# 11 COLOR VISION MECHANISMS

Andrew Stockman
*Department of Visual Neuroscience*
*UCL Institute of Opthalmology*
*London, United KIngdom*

David H. Brainard
*Department of Psychology*
*University of Pennsylvania*
*Philadelphia, Pennsylvania*

## 11.1 GLOSSARY

**Achromatic mechanism.** Hypothetical psychophysical mechanisms, sometimes equated with the luminance mechanism, which respond primarily to changes in intensity. Note that achromatic mechanisms may have spectrally opponent inputs, in addition to their primary nonopponent inputs.

**Bezold-Brücke hue shift.** The shift in the hue of a stimulus toward either the yellow or blue invariant hues with increasing intensity.

**Bipolar mechanism.** A mechanism, the response of which has two mutually exclusive types of output that depend on the balance between its two opposing inputs. Its response is nulled when its two inputs are balanced.

**Brightness.** A perceptual measure of the apparent intensity of lights. Distinct from luminance in the sense that lights that appear equally bright are not necessarily of equal luminance.

**Cardinal directions.** Stimulus directions in a three-dimensional color space that silence two of the three "cardinal mechanisms." These are the isolating directions for the L+M, L–M, and S–(L+M) mechanisms. Note that the isolating directions do not necessarily correspond to mechanism directions.

**Cardinal mechanisms.** The second-site bipolar L–M and S–(L+M) chromatic mechanisms and the L+M luminance mechanism.

**Chromatic discrimination.** Discrimination of a chromatic target from another target or background, typically measured at equiluminance.

**Chromatic mechanism.** Hypothetical psychophysical mechanisms that respond to chromatic stimuli, that is, to stimuli modulated at equiluminance.

**Color appearance.** Subjective appearance of the hue, brightness, and saturation of objects or lights.

**Color-appearance mechanisms.** Hypothetical psychophysical mechanisms that mediate color appearance, especially as determined in hue scaling or color valence experiments.

**Color assimilation.** The phenomenon in which the hue of an area is perceived to be closer to that of the surround than to its hue when viewed in isolation. Also known as the von Bezold spreading effect.

**Color constancy.** The tendency of objects to retain their color appearance despite changes in the spectral characteristics of the illuminant, or, more generally, despite changes in viewing context.

**Color contrast.** The change in the color appearance of an area caused by the presence of a colored surround. The color change, unlike assimilation, is usually complementary to the surround color.

**Color-discrimination mechanisms.** Hypothetical psychophysical mechanisms that determine performance in chromatic detection or discrimination tasks. Assumed in some models to correspond to cone-opponent mechanisms.

**Color spaces.** Representations of lights either in terms of the responses of some known or hypothetical mechanisms thought to underlie the perception of color (such as cone or postreceptoral mechanisms), or in terms of the projection of the lights onto stimulus-based vectors (such as monochromatic primaries or mechanism-isolating vectors).

**Color valence.** A measure of the color of a light in terms of the amount of a cancelling light required to null one of the hue sensations produced by that light. Thus, if a light appears red it is cancelled by light that appears green, and the amount of this green light is its red valance. In opponent-colors theory, color appearance depends on the relative red-green and blue-yellow valences.

**Cone contrast.** The contrast (or relative change in quantal or energy catch) presented to each cone photoreceptor: $\Delta L/L$, $\Delta M/M$, and $\Delta S/S$.

**Cone contrast space.** A color space where the position along each axis represents the contrast of one cone class.

**Cone mechanisms.** Hypothetical psychophysical mechanisms, the performances of which are limited at the cone photoreceptors.

**Cone-opponent mechanism.** Hypothetical psychophysical mechanisms with opposed cone inputs.

**Derrington Krauskopf Lennie (DKL) space.** Color space, the axes of which are the stimulus strengths in each of the three cardinal mechanism directions. Closely related to the spaces proposed by Lüther[85] and MacLeod and Boynton.[86] In some accounts of this space the axes are defined in a different way, in terms of the three vectors that isolate each of the three cardinal mechanisms.

**Detection surface or contour.** Detection thresholds measured in many directions in color space form a detection surface. Confined to a plane, they form a contour. The terms threshold surface and threshold contour are synonymous with detection surface and detection contour, respectively.

**Field method.** A method in which the observer's sensitivity for detecting or discriminating a target is measured as a function of some change in context or in the adapted state of the mechanism of interest.

**First-site adaptation.** Adaptation, usually assumed to be cone-class specific, occurring at or related to the photoreceptor level.

**Habituation.** Loss of sensitivity caused by prolonged adaptation to chromatic and/or achromatic stimulus modulations, also known as contrast adaptation.

**Incremental cone-excitation space.** A color space in which the axes represent the deviations of each of the three classes of cones from a background. Deviations can be negative (decrements) as well as increments.

**Intensity.** Generic term to denote variation in stimulus or modulation strength when chromatic properties are held constant. In the particular context of modulations around a background, the vector length of a modulation may be used as a measure of intensity.

**Invariant hue.** A stimulus produces an invariant hue if that hue is independent of changes to stimulus intensity. Generally studied in the context of monochromatic stimuli.

**Isolating direction.** Direction in a color space that isolates the response of a single mechanism.

**Linear visual mechanisms.** Hypothetical mechanisms that behave linearly, usually with respect to the cone isomerization rates, but in some models with respect to the cone outputs after von Kries adaptation or contrast coding.

**Luminance.** A measure of the efficiency (or effectiveness) of lights often linked to the assumed output of the achromatic mechanism.

**Mechanism direction.** Stimulus color direction along which a specified mechanism is most sensitive. Note that the mechanism direction is not, in general, the same as the isolating direction for the same mechanism.

**Noise masking.** Threshold elevations caused by superimposing targets in noise.

**Nonlinear visual mechanisms.** Hypothetical mechanisms that behave nonlinearly either with respect to the cone inputs or with respect to their own (assumed) inputs.

**Opponent-colors theory.** A color theory that accounts for color appearance in the terms of the perceptual opposition of red and green (R/G), blue and yellow (B/Y), and dark and light (W/B).

**Pedestal effects.** Changes in sensitivity that occur when a target is superimposed on another stimulus, called the pedestal, which may have either identical or different spatio-chromatic-temporal characteristics to the target.

**Second-site desensitization.** Adaptation or sensitivity losses that act on the outputs of second-site cone-opponent and achromatic mechanisms, and thus on the combined cone signals processed by each mechanism.

**Test method.** A method in which the sensitivity for detecting or discriminating a target is measured as a function of some target parameter, such as wavelength, size, or temporal frequency.

**Threshold surface or contour.** Synonyms for detection surface or contour.

**Unique hues.** Hues that appear perceptually unmixed, such as unique blue and unique yellow (which appear neither red nor green).

**Unipolar mechanism.** A mechanism that responds to only one pole of bipolar cone-opponent excursions, thought to be produced by half-wave rectification of bipolar signals.

**Univariant mechanism.** A mechanism, in which the output varies unidimensionally, irrespective of the characteristics of its inputs.

**von Bezold spreading.** See Color assimilation.

**von Kries adaptation.** Reciprocal sensitivity adjustment in response to changing light levels assumed to occur independently within each of the three cone mechanisms.

**Weber's law.** $\Delta I/I$ = constant. The sensitivity to increments ($\Delta I$) is inversely proportional to the adaptation level ($I$).

## 11.2 INTRODUCTION

The first stage of color vision is now well understood (see Chap. 10). When presented in the same context under photopic conditions, pairs of lights that produce the same excitations in the long-, middle-, and short-wavelength-sensitive (L-, M-, and S-) cones match each other exactly in appearance. Moreover, this match survives changes in context and changes in adaptation, provided that the changes are applied equally to both lights. Crucially, however, while the match survives such manipulations, the shared appearance of the lights does not. Substantial shifts in color appearance can be caused both by changes in context and by changes in chromatic adaptation. The identity of lights matched in this way reflects univariance at the cone photoreceptor level, whereas their changed appearance reflects the complex activity of postreceptoral mechanisms acting on the outputs of the cone photoreceptors. Figure 1 shows examples of how color contrast and color assimilation can affect the color appearance of pairs of lights that are physically identical.

In addition to affecting color appearance, postreceptoral mechanisms play a major role in determining the discriminability of color stimuli. Indeed, measurements of color thresholds (detection and discrimination) are critical in guiding models of postreceptoral mechanisms. Models of color discrimination are also important in industrial applications, for instance, in the specification tolerances for color reproduction (see subsection "CIE Uniform Color Spaces" in Sec. 10.6, Chap. 10).

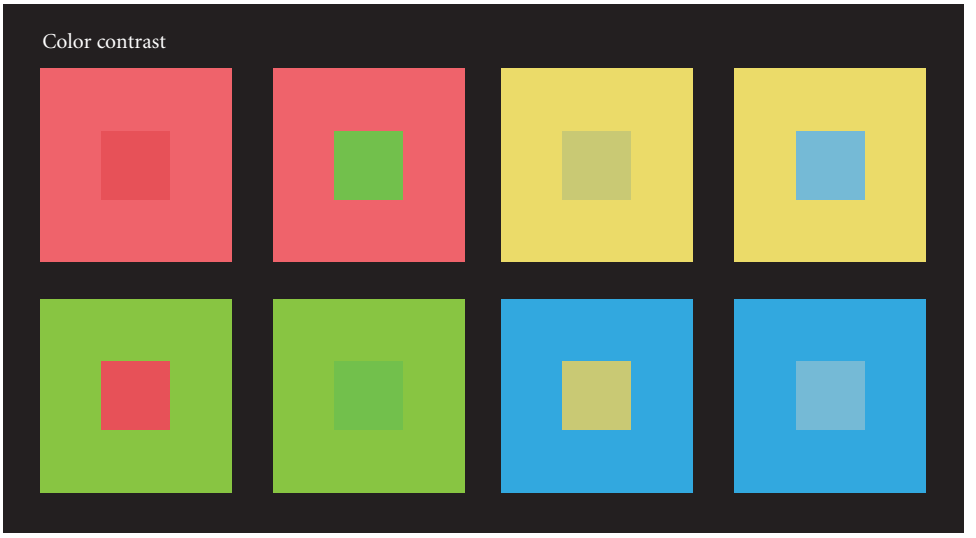


(a)

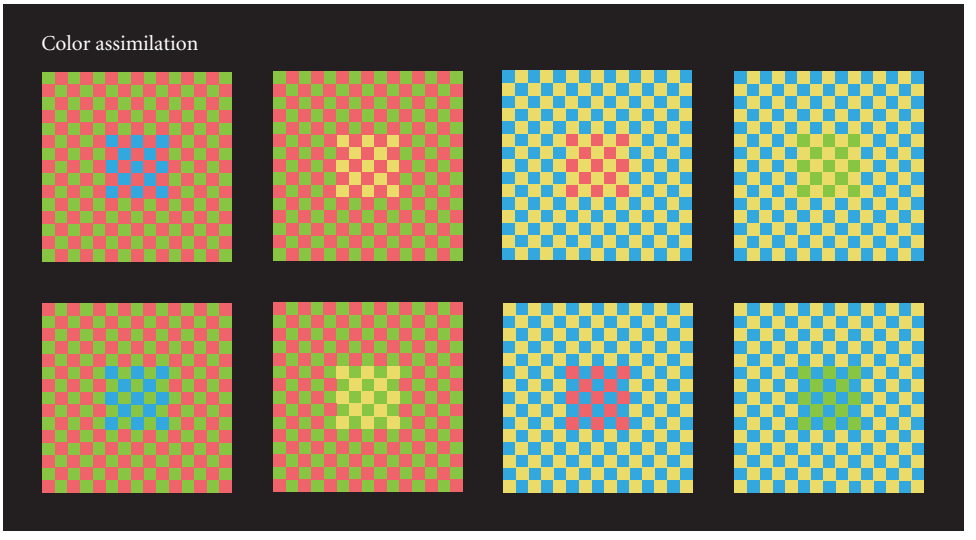


(b)

**FIGURE 1** (*a*) Color contrast: The pairs of smaller squares in each of the four vertical columns are physically the same, but their color appearances are very different. The differences arise because of the surrounding areas, which induce complementary color changes in the appearance of the central squares.[473] Comparable examples of color contrast have been produced by Akiyoshi Kitaoka,[474] which he attributed to Kasumi Sakai.[475] (*b*) Color assimilation or the von Bezold spreading effect:[476] The tiny squares that make up the checkerboard patterns in each of the four columns are identical, except in the square central areas. In those central areas, one of the checkerboard colors has been replaced by a third color. The replacement color is the same in the upper and lower patterns, but the colors of the checkers that it replaces are different. The result is that the replacement color is surrounded by a different color in the upper and lower patterns. Although the replacement color is physically the same in each column, it appears different because of the color of the immediately surrounding squares. Unlike color contrast, the apparent color change is toward that of the surrounding squares.

## The Mechanistic Approach

This chapter is about color vision after the photoreceptors. In the development, we adopt a mechanistic approach. The idea is to model color vision as a series of stages that act on the responses of the cones. Within the mechanistic approach, the central questions are: how many stages are needed, what are the properties of the mechanisms at each stage, and how are the mechanisms' outputs linked to measured performance? We focus on psychophysical (perceptual) data. Nonetheless, we are guided in many instances by physiological and anatomical considerations. For reviews of color physiology and anatomy, see, for example, Gegenfurtner and Kiper,[1] Lennie and Movshon[2], and Solomon and Lennie.[3] A useful online resource is Webvision at http://webvision.med.utah.edu/.

The distinction between color encoded at the photoreceptors and color encoded by postreceptoral mechanisms was anticipated by two theories that have dominated color vision research since the late nineteenth century. First, in the Young-Helmholtz trichromatic theory,[4,5] color vision is assumed to depend on the univariant responses of the three fundamental color mechanisms (see Chap. 10). Color vision is therefore trichromatic. Trichromacy allows us to predict which mixtures of lights *match*, but it does not address how those matches *appear*, nor the discriminability or similarity of stimuli that do not match.

Second, in Hering's[6,7] opponent colors theory, an early attempt was made to explain some of the phenomenological aspects of color appearance, and, in particular, the observation that under normal viewing conditions some combinations of colors, such as reddish-blue, reddish-yellow, and greenish-yellow, are perceived together, but others, such as reddish-green or yellowish-blue, are not. This idea is illustrated in Fig. 2. Hering proposed that color appearance arises from the action of three signed mechanisms that represent opposing sensations of red versus green, blue versus yellow, and light versus dark.[6,7] A consequence of this idea is that opposing or opponent pairs of sensations are exclusive, since they cannot both be simultaneously encoded. In this chapter, we will use the term "color-appearance mechanisms" to refer to model-constructs designed to account for the appearance of stimuli, and in particular the opponent nature of color appearance.

Early attempts to reconcile trichromacy with the opponent phenomenology of color appearance suggested that the color-appearance mechanisms reflect a postreceptoral stage (or "zone") of color processing that acts upon the outputs of the three Young-Helmholtz cone mechanisms. Modern versions of the two-stage theory explicitly incorporate the cone's characteristics as a first stage as well as

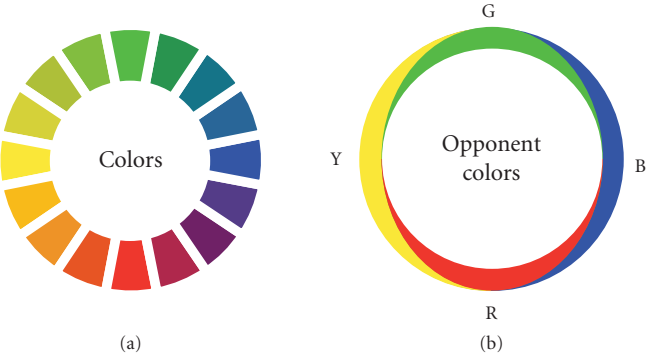


**FIGURE 2** Hering's opponent-colors diagram. A diagrammatic representation of opponent-colors theory. The ring on the left (*a*) shows a range of colors changing in small steps from green at the top clockwise to blue, red, yellow, and back to green. The ring on the right (*b*) shows the hypothetical contributions of each of the color-opponent pairs [red (R) vs. green (G), and blue (B) vs. yellow (Y)] to the appearance of the corresponding colors in (*a*). In accordance with opponent-colors theory, the opposed pairs of colors are mutually exclusive. (*Redrawn from Plate 1 of Ref. 7*).

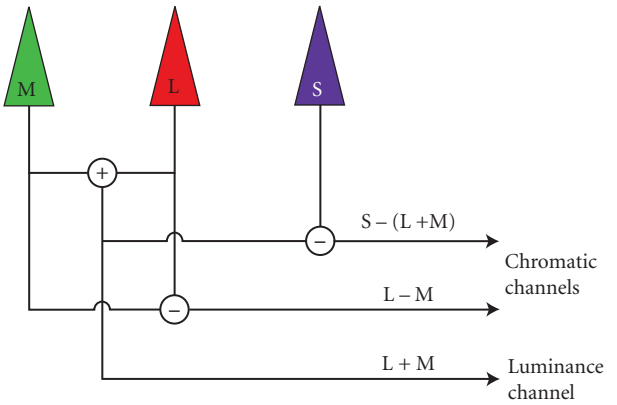


**FIGURE 3** Model of the early postreceptoral stages of the visual system. The signals from the three cone types, S, M, and L, are combined to produce an achromatic or luminance channel, L+M, and two cone-opponent channels, L–M and S–(L+M). Note that there is assumed to be no S-cone input to the luminance channel. (*Based on Fig. 7.3 of Ref. 15*).

a second stage at which signals from the separate cone classes interact (e.g., Refs. 8–14). A familiar version of the two-zone model from Boynton[15] with chromatic, L–M and S–(L+M), and achromatic, L+M, postreceptoral mechanisms is shown in Fig. 3.

Interestingly, the particulars of many modern two-stage models were formulated not to account for color appearance, but rather to explain threshold measurements of the detection and discrimination of visual stimuli. As Fig. 3 indicates, the opponent mechanisms in these models take on a simple form, represented as elementary combinations of the outputs of the three cone classes. We refer to opponent mechanisms that are postulated to explain threshold data as "color-discrimination mechanisms," to distinguish them from color-appearance mechanisms postulated to explain appearance phenomena. Here we use the omnibus term color-discrimination to refer both to detection (where a stimulus is discriminated from a uniform background) and discrimination (where two stimuli, each different from a background, are discriminated from each other.)

The distinction between color-appearance and color-discrimination mechanisms is important, both conceptually and in practice. It is important conceptually because there is no a priori reason why data from the two types of experiments (appearance and threshold) need be mediated by the same stages of visual processing. Indeed, as we will see below, the theory that links measured performance to mechanism properties is quite different in the two cases. The distinction is important in practice because the mechanism properties derived from appearance and discrimination data are not currently well reconciled.

The discrepancy between color-discrimination and color-appearance mechanisms has been commented on by recent authors,[11,14,16–22] but the discrepancy is implicit in early versions of the three-stage Müller zone theories,[23,24] Judd's version of which[24] was discussed again some years later in a more modern context (see Fig. 6. of Ref. 25). It is remarkable that models with separate opponent stages for the two types of data were proposed well before the first physiological observation of cone opponency in fish[26] and primate.[27]

Figure 4 illustrates a modern version of Judd's three-stage Müller zone theory, which is described in more detail in the subsection "Three Stage Zone Models" in Sec. 11.6. The figure shows the spectral sensitivities of each of the three stages. The spectral sensitivities of Stage 1 correspond to the cone spectral sensitivities of Stockman and Sharpe,[28] those of Stage 2 to the spectral sensitivities of

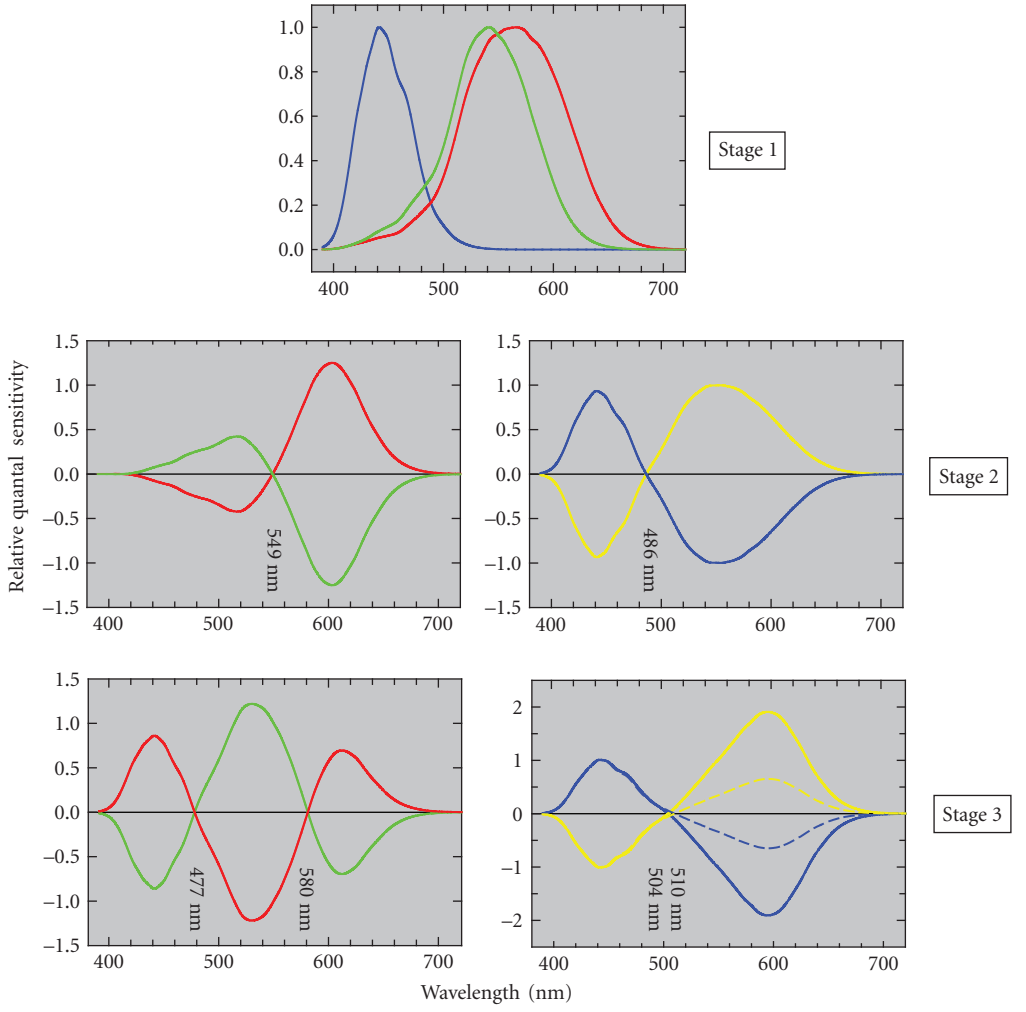


**FIGURE 4** Version of the three-stage Müller zone model with updated spectral sensitivities. The panels shows the assumed spectral sensitivities of the color mechanisms at Stages 1 (upper panel), 2 (middle panels), and 3 (lower panels). *Stage 1:* L- (red line), M- (green line), and S- (blue line) cone fundamental spectral sensitivities.[28] *Stage 2:* L–M (red line), M–L (green line), S–(L+M) (blue line), and (L+M)–S (yellow line) cone-opponent mechanism spectral sensitivities. *Stage 3:* R/G (red line), G/R (green line), B/Y (blue line), Y/B (yellow line) color-opponent spectral sensitivities. Our derivation of the cone-opponent and color-opponent spectral sensitivities is described in the subsection "Three-Stage Zone Models" in Sec. 11.6. The dashed lines in the lower right panel are versions of the B/Y and Y/B color-opponent spectral sensitivities adjusted so that the Y and B spectral sensitivity poles are equal in area. The wavelengths of the zero crossings of the Stage 2 and Stage 3 mechanisms are given in the figure. The spectral sensitivities of the achromatic mechanisms have been omitted.

color-discrimination mechanisms as suggested by threshold data, and those of Stage 3 to the spectral sensitivities of color-appearance mechanisms as suggested by appearance data.

Figure 4 sets the scene for this chapter, in which we will review the theory and data that allow derivation of the properties of color-discrimination and color-appearance mechanisms, and discuss the relation between the two. According to some commentators, one of the unsolved mysteries of color vision is how best to understand the relation between mechanisms referred to as Stages 2 and 3 of Fig. 4.

## Nomenclature

One unnecessary complication in the literature is that discrimination and appearance mechanisms are frequently described using the same names. Thus, the terms red-green (R/G), blue-yellow (B/Y), and luminance are often used to describe both types of mechanisms. We will attempt in this chapter to maintain a distinct nomenclature for distinct mechanisms.

It is now accepted that cones should be referred to as long-, middle-, and short-wavelength-sensitive (L-, M-, and S-), rather than red, green, and blue, because the color descriptions correspond neither to the wavelengths of peak cone sensitivity nor to the color sensations elicited by the excitation of single cones.[30] However, it is equally misleading to use color names to refer to color-discrimination mechanisms. Stimulation of just one or other side of such a mechanism does not necessarily give rise to a simple color sensation. Indeed, current models of opponent color-discrimination mechanisms have the property that modulating each in isolation around an achromatic background produces in one case a red/magenta to cyan color variation and in the other a purple to yellow/green variation.[31,32] Consequently, the perception of blue, green, and yellow, and to a lesser extent red, requires the modulation of *both* cone-opponent discrimination mechanisms (see subsection "Color Appearance and Color Opponency" in Sec. 11.5). We therefore refer to chromatic color-discrimination mechanisms according to their predominant cone inputs: L–M and S–(L+M). Although this approach has the unfortunate consequence that it neglects to indicate smaller inputs, usually from the S-cones (see subsection "Sensitivity to Different Directions of Color Space" in Sec. 11.5.), it has the advantage of simplicity and matches standard usage in much of the literature. We refer to the nonchromatic color discrimination mechanism as L+M. Note also that this nomenclature is intended to convey the identity and sign of the predominant cone inputs to each mechanism, but not the relative weights of these inputs.

In contrast, the perception of pure or "unique" red, green, yellow, and blue is, by construction of the theory, assumed to result from the responses of a single opponent color-appearance mechanism, the response of the other mechanism or mechanisms being nulled or in equilibrium (see subsection "Opponent-Colors Theory" in Sec. 11.5). We refer to opponent color-appearance mechanisms as R/G and B/Y, according to the color percepts they are assumed to generate. We refer to the nonopponent appearance mechanism as brightness.

## Guiding Principles

Behavioral measurements of color vision reflect the activity of an inherently complex neural system with multiple sites of processing that operate both in series and in parallel. Moreover, these sites are essentially nonlinear. The promise of the mechanistic approach lies in two main areas. First, in terms of developing an overall characterization of postreceptoral color vision, the hope is that it will be possible to identify broad regularities in the behavior of the system that can be understood in terms of models that postulate a small number of relatively simple mechanism constructs. Second, in terms of using psychophysics to characterize the behavior of particular neural sites, and to link behavior to physiology, the hope is that specific stimulus conditions can be identified for which the properties of the site of interest dominate the measured performance. In the conceptual limit of complexity, where a mechanistic model explicitly describes the action of every neuron in a given visual pathway, these models can, in principle, predict performance. But as a practical matter, it

remains unclear the degree to which parsimonious mechanistic models derived from behavioral measurements will succeed. Given the complexity of the underlying neural system, it is apparent that the mechanistic approach is ambitious.

In this context, several points are worth bearing in mind. First, the concept of a psychophysical mechanism will have the most utility when it can be shown to have an existence that extends beyond the particular stimulus and task conditions from which it was derived. Thus, we regard a mechanism as a theoretical construct whose usefulness depends on the range of data it can explain parsimoniously. This is a broader consideration than those sometimes used to determine the value of a mechanism.[33,34] In Secs. 11.3 and 11.4, we review two broad mechanism concepts that satisfy this criterion: opponency and adaptation.

Second, while some psychophysical techniques may emphasize the contribution of particular stages of the system, it is, with the exception of color matching, a simplification to ignore the contributions of earlier and/or later stages. For example, an often made but usually implicit assumption is that the cone quantal absorption rates are transmitted directly to postreceptoral mechanisms, as if the photoreceptors had no role other than to pass on a linear copy of their inputs. An interesting future direction for mechanistic models is to account for interactions between different stages of processing more fully.

Finally, in spite of our concerns, we have written this chapter primarily from the point of view of psychophysics. We readily acknowledge that over the past 50 years, results from molecular genetics, anatomy, and physiology have helped propel many psychophysical theories from intelligent speculation to received wisdom, particularly in the cases of cone spectral sensitivities and early retinal visual processing. Physiology and anatomy have also provided important evidence about color coding at different levels of the early visual system (e.g., Refs. 35–37), crucial information that is hard to obtain psychophysically. Obversely, as the increasing complexity of the visual system at higher levels of processing begins to limit the utility of a mechanistic psychophysical approach, it also constrains how much can be understood from a knowledge of the properties of the component neurons in the processing chain, the majority of which have yet to be characterized.

### Chapter Organization

The rest of this chapter is organized as follows: In the next two sections, we describe how mechanism concepts allow us to understand important features of both color discrimination and color appearance. Our treatment here is illustrative. We review a small selection of experimental data, and emphasize the logic that leads from the data to constraints on the corresponding models. In Sec. 11.3 we discuss discrimination data; in Sec. 11.4 we turn to appearance data. Two broad mechanistic concepts emerge from this initial review: those of color opponency and of adaptation. The initial review provides us with a basic model for postreceptoral color vision. Although this model is clearly oversimplified, it serves as the point of departure for much current work, and understanding it is crucial for making sense of the literature. The remainder of the chapter (Secs. 11.5 and 11.6) is devoted to a discussion of advanced issues that push the boundaries of the basic model.

## 11.3 BASICS OF COLOR-DISCRIMINATION MECHANISMS

### What Is a Mechanism?

Given the central role of the mechanism concept in models of color vision, one might expect that this concept is clearly and precisely defined, with a good consensus about its meaning. Our experience, however, is that although there are precise definitions of what constitutes a mechanism,[33,34] these are generally specific to a particular model and that the term is often used fairly loosely. In keeping with this tradition, we will proceed to discuss mechanisms through examples without attempting a rigorous definition.

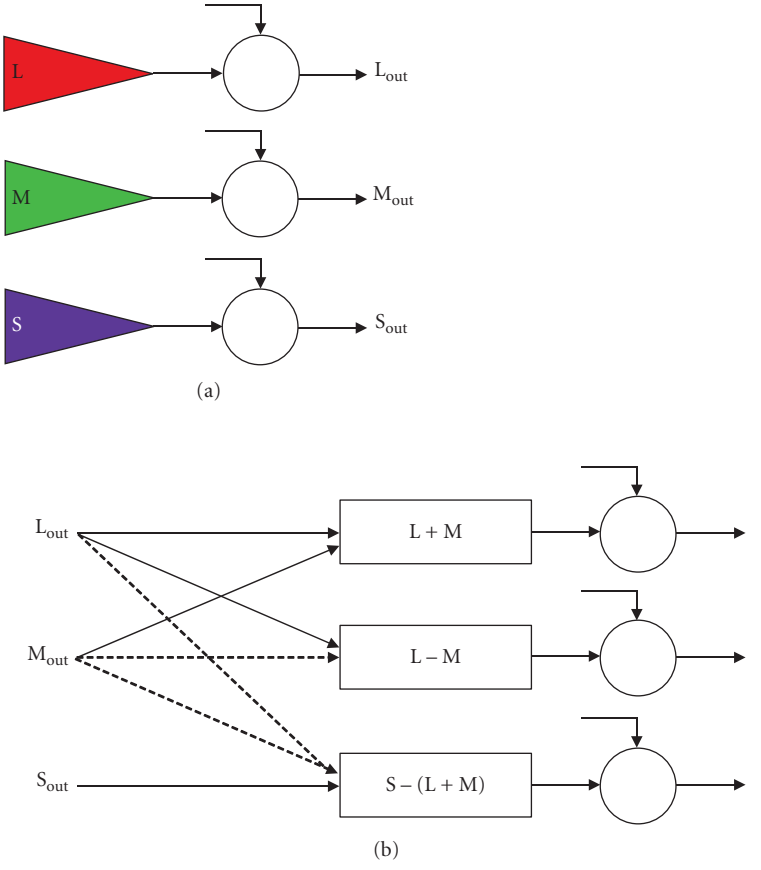


**FIGURE 5** Basic mechanisms. (*a*) First-stage cone mechanisms: L, M, and S. The cone outputs are subject to some form of gain control (open circles), which can, in principle, be modified by signals from the same or from different cone mechanisms. (*b*) Second-stage color-discrimination mechanisms: L+M, L–M, and S–(L+M). The inputs to these mechanisms are the adapted cone outputs from the cone mechanisms. As with the cone mechanisms, the outputs of the second-stage mechanism are subject to some gain control, which can be modified by signals from the same or from different second-stage mechanisms. Dashed arrows indicate inhibitory outputs.

Figure 5 illustrates the broad mechanism concept. Figure 5*a* shows the L, M, and S cones. Each of these cones is a mechanism and satisfies several key properties. First, we conceive of each cone mechanism as providing a spatiotemporal representation of the retinal image, so that the mechanism output may be regarded as a spatial array that changes over time. Second, at a single location and time, the output of each cone mechanism is univariate and conveys only a single scalar quantity. This means that the output of a single cone mechanism confounds changes in the relative spectrum of the light input with the overall intensity of the spectral distribution. Third, the relation between mechanism input and output is subject to adaptation. This is indicated in the figure by the open circle along the output pathway for each cone mechanism. Often the adaptation is characterized as a gain control, or a gain control coupled with a term that subtracts steady-state input (e.g., Refs. 38 and 39).

Key to the mechanism approach is that the behavior of the mechanism can be probed experimentally with adaptation held approximately fixed. This may be accomplished, for example, by presenting brief, relatively weak, flashes on spatially uniform backgrounds. In this case, the state of adaptation is taken to be determined by the background alone; that is, it is assumed that the weak flashes do not measurably perturb the state of adaptation and thus that the state of adaptation is independent of the flash.

The arrows pointing into each circle in Fig. 5 indicate that the signals that control the state of adaptation can be quite general, and need to be specified as part of the model. In the classical (von Kries) mechanism concept, however, these signals are assumed to arise entirely within the array of signals from the same cone mechanism.[33] For example, the gain (or adaptation) applied to the L-cone signals at a location would be taken to be determined entirely by the array of L-cone responses, and be independent of the responses of M and S cones. Adaptation that acts on the output of the cones is referred to as "first-site" adaptation.

Figure 5*b* shows a simple model of three second-stage color-discrimination mechanisms with the same basic wiring diagram as Fig. 3. These mechanisms have a similar structure to the cone mechanisms, in the sense that they are assumed to provide a spatial array of univariate responses. In addition, as with the cone mechanisms, the second-stage mechanisms can adapt. An important difference between these second-stage mechanisms and the cone mechanisms is the nature of their input. Where the cone mechanisms transduce light into a neural signal, the second-stage mechanisms take the adapted cone responses as their input. As shown in the Fig. 5, each of the postreceptoral mechanisms can be thought of as computing a weighted combination of cone signals. The three mechanisms are labeled by the manner in which they combine cone inputs. The first mechanism, (L+M), which is often referred to as the luminance mechanism, adds inputs from the L and M cones. The second mechanism, (L–M), takes a difference between L and M cone signals. And the third mechanism, S–(L+M), takes a difference between S-cone signals and summed L- and M-cone signals.

Although not necessary as part of the mechanism definition, making the input to the mechanism be a linear function of the output of the preceding stage simplifies the model, and enables it to make stronger predictions; whether the cone combinations are actually linear is an empirical question. Adaptation that acts on the outputs of the second-stage postreceptoral mechanisms is usually referred to as "second-site" adaptation or desensitization.

The cone mechanisms used in color vision models represent the action of a well-defined neural processing stage (the cone photoreceptors). The connection between postreceptoral mechanisms and neurons is not as tight. Although the cone inputs to different classes of retinal ganglion cells are similar to those used in models, these models often do not incorporate important features of real ganglion cells, such as their spatial receptive field structure (but see subsection "Multiplexing Chromatic and Achromatic Signals" in Sec. 11.5), cell-to-cell variability in cone inputs, and the fact that ganglion cells come in distinct ON and OFF varieties that each partially rectify their output (but see "Unipolar vs. Bipolar Chromatic Mechanisms" in Sec. 11.6).

## Psychophysical Test and Field Methods

Broadly speaking, two principal psychophysical techniques have been used to investigate the properties of color-discrimination mechanisms.[40–42] In the "test" (or "target") sensitivity method, the observer's sensitivity for detecting or discriminating a target is measured as a function of some target parameter, such as its wavelength, size, or temporal frequency. As noted above, implicit in the use of this method is the assumption that the presentation of the target does not substantially alter the properties or sensitivity of the detection mechanism, so that targets are usually presented against a background and kept near visual threshold.

In the "field" sensitivity method, the observer's sensitivity for detecting or discriminating a target is measured as a function of some change in the adaptive state of the mechanism. Field methods complement test methods by explicitly probing how contextual signals control adaptation. On the assumption that the control of adaptation occurs solely through signals within the mechanism mediating detection, the spectral properties of that mechanism can be investigated by, for example,

superimposing the target on a steady adapting field and changing the adapting field chromaticity and/or radiance, by habituating the observer to backgrounds temporally modulated in chromaticity and/or luminance just prior to the target presentation, or by superimposing chromatic and/or luminance noise on the target.

Both test and field methods have obvious limitations. In the test method, it is difficult to ensure that a target is detected by a single mechanism when the target parameters are varied, with the result that multiple mechanisms typically mediate most sets of test sensitivity measurements. As we discuss below, assigning different portions of chromatic detection contours to different mechanisms is problematic (see subsection "Sensitivity to Different Directions of Color Space" in Sec. 11.5). In the field method, it is often easier to ensure that a target is detected by a single mechanism. However, the assumption that adaptation is controlled entirely by signals from within the mechanism mediating detection is a strong one, and interpretation of results becomes much more complicated under conditions where this assumption is not secure. More generally, without an explicit and accurate model about the properties of the mechanism, both test and field sensitivity data may be uninterpretable.

## How Test Measurements Imply Opponency

In the next three sections, we introduce color-discrimination mechanisms. These are characterized by opponent recombination of cone signals at a second site (as shown in Fig. 5*b*), by adaptation in cone specific pathways (first-site adaptation, Fig. 5*a*), and by adaptation after the opponent recombination (second-site adaptation, Fig. 5*b*).

We begin with evidence from test sensitivity measurements that some sort of opponent recombination occurs. In the canonical test sensitivity experiment, a small test stimulus is presented against a uniform background. We denote the L-, M-, and S-cone excitations of the background by $L_b$, $M_b$, and $S_b$. If we fix the background, the test stimulus may be characterized by how much the cone excitations it produces deviate from the background. Denote these deviations by $\Delta L$, $\Delta M$, and $\Delta S$, so that the overall cone excitations of the test are given by $L = L_b + \Delta L$, $M = M_b + \Delta M$, and $S = S_b + \Delta S$. Note that the deviations $\Delta L$, $\Delta M$, and $\Delta S$ may be positive or negative.

For any background, we can consider a parametric family of test stimuli whose L-, M-, and S-cone deviations are in the same proportion. That is, we can define a test *color direction* by a triplet of deviations $\Delta L_d$, $\Delta M_d$, and $\Delta S_d$, normalized so that $\sqrt{\Delta L_d^2 + \Delta M_d^2 + \Delta S_d^2} = 1$. Test stimuli that share the same color direction have the form $\Delta L = c\Delta L_d$, $\Delta M = c\Delta M_d$, and $\Delta S = c\Delta S_d$. We refer to the constant $c$ as the *intensity* of the test stimulus along the given color direction. Figure 6*a* illustrates the test color direction and intensity concept for two vectors in the $\Delta L$, $\Delta M$ plane.

If the background and color direction of a test stimulus are held fixed, an experimenter can vary the test intensity and determine the psychophysical threshold for detection. This is the lowest intensity at which the observer can just see the test, and its value can be found experimentally using a variety of procedures.[43] The experiment can then be repeated for different choices of color direction, and the threshold intensity can be determined for each one.

Figure 6*b* plots one way in which the data from a threshold experiment might come out. For simplicity, we assume that $\Delta S_d$ was set to zero, and show data only in the $\Delta L$, $\Delta M$ plane. Each point in the plot represents the results of a threshold measurement for one color direction. The set of threshold points together trace out a "detection contour" (or "threshold contour"), since each point on the contour leads to an equal level of detection performance (the "threshold"). The two points that lie directly on the $\Delta L$ axis represent threshold for increments and decrements that drive only the L cones and leave the M cones silent; that is, these targets produce zero change in the M cones. Similarly two points that lie directly on the $\Delta M$ axis represent increments and decrements that produce only changes in the M cones. The other points on the contour show thresholds obtained when L- and M-cone signals are covaried in various ratios.

Understanding how threshold contours inform us about color-discrimination mechanisms is a key idea in the theory we present in this chapter. It is useful to begin by asking how the contour would come out if the visual system had a single color-discrimination mechanism consisting of, say,

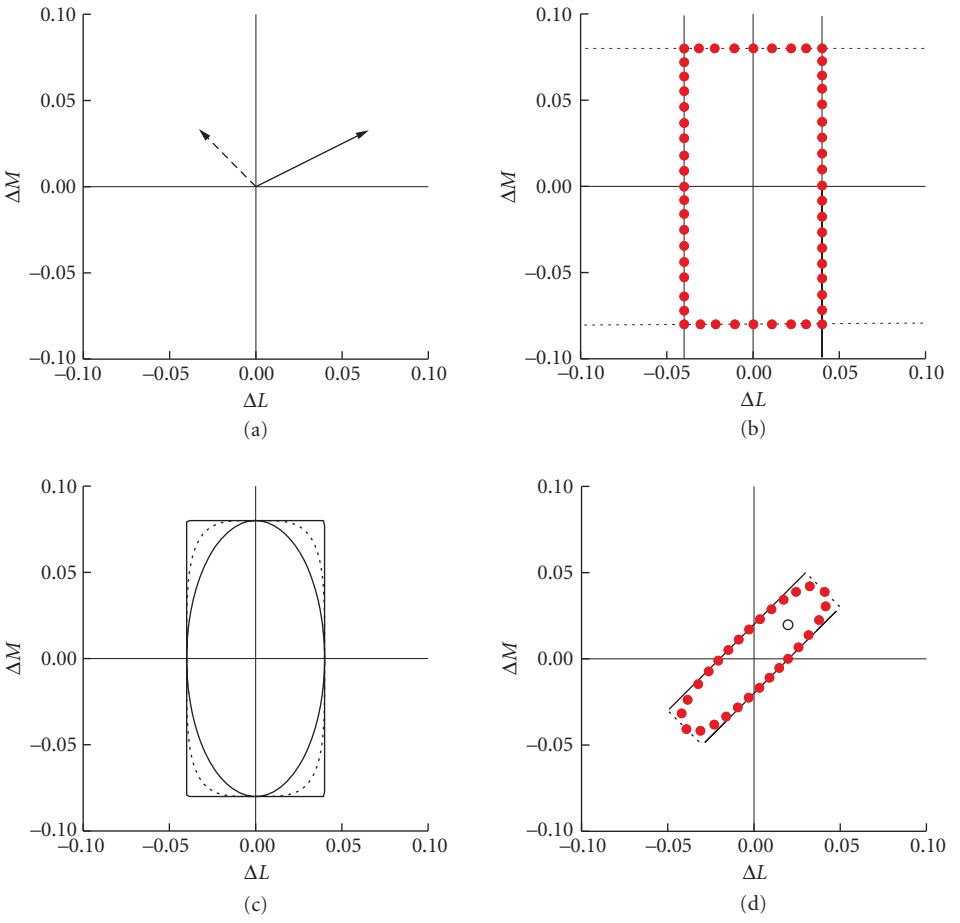


**FIGURE 6** Basic thresholds. (*a*) Two vectors plotted in the $\Delta L$, $\Delta M$ plane that represent two lights of different color directions and different intensities. (*b*) Incremental and decremental thresholds determined by an L-cone mechanism (vertical black lines) or by an M-cone mechanism (black, horizontal dotted lines). The points define the contour expected if threshold is determined independently and with no interactions between L- and M-cone detection mechanisms. (*c*) The joint detection contours when the L- and M-cone detection mechanisms show different degrees of summation. The inner, middle, and outer contours are for summation exponents of $k = 2$, 4, and 1000, respectively. (*d*) Idealized detection contours (red solid points) for thresholds determined by chromatic L–M (solid lines at 45°) and achromatic L+M (dotted lines at –45°) mechanisms. The single open circle shows the threshold expected in the $\Delta L_d = \Delta M_d$ direction if the threshold was determined by the cone mechanisms (i.e., by the thresholds along the axes $\Delta L_d = 0$ and $\Delta M_d = 0$).

only the L cones. In this case, only the $\Delta L$ component of the test modulation would affect performance, and the threshold contour would consist of two lines, both parallel to the $\Delta M$ axis. One line would represent threshold for incremental tests with a positive $\Delta L$ value, while the other would represent threshold for decremental tests with a negative $\Delta L$ value. This hypothetical detection contour is shown as two solid vertical lines in Fig. 6*b*. If there were no other mechanisms, the threshold contour would simply continue along the extensions of the solid vertical lines. The contour would not be closed, because modulations along the M-cone isolating direction produce $\Delta L$ values of zero and thus are invisible to the L-cone mechanism.

We can also consider a visual system with only an M-cone discrimination mechanism. By reasoning analogous to that used for the L-cone case above, the threshold contour for this system would consist of the two horizontal dotted lines also shown in the figure.

Finally, we can consider a system with independent L- and M-cone mechanisms and a threshold determined when either its $\Delta L$ or $\Delta M$ component reached the threshold for the corresponding mechanism. This would lead to a closed rectangular detection contour formed by the intersecting segments of the solid vertical and dotted horizontal lines shown in Fig. 6*b*. The threshold data plotted as solid red circles in the panel correspond to this simple model.

When signals from both L- and M-cone mechanisms mediate detection, the measured detection contour would be expected not to reach the corners of the rectangular contour shown in Fig. 6*b*. This is because even if the L- and M-cone mechanisms are completely independent, detection is necessarily probabilistic, and in probabilistic terms the likelihood that L, M, or both L and M together will signal the test is greater than the likelihood of either cone mechanism doing so alone even when the mechanisms are independent, especially when L and M are both near threshold. This "probability summation" will reduce thresholds in the corners where L and M signals are of similar detectability, rounding them. A number of simple models of how mechanisms outputs might combine in the presence of neural noise predict such rounding, with the exact shape of the predicted contour varying across models.

A convenient parametric form for a broad class of summation models is that test threshold is reached when the quantity $\Delta = \sqrt[k]{\sum_{i=1}^{N} |\Delta_i|^k}$ reaches some criterion value. In this expression, $N$ is the number of mechanism whose outputs are being combined, $\Delta_i$ is the output of the $i$th mechanism, and the exponent $k$ determines the form of summation. When $k = 2$, the quantity $\Delta$ represents the Euclidean vector length of the mechanism outputs. When $k \rightarrow \infty$, $\Delta$ represents the output of the mechanism whose output is greatest.

Figure 6*c* shows expected threshold contours for the output of the L and M mechanisms for three values of $k$. The outer rectangular contour (solid lines) shows the contour for $k = 1000$. Here there is effectively no summation, and the contour has the rectangular shape shown in Fig. 6*b*. The inner contour (solid line) shows the case for $k = 2$. Here the contour is an ellipse. The middle contour (dotted line) shows the case for $k = 4$. Determining the value of $k$ that best fits experimental data is a topic of current interest, as the answer turns out to have important implications for how to reason from sensitivity contours to mechanism properties (see subsection "Sensitivity to Different Directions of Color Space" in Sec. 11.5). Here, however, the key point is that we expect actual experimental data to show more rounded threshold contours than the one depicted in Fig. 6*b*. Under conditions where sensitivity is determined by the output of the L- and M-cone mechanisms, the expected shape of the threshold contour is a closed form whose major axes are aligned with the $\Delta L$ and $\Delta M$ axes.

Figure 6*d* shows an idealized representation of how the data actually come out when thresholds are measured against a neutral background (see also Fig. 20). Actual data deviate clearly from the predictions shown in Fig. 6*c*, which were based on the assumption that the color-discrimination mechanisms are the responses of the L and M cones. Instead, the data lie near an elongated ellipsoid whose axes are rotated intermediate to the $\Delta L$ and $\Delta M$ axes. The deviations from the predictions of the Fig. 6*c* are large and robust. In particular, note the location of the open circle in the figure. This circle shows an upper bound on threshold in the $\Delta L_d = \Delta M_d$ color direction; if the color-discrimination mechanisms were the L and M cones and they operated without summation, then threshold would be given by the open circle. If there was also summation between L- and M-cone mechanisms, then threshold would lie between the open circle and the origin, with the exact location depending on the degree of summation. Thresholds in this direction vastly exceed the bound shown by the open circle. This observation demonstrates unequivocally that the outputs of different cone mechanisms must be postreceptorally recombined.

A natural interpretation of the threshold contour shown in Fig. 6*d* is indicated by the rotated rectangle shown on the plot. The parallel solid lines represent the threshold contour that would be observed if detection were mediated by a single mechanism that computed as its output the difference between the L- and M-cone excitations to the test, and if threshold depended on $|\Delta L - \Delta M|$ reaching some criterion threshold level. Similarly, the dotted lines represent the threshold contours of a mechanism that sums the L- and M-cone excitations of the test. The idealized threshold data

shown is thus consistent with the first two color-discrimination mechanisms illustrated in Fig. 5*b*, with some amount of summation between mechanism outputs accounting for the quasi-ellipsoidal shape of the overall contour.

Logic similar to that shown, applied to data where $\Delta S$ is varied, leads us to postulate a third color-discrimination mechanism whose output is given by a weighted opposition of $\Delta S$ on the one hand and $\Delta L$ and $\Delta M$ on the other. Figure 21, later, shows detection contours in the equiluminant plane partially determined by the S–(L+M) mechanism.

Although it is straightforward to predict detection contours if the spectral properties of the underlying detection mechanisms and the interactions between them are known, it is harder, as we shall see below, to infer unequivocally the exact mechanism properties (e.g., the exact weights on signals from each cone class) from the contours.

## First-Site Adaptation

*Weber's law and contrast coding* The measurements described in the previous section assess sensitivity under conditions where the state of adaptation was held fixed. We now turn to how input signals from the cones depend on the conditioning or adapting background. The key idea here is that the cone excitations are converted to a contrast representation. Here we use L cones as an example and take the L-cone contrast of the test, $C_L$, to be given by $C_L = \Delta L/L_b$, where $\Delta L$ is (as above) the difference between the L-cone excitations produced by the test and background, and $L_b$ is the L-cone excitation produced by the background. Similar expressions apply for the M and S cones.

The conversion of raw cone excitations (photoisomerizations) to a contrast code implies an important adaptive function. The range of cone excitation rates encountered in the environment can be greater than $10^6$. This range greatly exceeds the limitations imposed by the individual neurons in the visual pathway, many of which have dynamic ranges of no more than about $10^2$ from the level of noise—their spontaneous firing rate in the absence of light stimulation—to their response ceiling.[44,45] If there were no adaptation, the cone visual response would often convey no useful information, either because it was too small to rise above the noise at the low end of the stimulus range or because it was saturated at the maximum response level and thus unable to signal changes. For adaptation to protect the cone-mediated visual system from overload as the light level increases, the primary mechanisms of sensitivity regulation are likely to be early in the visual pathways, most likely in the cone photoreceptors themselves.[46,48] Indeed, the molecular mechanisms of adaptation acting within the photoreceptor are now fairly well understood.[49–52]

The idea that signals leaving the cones are effectively converted to a contrast code makes a specific prediction about how thresholds should depend on the background. Suppose we consider test stimuli that only stimulate the L cones, and that we manipulate the L-cone component of the background, $L_b$. Because of the cone-specific adaptation, increasing $L_b$ will produce a proportional decrease in the contrast signal fed to the postreceptoral detection mechanisms. On the assumption that the noise limiting discrimination behavior remains constant across the change of background (see "Sites of Limiting Noise" in Sec. 11.3), this decrease means that the differential signal, $\Delta L$, required to bring a test stimulus to threshold will increase in proportion to $L_b$. This sort of behavior is often described as obedience to Weber's law; predictions of Weber's law models are shown by the blue line in Fig. 7*a*. Figure 7*a* shows a log-log plot of increment threshold $\Delta L$ against background component $L_b$. The predicted thresholds increase with a slope of unity on the log-log plot.

A feature of contrast-coding predictions that is clearly not realistic is that the threshold $\Delta L$ should decrease toward zero in complete darkness. A generalized and more realistic form of contrast coding is given by $C_L = \Delta L/(L_b + L_o)$, where $L_o$ is a constant. The dashed line in Fig. 7*a* shows a prediction of this form, which has the feature that thresholds approach a constant nonzero value as $L_b$ decreases below $L_o$. The value of $L_o$ may be thought of as the hypothetical excitation level—sometimes called a "dark light"—produced internally within the visual system in the absence of light that limits performance at low background levels.

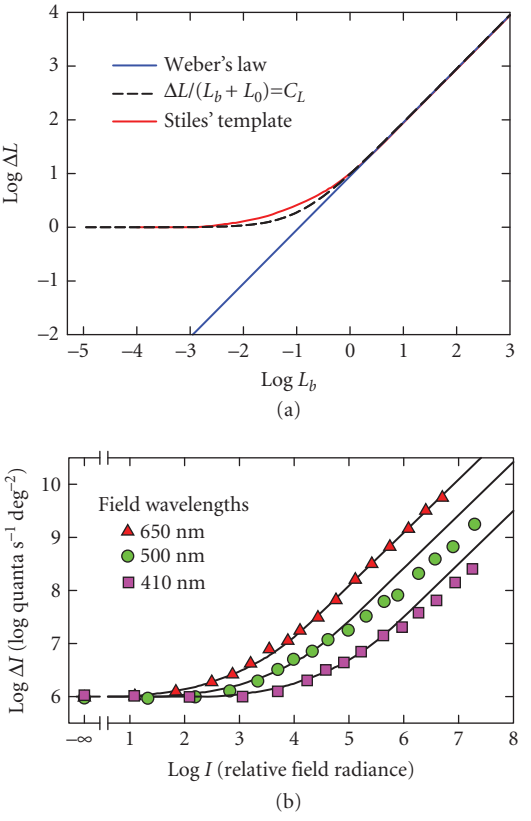


**FIGURE 7** Weber's law and increment thresholds. (*a*) Predictions of three first-site adaptation models for test lights detected by an L-cone mechanism as a function of background intensity. (*b*) Increment threshold data attributed to the L-cone mechanism ($\pi_5$, see subsection "Stiles' $\pi$ Mechanisms" in Sec. 11.5) replotted from Fig. 2 (Observer: EP) of Sigel and Pugh[54] obtained using a 200-ms duration, 667-nm target presented on background fields of 650 nm (red triangles), 500 nm (green circles), and 410 nm (purple squares). The solid lines aligned with each data set at low background radiances are Stiles' standard template [Table 1(7.4.3) of Ref. 53]. The horizontal position of the data is arbitrary.

Stiles' template shape [see Table 1(7.4.3) of Ref. 53], shown as the red line in Fig. 7*a*, has a form similar to that predicted by generalized contrast coding (dashed line). This template was derived to account for increment threshold data obtained under a variety of conditions (see subsections "Sensitivity to Spectral Lights" and "Stiles' $\pi$ Mechanisms" in Sec. 11.5). Figure 7*b* shows increment threshold data measured by Sigel and Pugh,[54] for three different background wavelengths under conditions where the L-cone mechanism is thought to dominate detection. These data fall approximately along Stiles' template, although deviations are clear at high background radiances for two of the three spectral backgrounds shown. The deviations are consistent with contributions of postreceptoral mechanisms to detection performance.[54,55] Data like these speak to the difficulties of distinguishing the contributions of different mechanisms from even the simplest data. Stiles, for example, accounted for the same sort of deviations by proposing an additional cone mechanism.[33]

*The signals reaching the second site* Although increment threshold data suggest a roughly Weber-type gain control, they do not by themselves determine whether the signal transmitted to the second site is of the contrast form $\Delta L/(L_b + L_o)$, as we have written above, or of the simpler form $L/(L_b + L_o)$, where to recap $L = \Delta L + L_b$. We cannot, in other words, determine from detection thresholds alone whether the adapted signal generated by the background is partially or wholly subtracted from the signal transmitted to the postreceptoral mechanisms.

To understand the ambiguity, define the gain $g$ as $g = 1/(L_b + L_o)$. In a gain control only model (with no background subtraction), the signal transmitted from the L cones in response to the background plus test would be $L' = gL$, where $L$ represents the combined cone excitations to the background plus test. Similarly, under this model, the gain adjusted response to the background alone would be $L_b' = gL_b$. If we assume that threshold requires the difference in response to background plus test on the one hand and background alone on the other to reach some criterion level, then the threshold will depend on $(L' - L_b') = g(L - L_b) = (L - L_b)/(L_b + L_o) = \Delta L/(L_b + L_o) = C$, which is the contrast form. Thus, predictions about detection threshold are independent of whether a constant is subtracted from the signals leaving the cones.

To deduce the need for a subtractive term (i.e., to differentiate contrast-like coding from gain control alone) from threshold data requires discrimination experiments, in which threshold is measured not just for detecting a test against the background, but also for detecting the test (often referred to as a probe in this context) presented against an incremental flash, both of which are presented against a steady background. In these experiments, the threshold intensity for the probe depends on the flash intensity, and changes in this dependence with the background may be used to infer the nature of the adaptive processes. We will not review these experiments or their analysis here; other papers provide detailed descriptions (e.g., Refs. 56–59). The conclusion drawn by these authors is that to account for steady-state adaptation a subtractive term is required in addition to multiplicative gain control.

## Second-Site Adaptation

The final piece of the basic model of color-discrimination mechanisms is a second stage of adaptation that modifies the output of the second-stage mechanisms (Fig. 5*b*). First-site adaptation is postulated to remove the effects of steady, uniform backgrounds by converting signals to a contrast representation; second-site adaptation is postulated to be driven by contrast signals in the background (see subsection "Field Sensitivities" in Sec. 11.5). Before proceeding, however, we should add two caveats. First, even with uniform, steady fields, first-site adaptation is usually incomplete. Were it complete, detection thresholds expressed as contrasts would be independent of background chromaticity, which they clearly are not (see Fig. 8 and subsection "Field Sensitivities" in Sec. 11.5). Second, first-site adaptation is not instantaneous. If it were, then in the extreme case of complete first-site adaptation being local to the photoreceptor as well as being instantaneous, neither local nor global changes in contrast would be transmitted to the second-site. In the less extreme case of complete, instantaneous adaptation being more spatially extended, then global changes in contrast would not be transmitted—with the result that large uniform field or Ganzfeld flicker should be invisible, which is not the case.[60] To understand the basic logic that connects threshold experiments to second-site contrast adaptation or desensitization, we first consider the effects of steady backgrounds and then the effects of habituation.

*Second-site desensitization by steady fields* Because first-site adaptation is incomplete, steady chromatic backgrounds can desensitize second-site mechanisms. The effect of this type of desensitization on detection contours is illustrated in Fig. 8. The colored circles in Fig. 8*a* show segments of detection contours in the $\Delta L/L$, $\Delta M/M$ plane of cone contrast space for two background chromaticities. The contours have a slope of 1, which is consistent with detection by a chromatic L–M mechanism with equal and opposite L- and M-cone contrast weights. If the background chromaticity is changed and adaptation at the first site follows Weber's law, then the contours plotted in cone contrast units should not change. What happens in practice, when for example, a field is changed

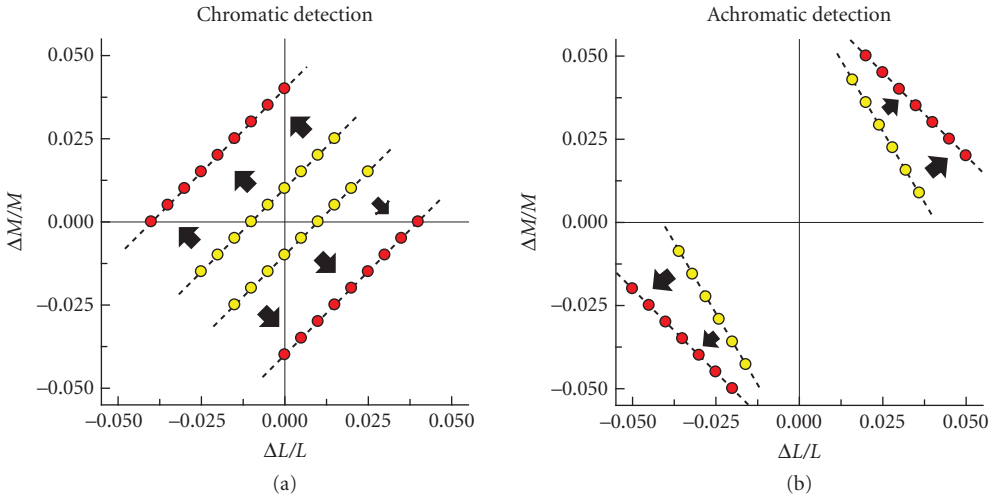


**FIGURE 8** Changes in contrast threshold caused by second-site adaptation to steady fields. (*a*) Hypothetical contours for detection mediated by the L–M mechanism plotted in cone contrast space before (yellow circles) and after (red circles) second-site desensitization (caused by, e.g., a change in background chromaticity from yellow to red). The L–M mechanism is assumed to have equal and opposite L-cone contrast weights at its input, and this equality is assumed to be unaffected by the desensitization. (*b*) Hypothetical detection contours for detection by the L+M mechanism before (yellow circles) and after (red circles) a change in background chromaticity from yellow to red. Initially, the L+M mechanism is assumed to have an L-cone contrast weight 1.7 times greater than the M-cone contrast weight. Changing the field to red suppresses the L-cone contrast weight, causing a rotation of the contour, as indicated by the arrows and the red circles.[63]

in chromaticity from spectral yellow to red, is that the contours move outward,[61] as indicated by the arrows and the red circles in Fig. 8*a*. (Actual data of this type are shown in Fig. 28.)

The constant slope of the L–M detection contours with changing background chromaticity is consistent with Weber's law operating at the first site. The loss of sensitivity in excess of Weber's law is most naturally interpreted as a second-site desensitization that depends on background chromaticity and acts on the joint L–M signals. Experimental evidence also supports the idea that first-site adaptation is in the Weber regime under conditions where supra-Weber desensitization is observed.[62]

The effect of second-site chromatic adaptation on the L+M luminance mechanism is different. The yellow circles show partial detection contours with a slope of –1.7, which is consistent with detection by an achromatic L+M mechanism with an L-cone contrast weight 1.7 times greater than the M-cone contrast weight (this choice is arbitrary, but, in general, the L-cone weight is found to be greater than the M-cone weight, see subsection "Luminance" in Sec. 11.5). If the background chromaticity is again changed from spectral yellow to red, the detection contours rotate, as indicated by the arrows and the yellow circles.[63] In this case, the rotation is due to a suppression by the long-wavelength field of the L-cone contribution to luminance detection relative to the M-cone contribution.[63,64] Given first-site adaptation that follows Weber's law independently in the L- and the M-cones, first-site adaptation should affect L- and M-cone inputs equally in all postreceptoral mechanisms. The fact that the L–M measurements show an equal effect on the L- and M-cone contrast inputs, whereas the L+M measurements show a differential effect, is most easily explained by positing adaptation effects at a second-site. The idea that the cone inputs to luminance and chromatic mechanisms undergo adaptation that is specific to each type of mechanism was framed by Ahn and MacLeod.[65] The same idea is also explicit in the earlier work of Stromeyer, Cole, and Kronauer.[61,63] The effects of steady fields on the L+M mechanism are discussed further in subsection "Achromatic Direction and Chromatic Adaptation" in Sec. 11.5.

*Second-site habituation* The effects of steady backgrounds at the second site are comparatively small because the background signals are attenuated by adaptation at the first site. Second-site effects can be enhanced by temporally modulating the chromaticity or luminance of the background as in an habituation experiment. Figure 9*a* shows an idealized threshold contour for detection thresholds

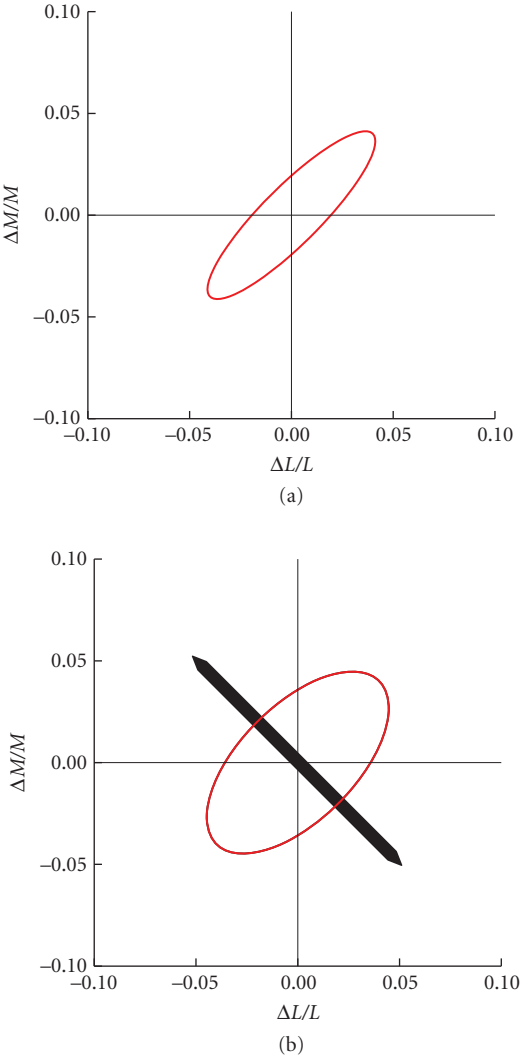


**FIGURE 9** Habituation predictions. (*a*) Hypothetical threshold contour under conditions where detection is mediated by second-site mechanisms. The contour is plotted in a cone contrast representation, and shows the contour in the $\Delta L/L$, $\Delta M/M$ contrast plane. The S-cone contrast is taken to be zero, so that thresholds are mediated by the L+M and L–M mechanisms. The contour was computed on the assumption that the gain of the L–M mechanism was four times that of the L+M mechanism, using a summation model with an exponent of 2. (*b*) Corresponding contour after habituation has reduced the gain of the L–M mechanism by a factor of 2 and left the L+M mechanism gain unchanged. The habituating direction is indicated by the black arrow. The result is the threshold contour becomes more elongated along the negative diagonal in the cone contrast plot.

in the $\Delta L/L$, $\Delta M/M$ plane obtained against a uniform background. This is the same type of data shown in Fig. 6*d*, but plotted on cone contrast axes. Detection is assumed to be mediated by L–M and L+M mechanisms with L–M being four times more sensitive to cone contrast than L+M. The elliptical contour reflects a summation exponent of 2, which we assume here for didactic purposes. If the same experiment is repeated after the subject has been habituated to contrast modulated in the L–M direction (as indicated by the black arrow Fig. 9*b*), the basic second-site model predicts that thresholds will be elevated for test stimuli that are modulated in that direction. On the other hand, for test stimuli modulated in the L+M direction, thresholds should be unaffected. Finally, for stimuli in intermediate directions, thresholds will be elevated to the extent that the L–M opponent mechanism contributes to detection. Figure 9*b* shows the predicted threshold contour, computed on the assumption that the L–M habituation cuts the gain of the L–M mechanism in half while leaving that of the L+M mechanism unaffected.

The data shown in Fig. 9 may be replotted by taking the difference of the post- and prehabituation threshold stimuli, for each color direction. Figure 10*a* shows an habituation effect plot of this sort. In this plot, the distance from the origin to the contour in each direction shows the threshold increase produced by the L–M habituation for test stimuli modulated in that color direction. The radius is large in the L–M test direction, and drops to zero for the L+M test direction.

Figure 10*b* and *c* show idealized habituation effect plots for habituation in the L+M direction and to an intermediate color direction, as shown by the black arrows. What the figure makes clear is that the effect of habituation on detection threshold should have a characteristic signature for each habituation direction.

Figure 11 replots the parts of Fig. 10 on axes that represent not cone contrast but rather stimulus directions that isolate the L+M and L–M discrimination mechanisms. These axes have been normalized so that a unit step along each axis direction corresponds to a threshold stimulus (without any habituation) for the corresponding mechanism. We discuss in more detail in subsection "Color Data Representations" in Sec. 11.5 the advantages and disadvantages of using an opponent representation of this type, but introduce it here to allow direct comparison of the idealized predictions of the basic model to the data reported by Krauskopf, Williams, and Heeley.[14] These authors made measurements of how habituation in different color directions affected threshold contours. Their data for observer DRW, as shown in Fig. 29 in subsection "Habituation or Contrast Adaptation Experiments" in Sec. 11.5, agree qualitatively with the predictions shown in Fig. 11, and provide fairly direct evidence to support habituation at a second site. As with other aspects of the basic model, we return below to discuss more subtle features of the data that deviate from its predictions.

## Sites of Limiting Noise

Before proceeding to color-appearance mechanisms, we pause to discuss a fundamental theoretical issue. This is the question of how the properties of a mechanism at an early stage of the visual processing chain could directly mediate observed detection thresholds, given that the signals from such a site must pass through many additional stages of processing before a perceptual decision is made. This question parallels one often asked in the context of colorimetry, namely, how it is that the very first stage of light absorption can mediate the overall behavior observed in color matching (see Chap. 10). Both questions have the same underlying answer, namely, that information lost at an early stage of visual processing cannot be restored at subsequent stages. The difference is the nature of the information loss. In the case of color matching, the information loss occurs because of the univariant nature of phototransduction. In the case of color thresholds, the information loss occurs because of noise in the responses of visual mechanisms. These sources of noise, relative to the signal strength, set the limits on visual detection and discrimination.

The link between thresholds and noise is well developed under the rubric of the theory of signal detection.[43,66–68] Here we introduce the basic ideas. Consider a test stimulus of intensity $c$ in the $\Delta L_d = 1$, $\Delta M_d = 0$ color direction. Only the L-cone mechanism responds to this stimulus, so for this initial example we can restrict attention to the L-cone response. If we present this same stimulus over many trials, the response of the L-cone mechanism will vary from trial-to-trial. This is indicated

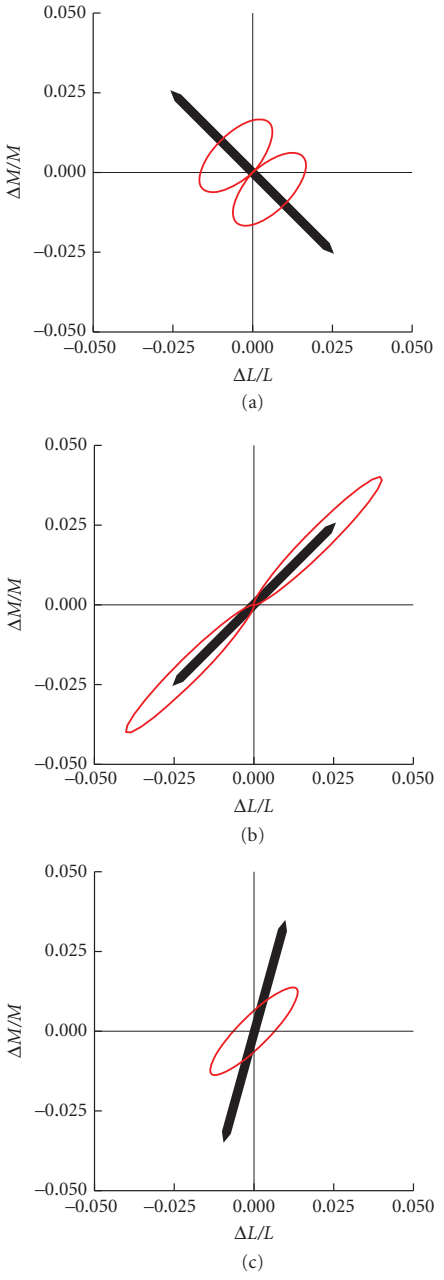


**FIGURE 10** Changes in contrast threshold caused by habituation. It is conventional to report the results of a habituation experiment using a plot that shows the change in threshold caused by habituation. (*a*) Depiction of the hypothetical data shown in Fig. 9 in this fashion. For each direction in the cone contrast plot, the distance between the origin and the contour shows the increase in threshold caused by habituation for tests in that color direction. For the example shown, there is no change in threshold in the L+M contrast direction, and the contour returns to the origin for this direction. (*b*) Changes in threshold that would be produced by a habituating stimulus that decreases the gain of the L+M mechanism by a factor of 2 and leaves the gain of the L–M mechanism unchanged. (*c*) Changes in threshold that would be produced by a habituating stimulus that decreases the gain of both mechanisms equally by a factor of 1.33. The habituating directions are indicated by the black arrows.

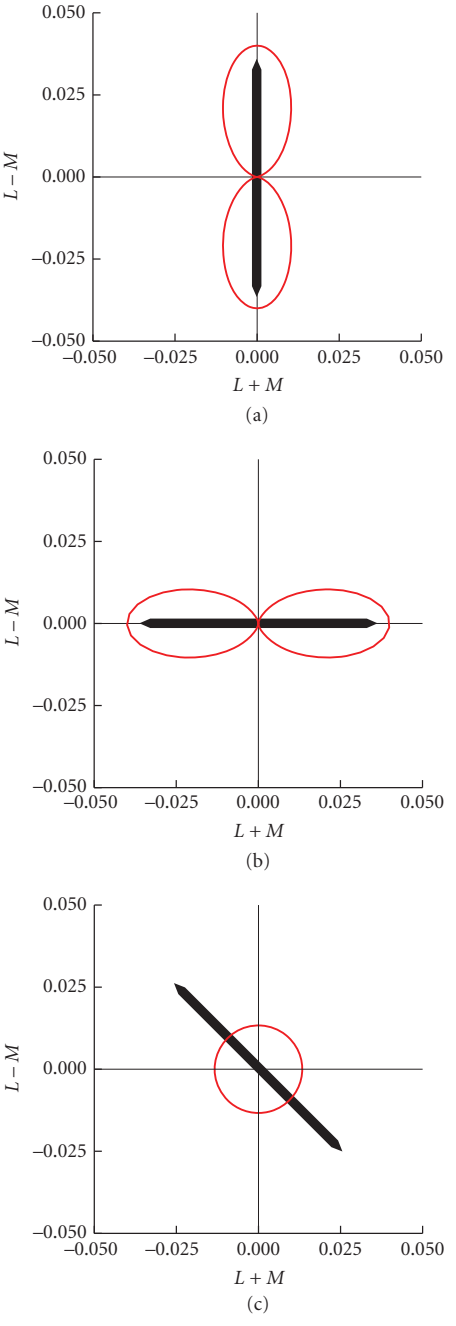


**FIGURE 11** Changes in L+M and L–M sensitivity caused by habituation. Panels (*a*) to (*c*) replot the threshold changes shown in the corresponding panels of Fig. 10. Rather than showing the effects in cone-contrast space, here the results are shown in a space where the axes correspond to the L+M and L–M color directions. In addition, the units of each of these rotated axes have been chosen so that detection threshold for tests along the axis is 1. This representation highlights the canonical pattern of results expected when habituation along each axis reduces sensitivity for only the corresponding mechanism, and where habituation along the 45° direction reduces sensitivity equally for the two mechanisms. The habituating directions are indicated by the black arrows.

by the probability distribution (solid red line) in Fig. 12*a*. Although the mean response here is 0.06, sometimes the response is larger and sometimes smaller. Similarly, the mechanism response to the background alone will also fluctuate (probability distribution shown as dotted blue line).

It can be shown[43,69] that optimal performance in a detection experiment occurs if the observer sets an appropriate criterion level and reports "background alone" if the response falls below this criterion

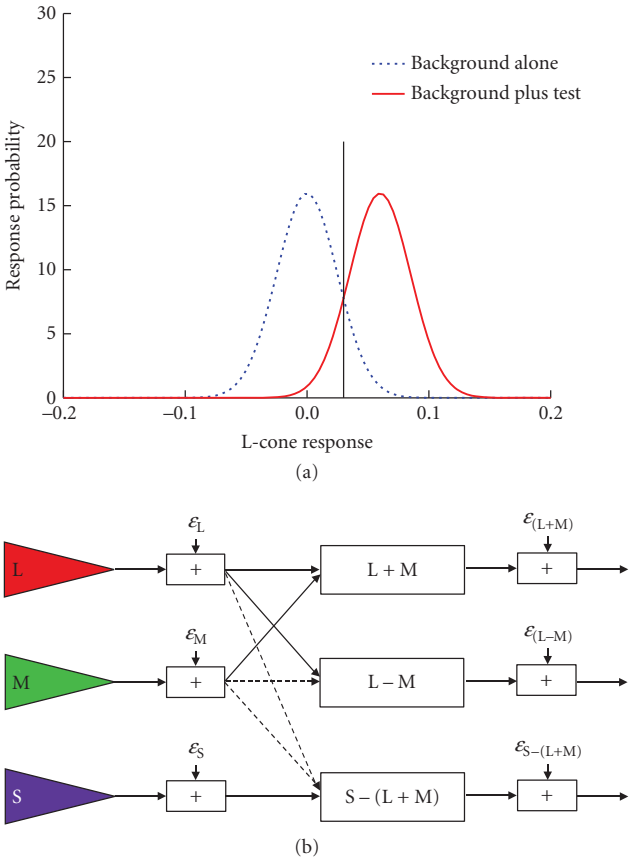


**FIGURE 12** Thresholds and noise. (*a*) The theory of signal detection's account of how noise determines thresholds, for a single mechanism. When the background alone is presented, the mechanism's responses vary somewhat from trial-to-trial because of additive response noise. The response variation is illustrated by the probability distribution centered on zero and shown by the dotted blue line. When the background and test are presented together, the average response increases but there is still trial-to-trial variability. This is illustrated by the probability distribution shown by the solid red line. When the two types of trial are presented equally often and the magnitudes of the costs associated with correct and incorrect responses are equal, it can be shown that the observer maximizes percent correct by reporting that the test was present whenever the mechanism response exceeds the criterion value shown in the figure by the vertical line. Different costs and prior probabilities simply move the location of this criterion. Even when this optimal criterion is used, there will still be some incorrect trials, those on which the response to background alone exceeds the criterion and those on which the response to background and test falls below the criterion. Threshold is reached when the test is intense enough that the observer is correct on a sufficient percentage of trials. How much the average response to background plus test must exceed that to background alone is determined by the magnitude of the noise. (*b*) The two-stage model of color-discrimination mechanisms, drawn in a manner that emphasizes that noise ($\varepsilon$) may be added both to the output of the first-site mechanisms and to the output of the second-site mechanisms. A full signal detection theoretic model of detection takes into account the response gain at each stage (which determines the separation of the average response to background and to background plus test) and the magnitude of noise at each stage. It also replaces the simple criterion shown in (*a*) with an optimal multivariate classifier stage.[70]

and "background plus test" otherwise. The plot shows the location of the optimal criterion (vertical line) for the special case when background-plus-test and background-alone events are presented equally often and when the benefits associated with both sorts of correct response (hits and correct rejections) have the same magnitude as the costs associated with both sorts of incorrect response (false alarms and misses). Note that even the optimal strategy will not lead to perfect performance unless the intensity of the test is large enough that the two distributions become completely separated. In this sense, the magnitude of response noise (which determines the widths of the distributions), relative to the effect of the test on the mean mechanism response, is what limits performance. More generally, the theory of signal detection allows computation of the probability of the observer performing correctly in the detection experiment as a function of the noise magnitude and test intensity.

With this idea in mind, we can turn to understanding how threshold measurements can reveal properties of early mechanisms, despite later processing by subsequent mechanisms. Figure 12*b* shows the basic model of color-discrimination mechanisms from Fig. 5, but without the adaptation stages shown explicitly. What is shown here, however, is that noise ($\varepsilon$) is added to the response of each mechanism. At the first stage, the cone responses are noisy. The noisy cone responses are then transformed at the second-site, and more noise is added. Thus the responses of the second-site mechanisms are subject both to noise that propagates from the first site, in addition to noise injected directly at the second site. For simplicity, we consider the noise added to each mechanism at each site to be independent; note that even with this assumption the noise at the opponent site will be correlated across the three color-discrimination mechanisms as a result of the way the first-site noise is transformed.

This model allows us to compute the expected shape of the threshold contours for a visual system that makes optimal use of the output of the second-site mechanisms. The computation is more involved than the simple unidimensional signal detection example illustrated in Fig. 12*a*, because optimal performance makes use of the output of all three second-site mechanisms and must take into account the correlated nature of the noise at this stage. Nonetheless, the ideas underlying the computation are the same as in the simple example, and the theory that allows the computation is well worked out.[70] We can thus ask how the expected discrimination contours, computed on the basis of the output at the second site, vary with the properties of the noise added at each stage.

Figure 13 shows threshold contours computed for three choices of noise. Figure 13*a* shows a case where the standard deviation of the noise injected at the first site is 5 times larger than that at the second site. The derived contour has the properties expected of detection by cone mechanisms, with the major axes of the contour aligned with the L- and M-cone contrast axes (see Fig. 6*b* and *c*). Figure 13*c* on the other hand, shows the opposite situation where the noise injected at the second site is 5 times larger than that at the first site. Simply changing the noise magnitude has major effects on the observed contour; the shape of the contour shown in Fig. 13*c* is the expected result for detection mediated by second-site mechanisms (see Fig. 6*d*). Finally, Fig. 13*b* shows an intermediate case, with equal noise injected at the two sites. Here the result is intermediate between the two other cases.

This example lets us draw a number of important conclusions. First, the result in Fig. 13*a* shows explicitly how, in a two-stage visual system, threshold contours can reveal properties of the first-stage mechanism. The necessary condition is that the noise added before the transformation to the second stage be large enough to dominate the overall performance. When a situation like this holds, we say that the first stage represents the *site of limiting noise*. As long as subsequent processing does not add significant additional noise, it is the site of limiting noise whose properties will be reflected by threshold measurements. Although Fig. 13*a* shows an example where the cones were the site of limiting noise, the fact that detection contours often have the shape shown in Fig. 13*c* suggests that often the second site limits performance, and that subsequent processing at sites past the second site do not add significant additional noise. As an aside, we note that much of threshold psychophysics is concerned with arranging auxiliary stimulus manipulations that manipulate mechanism properties so as to move the site of limiting noise from one stage of processing to another, or to shift it across mechanisms within a stage (e.g., to change the relative contribution of L+M and L–M mechanisms to performance), with the goal of enabling psychophysical probing of individual mechanisms at different stages of processing. Generally, the stimulus manipulations are thought to

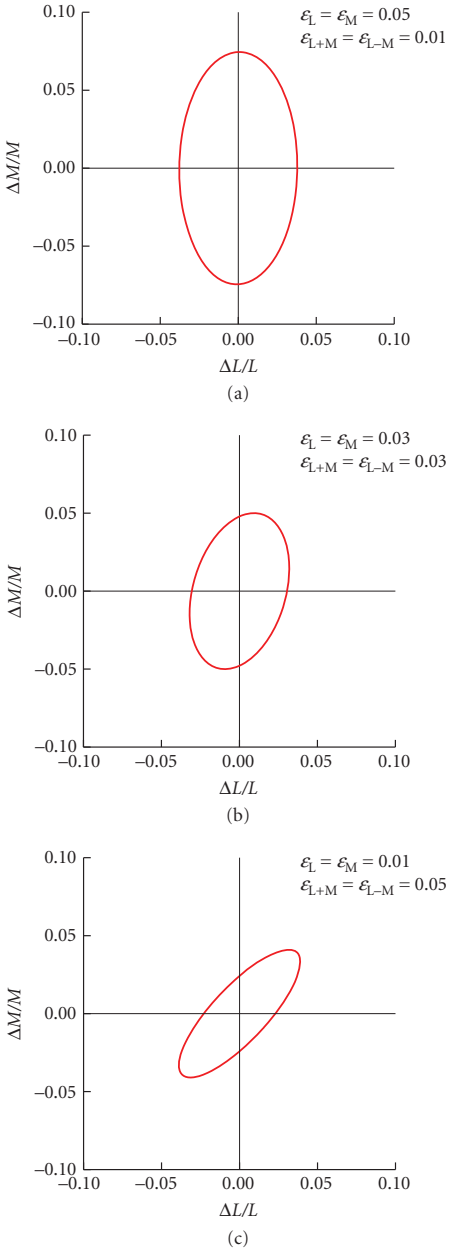


**FIGURE 13** Threshold predictions from signal detection theoretical model. The figure shows threshold contours predicted using the model shown in Fig. 12*b*, for various choices of noise amplitude. In all cases, only the L+M and L–M mechanisms were considered. The gain on L-cone contrast was set at 2, while the gain on M-cone contrast was set at 1. The gain of the L+M mechanism was set at 1, while that of the L–M mechanism was set at 4. The noise added at each site was assumed to be Gaussian, and for each test color direction and choice of noise magnitude, the test intensity that led to optimal classification performance of 75 percent was determined. (*a*) Resulting contour when the noise at the first site is five times that of the noise at the second site. In this case, the detection contour has the shape expected for the first-site mechanisms, because little additional information is lost at the second-site mechanisms. (*c*) Contour when the magnitude of the noise at the second site is five times that of the first. In this case, the properties of the second-site mechanisms dominate measured performance. (*b*) Contour when the noise at the two sites is of comparable magnitude, and here the result is itself intermediate between that expected from the properties of first- and second-site mechanisms.

act by changing the gains applied to mechanism outputs. This changes the effect of the stimulus relative to the noise, rather than the noise magnitude itself.

A second important point can be drawn from Fig. 13*b*. It is not unreasonable to think that noise at different stages of visual processing will be of a comparable magnitude, and Fig. 13*b* shows that in such cases observed performance will represent a mixture of effects that arise from mechanisms properties at different stages. This is a more formal development of a point we stressed in the introduction, namely, that in spite of our attempt to attribute performance under any given experimental conditions primarily to the action of a small number of mechanisms, this is likely to be a highly simplified account. Eventually, it seems likely that models that explicitly account for the interactions between mechanisms at different stages will be needed. The theory underlying the production of Fig. 13, which explicitly accounts for the role of noise at each stage, would be one interesting approach toward such models.

Finally, note that the development of Fig. 13 is in the tradition of ideal-observer models, where performance is derived from an explicit model of a set of stages of visual processing, followed by the assumption that further processing is optimal.[71–74] Although the assumption of optimal processing is unlikely to be exactly correct, ideal-observer models are useful because they can provide theoretical clarity and because cases where the data deviate from the predictions of such a model highlight phenomena that require further exploration and understanding. For example, the rounded shape of threshold contours, which we initially described using a descriptive vector length account, emerges naturally from the ideal-observer analysis. Indeed, for the ideal observer the predicted shape of the threshold contours is essentially ellipsoidal (summation exponent of 2). This prediction is another reason why careful assessment of the observed shape of threshold contours is of theoretical interest.

In subsection "Noise-Masking Experiments" in Sec. 11.5, we consider the effects of adding external noise to the system.

## 11.4 BASICS OF COLOR-APPEARANCE MECHANISMS

We now turn to consider how a different class of observations can inform us about mechanisms. These are measurements that assess not the observer's ability to detect or discriminate stimuli, but rather measurements of how stimuli look to observers. More specifically, we will consider measurements of color appearance.

As with threshold measurements, color-appearance measurements may be divided into two classes, those that assess the appearance of test stimuli as some function of those stimuli (test measurements) and those that assess how the color appearance of a test stimulus depends on the context in which it is viewed (field measurements). We review how both sorts of measurements can inform a model of color-appearance mechanisms. This treatment parallels our development for color-discrimination mechanisms in order to highlight similarities and differences between models that account for the two types of data.

### Appearance Test Measurements and Opponency

As described in the introduction, one of the earliest suggestions that the output of the cone mechanisms were recombined at a second site came from Hering's observation that certain pairs of color sensations (i.e., red and green, blue and yellow) are mutually exclusive. Hurvich and Jameson elaborated this observation into a psychophysical procedure known as hue cancellation (see subsection "Spectral Properties of Color-Opponent Mechanisms" in Sec. 11.5). Hue cancellation can be performed separately for the red/green opponent pair and the blue/yellow opponent pair.

In the red/green hue-cancellation experiment, the observer is presented with a test stimulus, which is usually monochromatic, and asked to judge whether its appearance is reddish or greenish. The results may be used to derive the properties of an opponent mechanism, under the "linking

hypothesis" that when the mechanism's response is of one sign the stimulus appears reddish, while when it is of the opposite sign the stimulus appears greenish. That is, color-appearance measurements are used to derive mechanism properties on the assumption that the mechanism output provides an explicit representation of the sensation experienced by the observer.

To understand the hue-cancellation procedure in more detail, imagine that the experimenter picks a fixed monochromatic reference light that in isolation appears greenish to the observer. The experimenter then chooses a series of monochromatic test lights of unit intensity, each of which appears reddish in isolation. The observer judges mixtures of each test light and the reference light. If the mixture appears reddish, the intensity of the greenish reference light is increased. If the mixture appears greenish, the intensity of the greenish reference light is decreased. Repeating this procedure allows the experimental determination of a balance or equilibrium point for the red-green mechanism, where the result of the mixture appears neither reddish nor greenish. (Depending on the test stimulus, the balanced mixture will appear either as yellow or blue or achromatic.) Colored stimuli that appear neither reddish nor greenish are referred to as "unique yellow" or "unique blue." The intensity of the green reference light in the balanced mixture may be taken as a measure of the amount of redness in the test stimulus, in the same way that the amount of weight added to one side of a balance scale indexes the weight on the other side when the balance is even (see Krantz's "force table" analogy.[75])

A similar procedure may be used to determine the amount of greenness in test stimuli that have a greenish component, by choosing an adjustable reference stimulus that appears reddish. Moreover, the units of redness and greenness may be equated by balancing the two reference stimuli against each other. Figure 14*a* and *b* show prototypical results of such measurements for spectral test lights, as well as results for an analogous procedure used to determine the amount of blueness and yellowness in the same set of spectral test lights. Such data are referred to as "chromatic valence" data.

Krantz[75,76] showed that if the amount of redness, greenness, blueness, and yellowness in any test light is represented by the output of two opponent color-appearance mechanisms, and if these mechanisms combine cone signals linearly, then the spectral hue-valence functions measured in the cancellation experiment must be a linear transformation of the cone spectral sensitivities. Although the linearity assumption is at best an approximation (see subsection "Linearity of Color-Opponent Mechanisms" in Sec. 11.5), Krantz's theorem allows derivation of the cone inputs from the data shown in Fig. 14. Such fits are shown in Fig. 14*a* and *b*, and lead to the basic wiring diagram shown in Fig. 14*c*. This shows two opponent color-appearance mechanisms, labeled R/G and B/Y. The cone inputs to these mechanisms are similar to those for the opponent color-discrimination mechanisms, with one striking difference: the S cones make a strong R contribution to the R/G appearance mechanism. By contrast, the S-cone input to the L–M discrimination mechanism is small at most. Another difference, which we address later, is that the M-cone contribution to B/Y in some models is of the same sign as the S-cone contribution (see "Three-Stage Zone Models" in Sec. 11.6).

Although the hue-cancellation procedure may be used to derive properties of opponent-appearance mechanisms, it is less suited to deriving the properties of a third mechanism that signals the brightness of colored stimuli. This aspect of color appearance may be assessed using heterochromatic brightness matching, where subjects are asked to equate the brightness of two stimuli, or scaling methods, where observers are asked to directly rate how bright test stimuli appear (see subsection "Luminance and Brightness" in Sec. 11.5).

## Appearance Field Measurements and First-Site Adaptation

It is also possible to make field measurements using appearance judgments. A common method is known as asymmetric matching, which is a simple extension of the basic color-matching experiment (see Chap. 10). In the basic color-matching experiment, the observer adjusts a match stimulus to have the same appearance as a test stimulus when both are seen side-by-side in the same context. The asymmetric matching experiment adds one additional variable, namely that the test and match are each seen in separate contexts. As illustrated in Fig. 1, when an identical test patch is presented

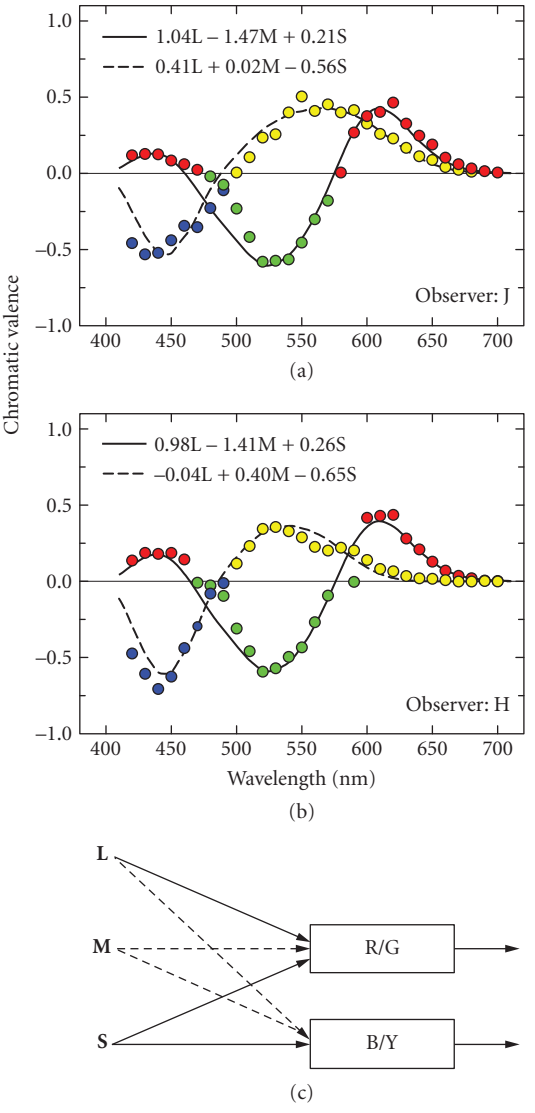


**FIGURE 14** Chromatic valence data and wiring. (*a*) and (*b*) Valence data (colored symbols) replotted from Figs. 4 and 5 of Jameson and Huryich[279] for observers "J" (*a*) and "H" (*b*) fitted with linear combinations of the Stockman and Sharpe[28] cone fundamentals (solid and dashed curves). The best-fitting cone weights are noted in the key. (*c*) Wiring suggested by this (*a*) and subsequent color valence data. In the diagram, the sign of the M-cone contribution to B/Y is shown as negative (see subsection "Spectral Properties of Color-Opponent Mechanisms" in Sec. 11.5).

against two different surrounds, it can appear quite different. In the asymmetric matching experiment, the observer compares test patches seen in two different contexts (e.g., against different adapting backgrounds) and adjusts one of them until it matches the other in appearance. The cone coordinates of the match test patches typically differ, with the shift being a measure of the effect of changing from one context to the other.

Figure 15*a* plots asymmetric matching data from an experiment of this sort reported by MacAdam.[77] The filled circles show the L- and S-cone coordinates of a set of test stimuli, seen in a region of the retina adapted to a background with the chromaticity of a typical daylight. The open circles show a subset of the corresponding asymmetric matches seen in a region of the retina adapted to a typical tungsten illuminant. The change in adapting background produces a change in test appearance, which observers have compensated for in their adjustments.

Asymmetric matching data can be used to test models of adaptation. For example, one can ask whether simple gain control together with subtractive adaptation applied to the cone signals can account for the matches. Let $(L_1, M_1, S_1)$, $(L_2,M_2,S_2)$, . . ., $(L_N,M_N,S_N)$ represent the L-, M-, and S-cone coordinates of $N$ test stimuli seen in one context. Similarly, let $(L'_1,M'_1,S'_1)$, $(L'_2,M'_2,S'_2)$, . . ., $(L'_N,M'_N,S'_N)$ represent the cone coordinates of the matches set in the other context. If the data can be accounted for by cone-specific gain control together with subtractive adaptation, then we should be able to find gains $g_L$, $g_M$, $g_S$, and subtractive terms $L_0$, $M_0$, $S_0$ such that $L'_i \approx g_L L_i - L_0$, $M'_i \approx g_M M_i - M_0$, and $S'_i \approx g_S S_i - S_0$ for all of the $N$ matches. The asterisks plotted in Fig. 15*a* show predictions of this gain control model in the L,-S cone plane. Figure 15*b*, *c*, and *d* show predicted shifts against the measured shifts for all three cone classes. The model captures the broad trends in the data, although it misses some of the detail. The first-site adaptation captured by this model is often taken to be the same adaptation revealed by sensitivity experiments.[78]

## Appearance Field Measurements and Second-Site Adaptation

Asymmetric matching may also be used to investigate the effect of contrast adaptation on color appearance. In a series of experiments, Webster and Mollon[32,79] investigated the effect of contrast adaptation (or habituation) on the color appearance of suprathreshold lights (see also Refs. 80 and 81). Observers habituated to a background field that was sinusoidally modulated at 1 Hz along various color directions. The habituating field was interleaved with a stimulus presented at the same location. The observer's task was to adjust the chromaticity and luminance of a match stimulus so that its appearance matched that of the test field. Webster and Mollon found that habituation affected the appearance of the test stimulus.

The motivation behind these experiments was to test whether or not the changes in color appearance caused by contrast adaptation were consistent with the type of second-site adaptation that characterizes sensitivity experiments, namely independent adaptation of three cardinal mechanisms with cone inputs: L–M, L+M, and S–(L+M). The prediction for this case is that the appearance effects should always be greatest along the color axis corresponding to the mechanism most adapted by the habituating stimulus, and least along the axis corresponding to the mechanism least adapted by the stimulus—and this pattern should be found whatever the chromatic axis of the habituating stimulus. Thus the *relative* changes in chromaticity and/or luminance caused by habituation should be roughly elliptical with axes aligned with the mechanism axes.

The results showed that the sensitivity changes did not consistently align with the axes of the cardinal mechanisms. Instead, the largest selective sensitivity losses in the equiluminant plane, for two out of three subjects, aligned with the adapting axis, while the smallest losses aligned with an axis approximately 90° away. Comparable results were found when the habituating and test stimuli varied in color and luminance in either the plane including the L−M and L+M+S axes or the plane including the S and L+M+S axes. Thus, contrast adaptation produces changes in color appearance that are, in general, selective for the habituating axis rather than selective for the purported underlying mechanism axes. Nevertheless, greater selectivity was found for habituation along the three cardinal axes, which suggests their importance. See Ref. 32 for further details.

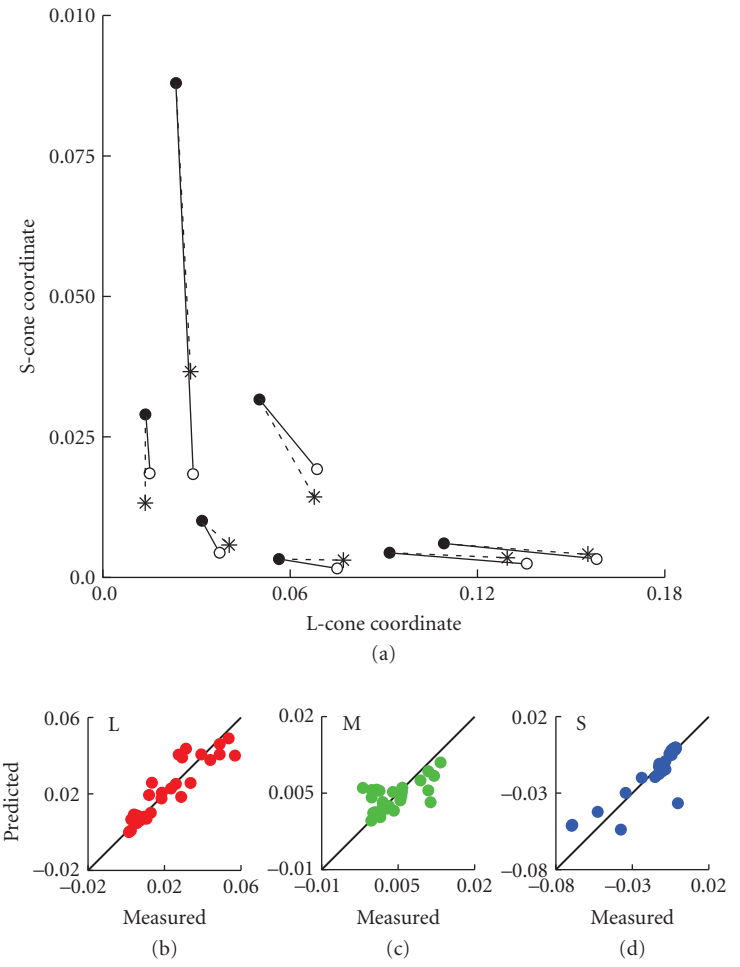


**FIGURE 15** Analysis of asymmetric matching data. (*a*) Subset of the data from Observer DLM reported by MacAdam.[77] The closed circles show L- and S-cone coordinates of tests viewed on part of the retina adapted to a background with the chromaticity of daylight. The connected open circles show the asymmetric matches to these tests, when the matching stimulus was viewed on part of the retina adapted to the chromaticity of a tungsten illuminant. The star symbols show the predictions of a model that supposes first-site gain control and subtractive adaptation, operating separately within each cone mechanism. (*b*), (*c*), and (*d*) Model predictions for the full set of 29 matches set by Observer DLM. Each panel shows data for one cone class. The *x* axis shows the measured difference between the test and match, and represents the size of the asymmetric matching effect. The *y* axis shows the corresponding predicted difference. If the model were perfect, all of the data would lie along the positive diagonals. The model captures the broad trend of the data, but misses in detail.

Webster and Mollon[32] conclude that the changes in color appearance following habituation are inconsistent with models of color vision that assume adaptation in just three independent postreceptoral channels. Given, however, that the properties of the color-appearance mechanisms as revealed by test methods differ from those of color-discrimination mechanisms, this result is hardly surprising. Also note that comparisons between sensitivity measurements made for test stimuli near detection threshold and appearance measurements made for suprathreshold tests are complicated by the presence of response nonlinearities at various stages of processing. See Refs. 78 and 82 for discussion.

## 11.5 DETAILS AND LIMITS OF THE BASIC MODEL

Sections 11.3 and 11.4 introduce what we will refer to as a "basic model" of color-discrimination and color-appearance mechanisms. There is general agreement that the components incorporated in this model are correct in broad outline. These are (1) first-site, cone specific, adaptation roughly in accord with Weber's law for signals of low temporal frequency, (2) a recombination of cone signals that accounts for opponent and nonopponent postreceptoral second-site signals, (3) second-site desensitization and habituation, and (4) the necessity for distinct mechanistic accounts of discrimination and appearance.

In the earlier sections, we highlighted example data that strongly suggest each feature of the basic model. Not surprisingly, those data represent a small subset of the available experimental evidence brought to bear on the nature of postreceptoral color vision. In this section we provide a more detailed review, with the goal of highlighting both data accounted for by the basic model, as well as data that expose the model's limitations. Current research in the mechanistic tradition is aimed at understanding how we should elaborate the basic model to account parsimoniously for a wider range of phenomena, and at the end of this chapter we outline approaches being taken toward this end.

Sections "Test Sensitivities" through "Color Appearance and Color Opponency" follow the same basic organization as the introductory sections. We consider discrimination and appearance data separately, and distinguish between test and field methods. We begin, however, with a discussion of color data representations.

### Color Data Representations

Over the past 50 years, color vision research has been driven in part by the available technology. Conventional optical systems with spectral lights and mechanical shutters largely restricted the volume of color space that could be easily investigated to the 1/8 volume containing positive, incremental cone modulations. When such data are obtained as a function of the wavelength of monochromatic stimuli, a natural stimulus representation is to plot the results as a function of wavelength (e.g., Fig. 14*a* and *b*). This representation, however, does not take advantage of our understanding of the first stage of color processing, transduction of light by the cone photoreceptors. Moreover, with the availability of color monitors and other three-primary devices, stimuli are now routinely generated as a combination of primaries, which makes increments, decrements, and mixtures readily available for experimentation. Spectral plots are not appropriate for such stimuli, which instead are represented within some tristimulus space (see Chap. 10).

Our estimates of the human cone spectral sensitivities have become increasingly secure over the past 30 years (see Chap. 10). This allows stimulus representations that explicitly represent the stimulus in terms of the L-, M-, and S-cone excitations and which therefore connect data quite directly to the first-stage color mechanisms. Such representations are called "cone-excitation spaces," and an example of this sort of representation is provided in Fig. 7 of Chap. 10.

An extension of cone-excitation space is one in which the cone excitations are converted to increments and decrements of each cone type relative to a background. Thus, the three axes are the changes in cone excitations: $\pm\Delta L$, $\pm\Delta M$, and $\pm\Delta S$. We introduced such spaces in Fig. 6; they are useful when

the stimulus is most naturally conceived as a modulation relative to a background, and where the properties of the background per se are of less interest. We will use the shorthand "incremental cone spaces" to refer to this type of representation, although clearly they allow expression of both increments and decrements.

Closely related to incremental cone spaces are "cone contrast spaces," in which the incremental/decremental changes in cone excitations produced by the target are divided by the cone excitations produced by the background.[61,83] Here, the three axes are dimensionless cone contrasts: $\Delta L/L_b$, $\Delta M/M_b$, and $\Delta S/S_b$. If Weber's law holds independently for each cone type then $\Delta L/L_b$, $\Delta M/M_b$, and $\Delta S/S_b$ all remain constant. Thus a particular advantage of this space is that it factors out the gross effects of first-site cone-specific adaptation, which tends to follow Weber's law at higher intensities (see subsection "First-Site Adaptation" in Sec. 11.3). Plots in cone contrast space help to emphasize desensitization that occurs after the receptors, and, to the extent that Weber's law holds, provide an explicit representation of the inputs to postreceptoral mechanisms. (We introduced a cone contrast representation in Fig. 8 exactly for this reason.)

At lower adaptation levels, when adaptation falls short of Weber's law (see Fig. 7) or under conditions where Weber's law does not hold (such as at high spatial and temporal frequencies; see, e.g., Ref. 84), cone contrast space is less useful. However, for targets of low temporal and spatial frequencies, Weber's law has been found to hold for chromatic detection down to low photopic levels.[62]

A final widely used color space is known as the "Derrington-Krauskopf-Lennie" (DKL) space[36,85,86] in which the coordinates represent the purported responses of the three second-site color-discrimination mechanism, L+M, L–M, and S–(L+M). In this context, modulation directions that change the response of one of these mechanisms while leaving the response of the other two fixed are referred to as "cardinal directions."[14] The DKL representation was introduced in Fig. 11 and is further illustrated in Fig. 16. See Ref. 87 for further discussion of color spaces and considerations of when each is most appropriately used.

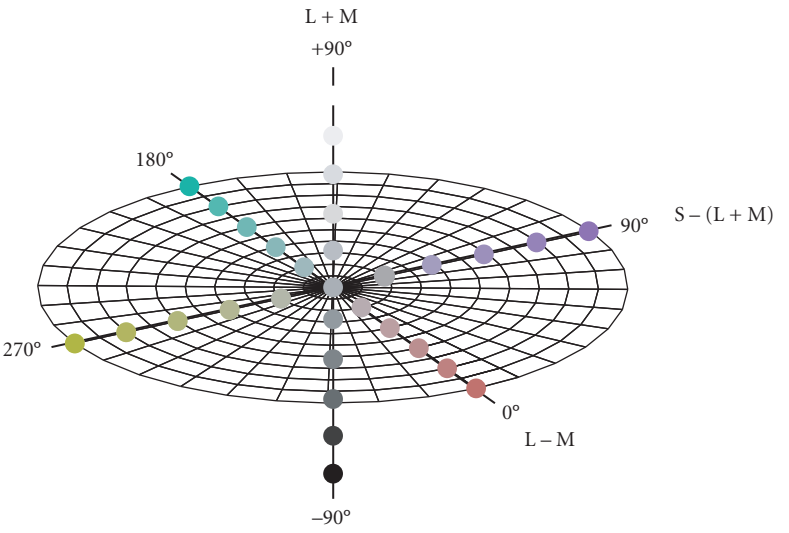


**FIGURE 16** Derrington-Krauskopf-Lennie (DKL) color space. The grid corresponds to the equiluminant plane, which includes the L–M (0°–180°) and S–(L+M) (90°–270°) cardinal mechanisms axes. The vertical axis is the achromatic L+M axis (–90° – +90°). The colors along each axis are approximate representations of the appearances of lights modulated along each cardinal axis from an achromatic gray at the center. Notice that the unique hues do not appear. The axes are labeled according to the mechanisms that are assumed to be uniquely excited by modulations along each cardinal axis. (*Figure provided by Caterina Ripamonti.*)

Although the conceptual ideas underlying the various color spaces discussed here are clear enough, confusion often arises when one tries to use one color space to represent constructs from another. The confusion arises because there are two distinct ways to interpret the axes of a three-dimensional color space. The first is in terms of the responses of three specified mechanisms, while the second is in terms of how the stimulus is decomposed in terms of the modulation directions that isolate the three mechanisms. To understand why these are different, note that to compute the response of a particular mechanism, one only needs to know its properties (e.g., that it is an L–M mechanism). But, in contrast, the stimulus direction that isolates that same mechanism is the one that silences the responses of the other two mechanisms. The isolating stimulus direction depends not on the properties of the mechanism being isolated but on those of the other two. For this reason, it is important to distinguish between the *mechanism direction*, which is the stimulus direction that elicits the maximum positive response of a given mechanism per unit intensity, and the *isolating direction* for the same mechanism, which produces no response in the other two mechanisms. For the triplet of mechanisms L+M, L–M, and S–(L+M), the mechanism and isolating directions align (by definition) in DKL space, but this property does not hold when these directions are plotted in the antecedent incremental cone space or cone contrast space. Note that in some descriptions of DKL space, the axes are defined in terms of the cone modulations that isolate mechanisms rather than in terms of the mechanism responses. These conflicting definitions of DKL space have led to a good deal of confusion. See Chap. 10 and Refs. 87–89 for further discussion of transformations between color spaces and the relation between mechanism sensitivities, mechanism directions, and isolating directions.

***Caveats*** Crucial for the use of any color space based on the cone mechanisms either for generating visual stimuli or for interpreting the resulting data is that the underlying cone spectral sensitivities are correct. Our estimates of these are now secure enough for many applications, but there are uncertainties that may matter for some applications, particularly at short wavelengths. These are compounded by individual differences (see Chap. 10), as well as issues with some of the sets of color-matching functions used to derive particular estimates of cone spectral sensitivities (again see Chap. 10, and also Ref. 90 for further discussion).

Such concerns are magnified in the use of postreceptoral spaces like the DKL space, because as well as the cone spectral sensitivities needing to be correct, the rules by which they are combined to produce the spectral sensitivities of the postreceptoral mechanisms must also be correct. For example, to silence the L+M luminance mechanism it is necessary to specify exactly the relative weights of the M and L cones to this mechanism. However, these weights are uncertain. As discussed in subsection "Luminance" in Sec. 11.5, the M- and L-cone weights show large individual differences. Furthermore, the assumption typically used in practice, when constructing the DKL space, is that luminance is a weighted sum of M and L cones and that the S cones therefore do not contribute to luminance. This may not always be the case.[91–94] Luminous efficiency also varies with chromatic adaptation, the spatial and temporal properties of the stimulus, and the experimental task used to define luminous efficiency. Lastly, the standard 1924 CIE $V(\lambda)$ luminous efficiency function, which determines candelas/m$^2$, and has been used by several groups to define the spectral sensitivity of the luminance mechanism, seriously underestimates luminous efficiency at shorter wavelengths (see Ref. 90).

One final note of caution is that it is useful to keep in mind that independently representing and manipulating the responses of mechanisms at a particular stage of visual processing only makes sense if there are three or fewer mechanisms. If there are more than three photopic mechanisms at the second stage of color processing (see also subsection "Low-Level and Higher-Order Color-Discrimination Mechanisms" in Sec. 11.6), independently manipulating all of them is not possible because of the inherent three-dimensionality of the first stage.

These caveats are not meant to discourage entirely the use of physiologically motivated color spaces for data representation; on the contrary we believe such representations offer important advantages if used judiciously. It is crucial, however, to bear in mind that such spaces usually assume particular theories of processing, and that interpreting data represented within them should be done in the context of a clear understanding of the limitations of the corresponding theories.

## Test Sensitivities

The most direct method of studying the chromatic properties of color mechanisms is the test method. Variations of this method have been tailored to investigate the properties of different visual mechanisms, including cone, chromatic, and achromatic (or luminance) mechanisms.

*Sensitivity to Spectral Lights* Perhaps the most influential chromatic detection data have been the two-color threshold data of Stiles,[41,42,95–98] so called because the threshold for detecting a target or test field of one wavelength is measured on a larger adapting or background field usually of a second wavelength (or mixture of wavelengths). These data were collected within the context of an explicit model of color mechanisms, referred to as "$\pi$-mechanisms," and how they adapt. Enoch[99] provides a concise review of Stiles' work.

An important limitation of Stiles' model is that it did not allow for opponency: the $\pi$-mechanisms had all-positive spectral sensitivities and interactions between them were required to be summative. In some instances, the deviations caused by opponency were accommodated in Stiles' model by the postulation of new $\pi$-mechanisms, such as $\pi_5'$ (see Refs. 54 and 55). As data in the two-color tradition accumulated, this limitation led to the demise of the $\pi$-mechanism framework and the development of the basic model we introduced in Sec. 11.3. Nonetheless, any correct model must be consistent with the experimental data provided by the two-color threshold technique, and we review some key aspects in the context of current thinking.

Two-color threshold test spectral sensitivity measurements obtained on steady backgrounds as a function of target wavelength have characteristic peaks and troughs that depend on the background wavelength (see Fig. 1 of Ref. 98). These undulations were interpreted as the envelope of the spectral sensitivities of the underlying cone mechanisms (or "$\pi$-mechanisms," see Fig. 23), but crucially they are now known also to reflect opponent interactions between mechanisms.[100]

The shape of test spectral sensitivity functions depend not only on background wavelength but also on the type of target used in the detection task. Detection by second-site opponent color-discrimination mechanisms is generally favored by targets comprised mainly of low temporal and spatial frequency components, whereas detection by achromatic mechanisms, which sum cone signals, is favored by targets with higher temporal and spatial frequency components.[83,101,102] Stiles typically used a flashed target of 1° in visual diameter and 200 ms in duration, which favors detection by chromatic mechanisms. When Stiles' two-color threshold experiments are carried out using brief, 10-ms duration targets, the results are more consistent with detection being mediated by achromatic mechanisms.[103]

Detection by chromatically opponent mechanisms is most evident in test spectral sensitivity functions measured using targets of low temporal and/or spatial frequency. Measured on neutral fields, chromatic detection is characterized by peaks in the spectral sensitivity curves at approximately 440, 530, and 610 nm that are broader than the underlying cone spectral sensitivity functions and separated by pronounced notches.[102,104–108] The so-called "Sloan notch"[109] corresponds to the loss of sensitivity when the target wavelength is such that the target produces no chromatic signal (e.g., when the L- and M-cone inputs to the L−M chromatic mechanism are equal), so that detection is mediated instead by the less-sensitive achromatic mechanism. By contrast, the broad peaks correspond to target wavelengths at which the target produces a large chromatic signal.[101,102,105–108,110,111] Examples of detection spectral sensitivities with strong contributions from opponent mechanisms are shown in Fig. 17*a* and Fig. 18*a*. Those shown as circles in Fig. 17 and Fig. 18 were measured on a white background. The other functions in Fig. 17 were measured on backgrounds of 560 nm (green squares), 580 nm (yellow triangles), and 600 nm (orange triangles).

The nature of the mechanisms responsible for the spectral sensitivity data in Fig. 17*a* can be seen clearly by replotting the data as cone contrasts, as illustrated in Fig. 17*b* for the three chromatic backgrounds (from Ref. 89). As indicated by the straight lines fitted to each set of data, the detection contours have slopes close to one in cone contrast space, which is consistent with detection by L–M chromatic mechanisms with equal cone contrast weights (see subsection "Sensitivity to Different Directions of Color Space" in Sec. 11.5). Note also that the contours move outward with increasing field wavelength. This is consistent with second-site desensitization (see Fig. 8). The dependence

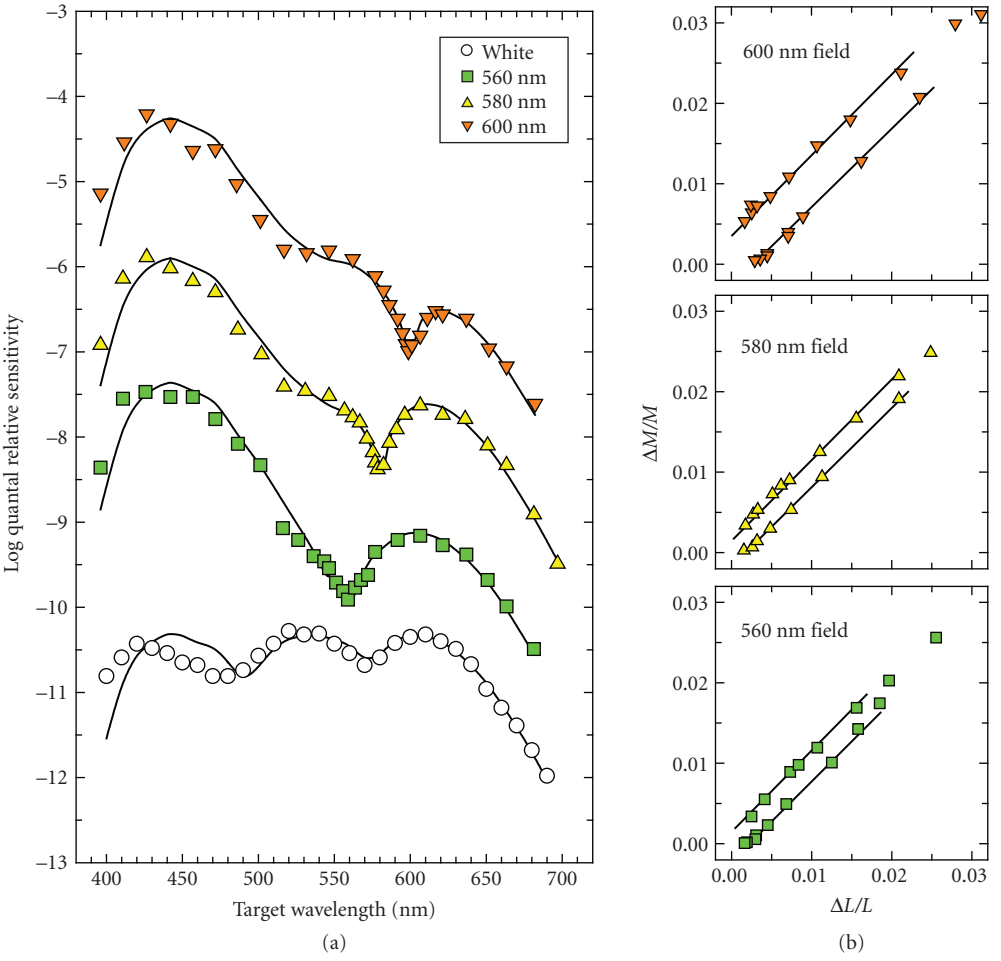


**FIGURE 17** Sloan notch and chromatic adaptation. The three data sets in (*a*) are spectral sensitivity data replotted from Fig. 1 of Thornton and Pugh[107] measured on $10^{10}$ quanta $sec^{-1}$ $deg^{-2}$ fields of 560 nm (green squares), 580 nm (yellow triangles), and 600 nm (orange inverted triangles) using a long duration (one period of a 2-Hz cosine), large (3° diameter, Gaussian-windowed) target. The lowest data set in (*a*) are data replotted from Fig. 4 (Observer JS) of Sperling and Harwerth[105] measured on 10,000 td, 5500 K, white field (open circles) using a 50-ms duration, 45-min diameter target. The data have been modeled (solid lines) by assuming that the spectral sensitivities can be described by $b|aL - M| + c|M - aL| + d|S - e(L + 0.5M)|$, where L, M, and S are the quantal cone fundamentals[28] normalized to unity peak, and $a$–$e$ are the best-fitting scaling factors. These fits are comparable to the ones originally carried out by Thornton and Pugh[107] using different cone fundamentals. Notice that the Sloan notch (on colored backgrounds) coincides with the field wavelength. The detection contours in (*b*) have been replotted from Fig. 18.4B of Eskew, McLellan, and Giulianini.[89] The data are the spectral sensitivities measured on 560 nm (green squares), 580 nm (yellow triangles), and 600 nm (orange inverted triangles) fields already shown in (*a*), but transformed and plotted in cone-contrast space. Only data for target wavelengths ≥ 520 nm are shown. As indicated by the straight lines fitted to each set of data, the detection contours have slopes close to one in cone contrast space, which is consistent with detection by L–M chromatic mechanisms with equal L- and M-cone contrast weights.

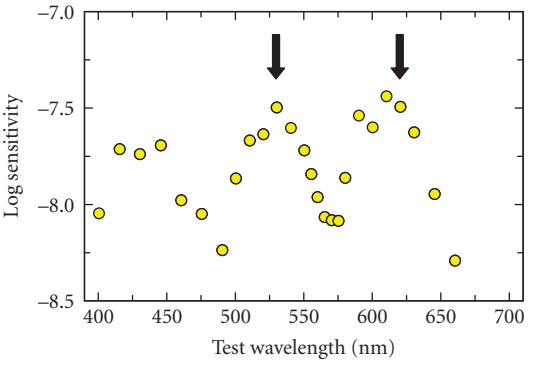


(a)

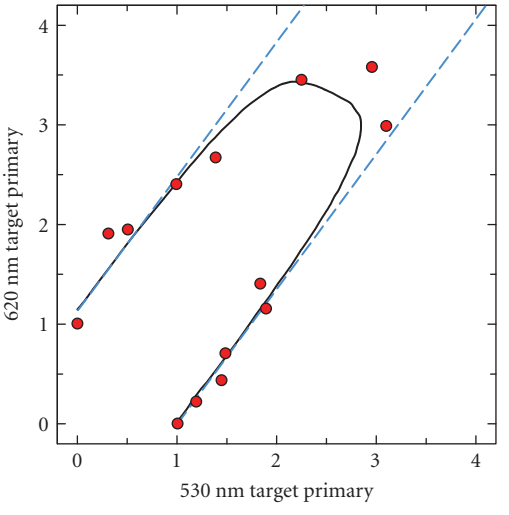


(b)

**FIGURE 18** Test additivity. (*a*) Spectral sensitivity for the detection of a low frequency target measured on a 6000 td xenon (white) background (yellow circles). The shape is characteristic of detection by chromatic channels. The arrows indicate the wavelengths of the two primaries used in the test additivity experiment shown in (*b*). (*b*) Detection thresholds measured on the same field for different ratios of the two primaries. Data and model fits replotted from Fig. 2 of Thornton and Pugh.[164] The solid curve is the fit of a multi-mechanism model comprising an achromatic (L+M) and chromatic mechanisms (L–M and M–L with the same but opposite weights). The sensitivities of the chromatic mechanisms are shown by the dashed blue line. (See Ref. 164 for details.)

of the spectral position of the Sloan notch on background wavelength is discussed in subsection "Chromatic Adaptation and the Sloan Notch" in Sec. 11.5.

### *Luminance*

*Luminous efficiency* The target parameters (and the experimental task) can also be chosen to favor detection by achromatic mechanisms. For example, changing the target parameters from a 200-ms duration, 1° diameter flash to a 10 ms, 0.05° diameter flash presented on a white background changes the spectral sensitivity from a chromatic one to an achromatic one, with chromatic peaks at approximately 530- and 610-nm merging to form a broad peak near 555 nm.[102] Measurements that favor detection by achromatic mechanisms have been carried out frequently in the applied field of photometry as a means of estimating scotopic (rod), mesopic (rod-cone), or photopic (cone) "luminous efficiency" functions.

Luminous efficiency was introduced by the CIE (Commission Internationale de l'Éclairage) to provide a perceptual analog of radiance that could be used to estimate the visual effectiveness of lights. The measurement of luminous efficiency using tasks that favor achromatic detection is a practical solution to the requirement that luminous efficiency should be additive. Additivity, also known as obedience to Abney's law,[112,113] is necessary in order for the luminous efficiency of a light of arbitrary spectral complexity to be predictable from the luminous efficiency function for spectral lights, $V(\lambda)$.

Some of the earlier luminous efficiency measurements[114–117] incorporated into the original 1924 CIE photopic luminous efficiency function, $V(\lambda)$, used techniques that are now known to fail the additivity requirement. Techniques that satisfy the additivity requirement, and depend mainly on achromatic or luminance mechanisms, include heterochromatic flicker photometry (HFP), heterochromatic modulation photometry (HMP), minimally distinct border (MDB), and minimum motion (MM). Details of these techniques can be found in several papers.[28,53,90,118–124]

In visual science, $V(\lambda)$ or its variants, has often been assumed to correspond to the spectral sensitivity of the human postreceptoral achromatic or "luminance" mechanism, which is assumed to add positively weighted inputs from the L and M cones.[125] As a result, estimates of luminous efficiency have taken on an important theoretical role in studies of the opponent mechanisms, because they are used to produce stimulus modulations that produce no change in the purported luminance mechanism. In this context, the $V(\lambda)$ standard is often overinterpreted, since it obscures a number of factors that affect actual measurements of luminous efficiency. These include (1) the strong dependence of luminous efficiency on the mean state of chromatic adaptation (see subsection "Achromatic Detection and Chromatic Adaptation" in Sec. 11.5), (2) the sizeable individual differences in luminous efficiency that can occur between observers (see below), and (3) the fact that luminous efficiency is affected both by the spatial properties of the target, as well by where on the retina it is measured.

A more fundamental problem is that the CIE photopic 1924 $V(\lambda)$ function seriously underestimates luminous efficiency at short wavelengths, because of errors made in its derivation. Consequently, $V(\lambda)$ is seldom used in visual science, except for the derivation of troland values (with the result that luminance is often underestimated at short wavelengths). Attempts to improve $V(\lambda)$[126,127] have been less than satisfactory,[28,90] but are continuing in the form of a new estimate referred to as $V^*(\lambda)$.[128,129] The $V^*(\lambda)$ (green line) and the CIE 1924 $V(\lambda)$ (green circles) luminous efficiency functions for centrally viewed fields of 2° in visual diameter, and the $V_{10}{}^*(\lambda)$ (orange line) and the CIE 1964 $V_{10}(\lambda)$ (orange squares) luminous efficiency functions for centrally viewed fields of 10° in visual diameter can be compared in Fig. 19. The functions differ mainly at short wavelengths. The $V^*(\lambda)$ and $V_{10}{}^*(\lambda)$ functions have been recommended by the CIE for use in "physiologically relevant" colorimetric and photometric systems.[130]

In general, luminous efficiency functions can be approximated by a linear combination of the L-cone $[\bar{l}(\lambda)]$ and M-cone $[\bar{m}(\lambda)]$ spectral sensitivities, thus: $V(\lambda)=a\bar{l}(\lambda)+\bar{m}(\lambda)$, where $a$ is the L-cone weight relative to the M-cone weight. Luminous efficiency shows sizeable individual differences even after individual differences in macular and lens pigmentation have been taken into account. For example, under neutral adaptation, such as daylight D65 adaptation, the L-cone weight in a group of 40 subjects, in whom 25-Hz HFP spectral sensitivity data were measured on a 3 log td white D65 background, varied from 0.56 to 17.75, while the mean HFP data were consistent with an L-cone weight of 1.89.[128,129]

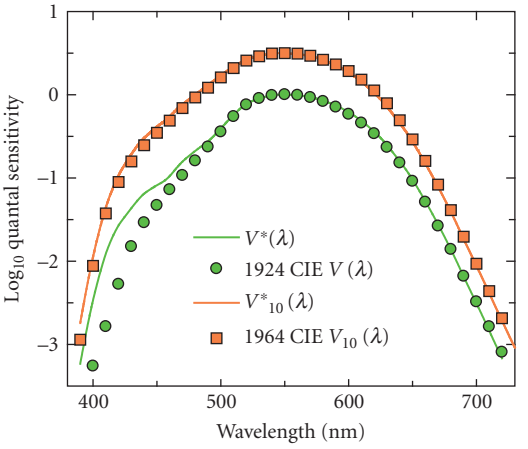


**FIGURE 19** Luminous efficiency functions for 2° and 10° central viewing conditions. The lower pair of curves compare the CIE 1924 2° $V(\lambda)$ function (green circles) with the 2° $V^*(\lambda)$ function[128,129] (green line). The upper pair of curves compare the CIE 1964 10° $V_{10}(\lambda)$ function (orange squares) with the 10° $V^*(\lambda)$ function (orange line). The main discrepancies are found at short wavelengths.

*Cone numerosity* On the assumption that the variation in L:M cone contribution to luminous efficiency is directly related to the variation in the ratio of L:M cone numbers in the retina, several investigators have used luminous efficiency measurements to estimate relative L:M cone numerosity.[125,131–141] It is important to note, however, that luminous efficiency depends on factors other than relative L:M cone number, and is affected, in particular, by both first-site and second-site adaptation.[63,64,142] Indeed, the L:M contribution to luminous efficiency could in principle have little or nothing to do with the relative numbers of L and M cones, but instead reflect the relative L- and M-cone contrast gains set in a manner independent of cone number. Such an extreme view seems unlikely to hold, however. Population estimates of relative L:M cone numerosity obtained using luminous efficiency, correlate reasonably well with estimates obtained using direct imaging,[30] flicker ERG,[143,144] and other methods.[134,137–139,145–148] More precise delineation of the relation between luminous efficiency and relative L:M cone numerosity awaits further investigation. Note that an important piece of this enterprise is to incorporate measurements of individual variation in L- and M-cone spectral sensitivity.[128,144,146]

*Multiple luminance signals* As developed later in subsection "Multiplexing Chromatic and Achromatic Signals" in Sec. 11.5, cone-opponent, center-surround mechanisms that are also spatially opponent, such as parvocellular or P-cells, encode not only chromatic information, but also luminance information (see Fig. 38). The fact that P-cells transmit a luminance signal suggests that there may be two distinct "luminance" signals at the physiological level: one generated by P-cells and another by magnocellular or M-cells, a possibility which has been discussed in several papers by Ingling and his coworkers.[149–152] The need for a P-cell-based luminance system is also suggested by the fact that the retinal distribution of M-cells is too coarse to support the observed psychophysical spatial acuity for luminance patterns[153] (but see Ref. 154). Others have also suggested that multiple mechanisms might underlie luminance spectral sensitivity functions.[124]

Luminance mechanisms based on M-cell and P-cells should have different spatial and temporal properties. Specifically, the mechanism more dependent on M-cell activity, which we refer to as $(L+M)_M$, should be more sensitive to high temporal frequencies, whereas the mechanism more dependent on

P-cell activity, which we refer to as $(L+M)_P$, should be more sensitive to high spatial frequencies. If, as has been suggested,[149–152] $(L+M)_P$ is multiplexed with L–M, we might also expect the interactions between $(L+M)_P$ and L–M to be different from those between $(L+M)_M$ and L–M. Similarly, chromatic noise may have a greater effect on $(L+M)_P$ than on $(L+M)_M$. Note, however, that if the stimulus temporal frequency is high enough for the spatially opponent surround to become synergistic with the center (i.e., when the surround delay is half of the flicker period), the P-cell will, in principle, become sensitive to any low spatial frequency luminance components of the stimulus.[151,155]

Psychophysical evidence for multiple luminance mechanisms is relatively sparse. Given the likely difference in the M- and L-cone weights into $(L+M)_M$, the conventional luminance mechanism, and into L-M, the chromatic mechanism [from which $(L+M)_P$ is assumed to derive], the spectral sensitivities for spatial acuity tasks, which favor $(L+M)_P$, and for flicker tasks, which favor $(L+M)_M$, should be different. However, little difference in spectral sensitivity is actually found.[122,156–158] Ingling and Tsou[152] speculate that this similarity is found despite there being different luminance mechanisms, because the spatial acuity task may depend on P-cell centers rather than on centers and surrounds. Averaged over many cells, the P-cell *center* spectral sensitivity may be similar to the M-cell sensitivity, particularly if the latter depends on relative cone numerosity (see previous subsection).

Webster and Mollon[17] looked at the effect of correlated chromatic and luminance contrast adaptation on four different measures of "luminous efficiency." They found that lightness settings and minimum-motion settings for 1-Hz counter-phase gratings were strongly biased by contrast adaptation, but that flicker settings and minimum-motion settings for 15-Hz counter-phase gratings were unaffected. On the face of it, these results are consistent with the idea that different luminance mechanisms mediate low- and high-temporal frequency tasks.

We speculate that some of the discrepancies found between the detection contours measured in the L,M plane might be related to detection being mediated by different luminance mechanisms under different conditions. Conditions chosen to favor the conventional luminance channel (e.g., the presence of chromatic noise and/or the use of targets of high temporal frequency) are likely to favor detection by $(L+M)_M$. Perhaps, under these conditions the $(L+M)_M$ luminance contours appear as distinct segments, because there is relatively little threshold summation with L–M (e.g., $k = 4$). Examples of such segments are shown by the dashed lines in Fig. 20*c*. Conditions *not* specially chosen to favor the conventional luminance channel (e.g., the use of targets of high spatial and/or low temporal frequencies) may favor instead detection by $(L+M)_P$. Perhaps, under these conditions the luminance $(L+M)_P$ contours form elliptical contours with L–M ($k = 2$). Examples of such contours are shown in Fig. 20*d*. Noorlander, Heuts, and Koenderink,[83] however, reported that elliptical contours were found across all spatial and temporal frequencies.

***Sensitivity to Different Directions of Color Space*** Before considering results obtained using trichromatic test mixtures, we first consider earlier results obtained using bichromatic mixtures.

*Sensitivity to bichromatic test mixtures* The use of spectral lights restricts the range of measurements to the spectrum locus in color space, thus ignoring the much larger and arguably environmentally more relevant volume of space that includes desaturated colors, achromatic lights, and extra-spectral colors (such as purples). Measuring detection sensitivity for mixtures of spectral targets probes the inner volume of color space. Studying these "bichromatic mixtures," moreover, can provide a direct test of the additivity of a mechanism. For example, under conditions that isolate a univariant linear mechanism, pairs of lights should combine additively, so that the observer should be more sensitive to the combination than to either light alone. For a cone-opponent mechanism, on the other hand, pairs of lights that oppositely polarize the mechanism should combine subadditively, so that the observer is less sensitive to the mixture than to either component (as illustrated in Fig. 6*d*). If different mechanisms detect the two targets, then other potential interactions include probability summation or gating inhibition (winner takes all). Boynton, Ikeda, and Stiles[100] found a complex pattern of interactions between various test fields that included most of the possible types of interactions.

Several workers have demonstrated subadditivity for mixtures of spectral lights that is consistent with either L–M or S–(L+M) cone opponency.[100,106,120,159–165] Clear examples of subadditivity were

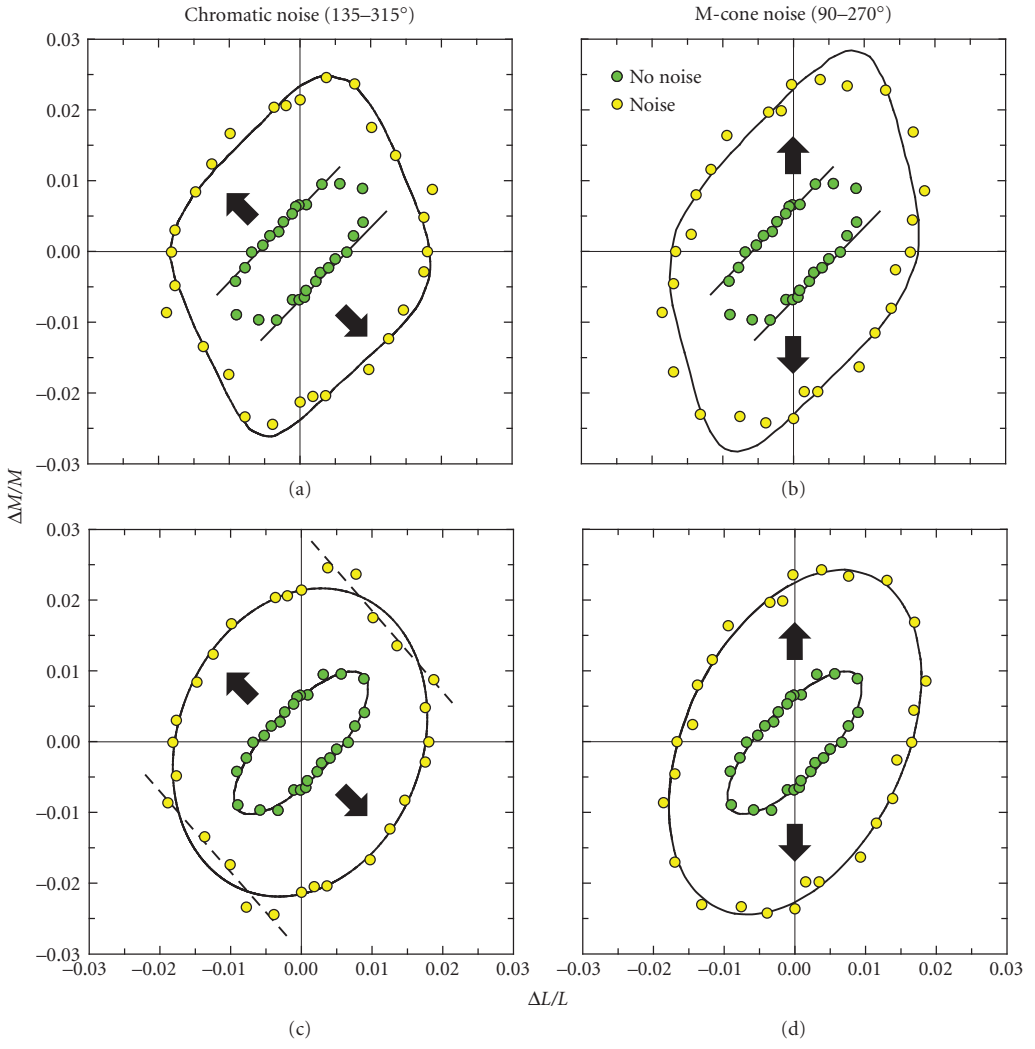


**FIGURE 20** Detection contours in the $\Delta L/L$, $\Delta M/M$ plane. Detection thresholds for a 1-cpd Gabor replotted from Fig. 5 of Giulianini and Eskew[175] obtained with (yellow circles) or without (green circles) noise made up of superposed flickering rings modulated along the $\Delta L/L = -\Delta M/M$ (chromatic) axis (*a* and *c*) or the $\Delta M/M$ (M-cone) axis (*b* and *d*). The arrows indicate the noise directions. (*a*) and (*b*). Model fits (solid lines) by Giulianini and Eskew[175] in which L–M chromatic detection is assumed to be mediated by a mechanism with relative cone contrast weights of 0.70 $\Delta L/L$ and 0.72 $\Delta M/M$ of opposite sign, while L+M achromatic detection is mediated by a mechanism with relative weights of 0.90 $\Delta L/L$ and 0.43 $\Delta M/M$ of the same sign. Without chromatic noise, the detection data are consistent with detection solely by the chromatic mechanism (as indicated by the parallel lines) except along the luminance axis. With added chromatic noise, the sensitivity of the chromatic mechanism is reduced, revealing the achromatic mechanism in the first and third quadrants. In the presence of noise, the data are consistent with detection by both chromatic and achromatic mechanisms (as indicated by the rounded parallelogram). The combination exponent for the two mechanisms, *k*, was assumed to be 4 (see subsection "How Test Measurements Imply Opponency" in Sec. 11.3). (*c*) and (*d*) Alternative fits to the data using elliptical contours, which provide a surprisingly good fit to the detection data, except in the achromatic direction with chromatic noise (*c*). The ellipse fitted to the yellow circles in (*c*) has the formula $3332x^2 + 2021y^2 + 873xy = 1$ (major axis 73.16°), while that fitted to the green circles has the formula $27{,}191x^2 + 24{,}842y^2 + 43{,}005xy = 1$ (major axis 46.56°), where $x = \Delta L/L$ and $y = \Delta M/M$. Those data with noise that are poorly accounted for by the ellipse have been fitted with a straight line of best-fitting slope –1.14 (dashed line). The ellipse fitted to the yellow circles in (*d*) has the formula $3648x^2 + 1959y^2 + 1992xy = 1$ (major axis 65.15°), while that fitted to the green circles has the formula $26{,}521x^2 + 23{,}587y^2 + 38{,}131xy = 1$ (major axis 47.20°).

obtained by Thornton and Pugh,[164] who presented targets chosen to favor chromatic detection on a white (xenon-arc) background. Figure 18*a* shows the test spectral sensitivity obtained on the white field characteristic of chromatic detection. The spectral positions of the test mixture primaries used in the additivity experiment are indicated by the arrows. Figure 18*b* shows the results of the text mixture experiment. Detection contours aligned with the parallel diagonal contours (dashed blue lines) is consistent with chromatic detection by an L–M mechanism, whereas detection along the 45° vector (parallel to the contours) is consistent with achromatic detection by an L+M mechanism. Thornton and Pugh[164] also used test primaries of 430 and 570 nm, which were chosen to favor detection by the S cones and by luminance (L+M), respectively. Although less clear than the L–M case shown here, they found evidence for inhibition between the 430- and 570-nm target consistent with detection by an S–(L+M) cone-opponent mechanism.

Guth and Lodge[11] and Ingling and Tsou[12] both used models that incorporated opponency to analyze bichromatic and spectral thresholds. Both found that the threshold data could be accounted for by two opponent-color mechanisms [which can be approximated to the basic cone-opponent discrimination mechanisms, L+M and S–(L+M)], and a single nonopponent mechanism (L+M). Both also developed models that could better account for "suprathreshold" data, such as color valence data, by modifying their basic models. These modifications took the form of an increase in the contribution of the S–(L+M) mechanism and either inhibition between the two cone-opponent mechanisms[11] or addition of an S-cone contribution to the L-cone side of the L–M mechanism.[12] These suprathreshold models are related to the color-appearance models discussed in subsection "Color Appearance and Color Opponency" in Sec. 11.5. It is worth noting that Guth and Lodge acknowledge that modulations of their cone-opponent discrimination mechanisms do not produce strictly red-green or yellow-blue appearance changes, but rather yellowish-red versus blue-green and greenish-yellow versus violet. That is, their threshold discrimination mechanisms do not account for unique hues (see subsection "Spectral Properties of Color-Opponent Mechanisms" in Sec. 11.5).

Kranda and King-Smith[106] also modeled bichromatic and spectral threshold data, but they required four mechanisms: an achromatic mechanism (L+M), two L–M cone-opponent mechanisms of opposite polarities (L–M and M–L), and an S-cone mechanism (S). The main discrepancy from the previous models is that they found no clear evidence for an opponent inhibition of S by L+M. Two opposite polarity, L–M mechanisms were required because Kranda and King-Smith assumed that only the positive lobe contributed to detection, whereas previous workers had assumed that both negative and positive lobes could contribute. This presaged the unipolar versus bipolar mechanism debate (see "Unipolar versus Bipolar Chromatic Mechanisms" in Sec. 11.6).

With the exception of Boynton, Ikeda, and Stiles,[100] most of the preceding studies used incremental spectral test lights, which confined the measurements to the eighth volume of color space in which all three cone signals increase. To explore other directions in color space, both incremental and decremental stimuli must be used.

*Detection contours in the L,M plane* The first explicit use of incremental and decremental stimuli in cone contrast space was by Noorlander, Heuts, and Koenderink,[83] who made measurements in the L,M plane. They fitted their detection contours with ellipses, and found that the alignment of the minor and major axes depended on temporal and spatial frequency. At lower frequencies, the minor and major axes aligned with the chromatic ($\Delta M/M = -\Delta L/L$) and achromatic ($\Delta M/M = \Delta L/L$) directions, respectively. By contrast, at higher frequencies, the reverse was the case. Such a change is consistent with relative insensitivity of chromatic mechanisms to higher temporal and spatial frequencies (see subsection "Spatial and Temporal Contrast Sensitivity Functions" in Sec. 11.5).

If the individual detection contours are truly elliptical in two-dimensional color space or ellipsoidal in three, then the vectors of the underlying linear detection mechanisms cannot be unambiguously defined. This ambiguity arises because ellipses or ellipsoids can be linearly transformed into circles or spheres, which do not have privileged directions.[165] Consequently, whether or not detection contours are elliptical or ellipsoidal has become an important experimental question. Knoblauch and Maloney[166] specifically addressed this question by testing the shapes of detection contours measured in two color planes. One plane was defined by modulations of the red and green phosphors of their display (referred to by them as the $\Delta R$, $\Delta G$ plane), and the other by the modulations of the red and green phosphors together and the blue phosphor of their display (referred to as the $\Delta Y$, $\Delta B$ plane). The

detection contours they obtained did not differ significantly in shape from an elliptical contour.[166] Note, however, that a set of multiple threshold contours, each ellipsoidal but measured under related conditions, can be used to identify mechanisms uniquely, given a model about how the change in conditions affects the contours (see, e.g., Ref. 167; discussed in subsection "Spatial and Temporal Contrast Sensitivity Functions" in Sec. 11.5).

Deviations from an ellipse, if they do occur, are most likely to be found under experimental conditions that maximize the probability that different portions of the contour depend on detection by different mechanisms. Such a differentiation is unlikely to be found under the conditions used by Knoblauch and Maloney.[166] At lower temporal frequencies (1.5-Hz sine wave or a Gaussian-windowed, $\sigma = 335$ ms, 1.5-Hz cosine wave), the detection contour in the $\Delta R$, $\Delta G$ phosphor space is likely to be dominated by the much more sensitive L–M mechanisms, whereas the contour in $\Delta Y$, $\Delta B$ space is likely to depend upon detection by all three mechanisms [L–M, L+M, and S–(L+M)]. A comparable conclusion about the shape of threshold contours was reached by Poirson, Wandell, Varner, and Brainard,[168] who found that color thresholds could be described well by ellipses, squares, or parallelograms. Again, however, they used long duration (a Gaussian envelope lasting 1 s, corresponding to +5 to –5 standard deviations) and large (2° diameter) target that would favor detection by L–M.

The relatively high sensitivity of the L–M mechanism to foveally viewed, long-duration flashed targets[169–171] means that the L–M mechanism dominates the detection contours unless steps are taken to expose the L+M luminance mechanisms, such as by the use of flickering targets,[63,172] very small targets,[173] or chromatic noise (see subsection "Noise-Masking Experiments" in Sec. 11.5). Detection threshold contours measured in the L,M plane that expose both L–M and L+M contours are arguably better described by a parallelogram with rounded corners rather than an ellipse, with the parallel sides of positive slope corresponding to detection by the L–M chromatic mechanism and those of negative slope corresponding to detection by the L+M luminance mechanism.[61,63,173,174] Examples of detection contours that appear nonelliptical include parts of Figs. 3 and 4 of Ref. 63; Fig. 3, 5, and 7 of Ref. 175; and Fig. 2 of Ref. 176.

Figure 20 shows the detection data replotted from Fig. 5 of Ref. 175. The data are shown twice: once in the upper panels (a, b) and again in the lower panels (c, d). The data shown as green circles were measured without noise. The data shown as yellow circles in Fig. 20*a* and *c* were measured in the presence of chromatic noise, while those in Fig. 20*b* and *d* were measured in the presence of M-cone noise. The noise directions are indicated by the black arrows.

If, for the sake of argument, we accept that the mechanism vectors of the detection mechanisms can be unambiguously defined from detection contours (as illustrated in Fig. 20*a* and *b*), it is possible to estimate their cone weights and therefore their spectral sensitivities. The chromatic L–M detection contours in Fig. 20*a* and *b* obtained without noise (green circles) have been fitted with lines of parallel slopes of approximately 1.0, which indicates that the L–M chromatic mechanism responds to the linear difference of the L- and M-cone *contrast* signals; $|c\Delta L/L - d\Delta M/M| = \text{constant}$, where $c = d$.[61,63,173,174] The equality of the L- and M-cone weights, unlike the underlying relative L-and M-cone numerosities (e.g., Ref. 30), shows a remarkable lack of individual variability across observers (see Ref. 89). Similarly, color appearance settings (see subsection "Color Appearance and Color Opponency" in Sec. 11.5) in the form of unique yellow settings show much less variability than would be expected if unique yellow depended on the relative number of L and M cones in the retina.[146]

As suggested by the yellow circles in Fig. 20*a* and *c*, the use of a high frequency flickering target in chromatic noise exposes more of the L+M contour in the first and third quadrants. Unlike the L–M contour, the L+M contour has a negative slope, which indicates that the L+M achromatic chromatic mechanism responds to the linear sum of the L- and M-cone *contrast* signals; $|a\Delta L/L + b\Delta M/M| = \text{constant}$, where $a$ is typically greater than $b$.[61,63,89,173,174]

*Mechanism interactions* The shapes of the detection contours when two or more postreceptoral mechanisms mediate threshold depends upon the way in which those mechanisms interact (see Fig. 6*c*). In principle, such interactions can range from complete summation, through probability summation to exclusivity (winner takes all) and inhibition (see Ref. 100). The usual assumption is that L–M, S–(L+M), and L+M are stochastically independent mechanisms that combine by probability summation. That is, if two or three mechanisms respond to the target, then the threshold will be lower than if only one responds to it. How much the threshold is lowered depends upon the

underlying frequency-of-seeing curve for each mechanism. Steep frequency-of-seeing curves result in a relatively small drop in threshold, whereas shallow curves result in a larger drop. Several groups have mimicked probability summation by using the summation rule introduced in "How Test Measurements Imply Opponency" in Sec. 11.3. The summation exponent can be varied to mimic the effects of probability summation for psychometric functions with different slopes (see Refs. 174 and 89). A closely related geometrical description of the threshold contours was used by Sankeralli and Mullen.[172] For the fits in Fig. 20*a* and *b*, the summation exponent was assumed to be 4, which produces a contour shaped like a rounded parallelogram.[89,175]

The superiority of a rounded parallelogram over an ellipse (summation exponent of 2) is not always clear. For example, Fig. 20*c* and *d* show the same detection data as the *a* and *b*. In *c* and *d*, the data have been fitted with ellipses. As can be seen, each set of data is well fitted by an ellipse, except perhaps for a small part of the contour measured in the presence of chromatic noise shown in Fig. 20*c*. In this region, we have fitted a straight line plotted as the dashed line. Changing the direction of the noise from L–M chromatic to M cone between Fig. 20*c* and *d* rotates the ellipse slightly anticlockwise. The L–M data along the opponent diagonals clearly follow an elliptical rather than a straight contour in both cases. As previously noted, when an elliptical representation underlies the data, it does not uniquely determine the inputs to the underlying mechanisms.

Support for the summation exponent of 4 used to fit the data in Fig. 20*a* and *b* is also lacking from estimates of the slopes of the underlying psychometric functions, which are consistent with much smaller exponents.[171,177,178]

*Detection in the other planes* An investigation of mechanisms other than L–M and L+M (as well as information about whether or not there are S-cone inputs into those mechanisms) requires the measurement of responses outside the L,M plane of color space. Two systematic investigations have been carried out that include S-cone modulations. Cole, Hine, and McIlhagga[174] made measurements on a roughly 1000 log td white background using a Gaussian-blurred 2°, 200-ms spot that favors chromatic detection. Their data were consistent with three independent mechanisms: an L–M mechanism with equal and opposite L- and M-cone inputs but no S-cone input; an L+M mechanisms with unequal inputs and a small positive S-cone input, and an S–(L+M) mechanism. Sankeralli and Mullen[172] used three types of gratings with spatiotemporal properties chosen to favor either the chromatic L–M (1 cpd, 0 Hz), chromatic S–(L+M) (0.125 cpd, 0 Hz), or the achromatic L+M mechanism (1 cpd, 24 Hz). They confirmed that L–M had equal and opposite L- and M-cone inputs, but found a small S-cone input of about 2 percent added to either the L or the M cones for different observers. In addition, they found a small 5 percent S-cone input into the luminance mechanism that opposed the L+M input (see also Ref. 92). The S–(L+M) mechanism was assumed to have balanced opposed inputs.[172] Eskew, McLellan, and Giulianini[89] provide a separate analysis of both these sets of data (see Table 18.1 of Ref. 89).

Figure 21 shows chromatic detection data measured in the L–M,S plane by Eskew, Newton, and Giulianini.[179] The central panel shows detection thresholds with (filled circles) and without (open squares) L–M chromatic masking noise. Detection by the relatively insensitive S-cone chromatic mechanisms becomes apparent when detection by L–M chromatic mechanism is prevented by chromatic noise. The nearly horizontal portions of the black contour reflect detection by S–(L+M), while the vertical portions reflect detection by L–M (the model fit is actually of the unipolar mechanisms |L–M|, |M–L|, |S–(L+M)|, and |(L+M)–S|, see Ref. 34 for details; also "Unipolar versus Bipolar Chromatic Mechanisms" in Sec. 11.6).

The question of whether or not the S cones make a small contribution to the L–M detection mechanisms remains controversial. Boynton, Nagy, and Olsen[180] found that S cones show summation with L–M (+S with L–M, and –S with M–L) in chromatic difference judgments. Stromeyer et al.[181] showed that S-cone flicker facilitated detection and discrimination of L–M flicker, with +S facilitating L–M and –S facilitating M–L. Yet, the estimated S-cone contrast weight was only approximately 1/60th of the L- and M-cone contrasts weight into L–M (see p. 820 of Ref. 181). In general, in detection measurement the S-cone signal adds to redness (L–M) rather than greenness (M–L)—as expected from color-opponent theory (see Sec. 11.4), but the size of the contribution is much less than expected. Eskew and Kortick,[20] however, made both hue equilibria and detection measurements and estimated that the S-cone contrast weight was about 3 percent that of the L- and

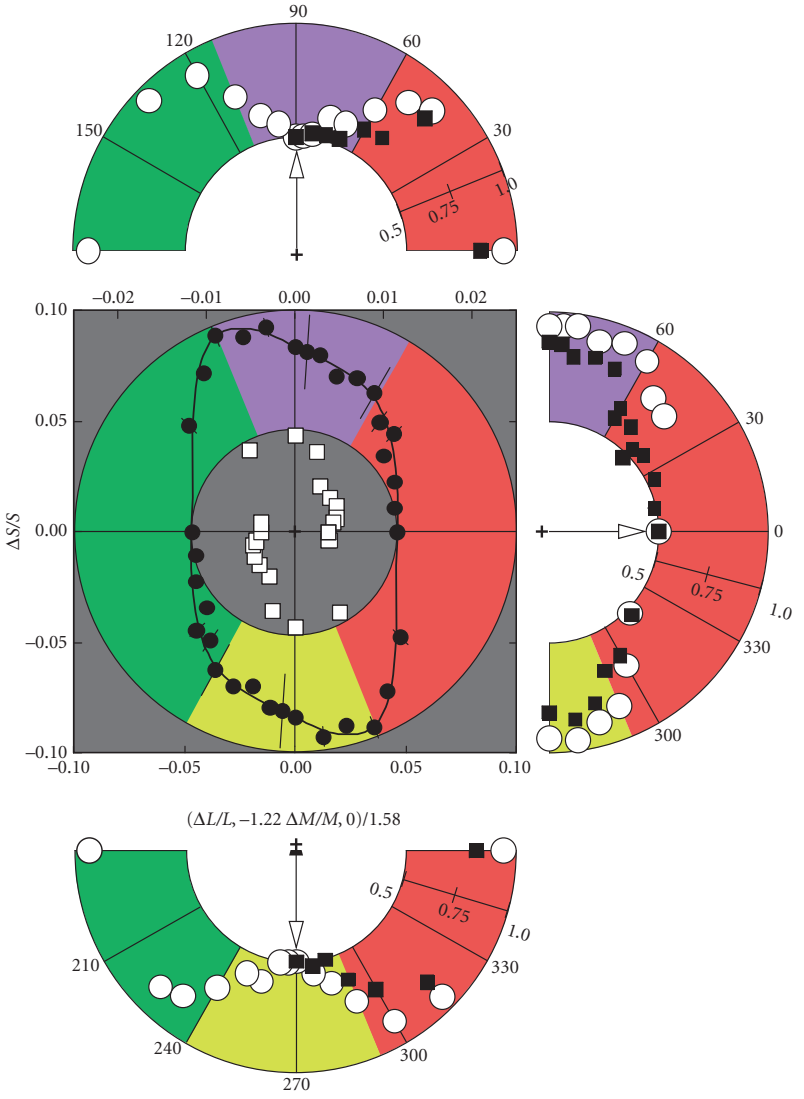


**FIGURE 21** Detection and discrimination contours in the equiluminant plane. This figure is a reproduction of Fig. 5 from Eskew.[34] The central panel shows thresholds for the detection of Gabor patches with (filled circles) and without (open squares) L–M chromatic masking noise (0°/180° color direction). For clarity, the horizontal scale for the no-noise thresholds (open squares) has been expanded as indicated by the upper axis. Data are symmetric about the origin due to the symmetric stimuli. Detection by the relatively insensitive S-cone chromatic mechanisms becomes apparent when detection by the L–M chromatic mechanism(s) is suppressed by L–M chromatic noise. The black contour fitted to the filled circles is the prediction of a model in which detection is mediated by probability summation between four symmetric unipolar linear mechanisms |L–M|, |M–L|, |S–(L+M)|, and |(L+M)–S|, (see subsection "Unipolar versus Bipolar Chromatic Mechanisms" Sec. 11.6). The three outlying semicircular polar plots are discriminability data (filled squares), in which the angular coordinate corresponds to the same stimuli, at the same angles, as in the detection data. The radial coordinate gives the discriminability between 0.5 (chance) and 1.0 (perfect discriminability) of the given test color angle relative to the standard color angle indicated by the arrow. The open circles are predictions of a Bayesian classifier model that takes the outputs of the four mechanisms fitted to the detection data as its inputs. Colored regions indicate bands of poorly discriminated stimuli, and are redrawn on the detection plot for comparison. These results suggest that just four univariant mechanisms are responsible for detection and discrimination under these conditions. See Ref. 34 for further details. [*Figure adapted by Eskew[34] from Fig. 4 (Observer JRN) of Ref. 179 Reprinted from The Senses: A Comprehensive Reference, Volume 2: Vision II, Fig. 5* from R. T. Eskew, Jr., "Chromatic Detection and *Discrimination," pp. 109–117. Copyright (2008), with permission from Elsevier.*]

M-cone contrast weights for both tasks. Yet, although test methods support an S-cone contribution to L–M, field methods do not (see Ref. 34). Changes in the S-cone adaptation level have little effect on L–M detection[182] or on L–M mediated wavelength discrimination.[183]

Given the uncertainties about cone spectral sensitivities and luminous efficiency at short wavelengths, as well as the substantial individual differences in prereceptoral filtering between observers (see, e.g., Ref. 90), evidence for small S-cone inputs should be treated with caution.

***Spatial and Temporal Contrast Sensitivity Functions*** The test method can also be used to determine the temporal and spatial properties of visual mechanisms. These properties are traditionally characterized by temporal and spatial "contrast sensitivity functions" (CSFs). These are sometimes incorrectly called "modulation transfer functions" (MTFs)—incorrectly because MTFs require phase as well as amplitude specifications.

In a temporal CSF determination, the observer's sensitivity for detecting sinusoidal flicker is measured as a function of temporal frequency. Generally, the chromatic mechanisms have a lowpass temporal frequency response with typically greater temporal integration and a poorer response to higher temporal frequencies than the more band-pass achromatic mechanism.[94,102,184–190] A lowpass CSF means that the temporal response is approximately independent of frequency at low frequencies but falls off at higher frequencies, whereas a band-pass CSF means that the response peaks at an intermediate frequency and falls off at both lower and higher frequencies.

On the grounds that different chromatic flicker frequencies can be discriminated near threshold, Metha and Mullen[190] suggest that at least two chromatic mechanisms with different temporal CSFs must underlie the measured chromatic CSF, one with a band-pass CSF and the other with a lowpass CSF. They argue that two mechanisms must operate, because a single *univariant* flicker mechanism will confound changes in contrast and flicker frequency, making frequency identification impossible. However, the assumption that flicker is encoded univariantly may be flawed. At low frequencies, flicker may be encoded as a moment-by-moment variation that matches the flicker frequency.[191]

In a spatial CSF determination, the observer's sensitivity for detecting sinusoidal gratings is measured as a function of their spatial frequency. Generally, the chromatic mechanisms have a lowpass spatial frequency response with greater spatial integration and a poorer response to higher spatial frequencies than the usually more band-pass achromatic mechanisms.[102,192–197]

Spatial CSFs are degraded by sensitivity losses introduced by the optics of the eye. In one study, laser interference fringes were used to project gratings directly on the retina, thereby effectively bypassing the MTF of the eye's optics.[198,199] However, because the red and green equiluminant interference fringes could not be reliably aligned to produce a steady artifact-free chromatic grating, they were drifted in opposite directions at 0.25 Hz. Thus, the gratings continuously changed from a red-green chromatic (equiluminant) grating to a yellow-black luminance (equichromatic) grating. The subject's task was to set the contrast threshold separately for the different spatial phases, which was apparently possible.[199] One concern about this method, however, is that the close juxtaposition of chromatic and luminance gratings in time and space might produce facilitation or interference (see subsection "Pedestal Experiments" in Sec. 11.5). For S-cone detection, a single grating was used.

The results for equiluminant, chromatic (red circles) and equichromatic, achromatic (blue circles) fringes are shown for three observers in the upper panels of Fig. 22. As expected, there is a steeper fall-off in high spatial-frequency sensitivity for chromatic gratings than for luminance gratings. By estimating the sensitivity losses caused by known factors such as photon noise, ocular transmission, cone-aperture size, and cone sampling, Sekiguchi, Williams, and Brainard[198] were able to estimate an ideal observer's sensitivity at the retina. Any additional losses found in the real data are then assumed to be due to neural factors alone. Estimates of the losses due to neural factors are shown in the lower panels of Fig. 22. Based on these estimates, the neural mechanism that detects luminance gratings has about 1.8 times the bandwidth of the mechanisms that detect chromatic gratings. Interestingly, the neural mechanisms responsible for the detection of equiluminant L–M gratings and S-cone gratings have strikingly similar (bandpass) contrast sensitivities, despite the very different spatial properties of their submosaics.[200] This commonality may have important implications for color processing (see "Three-Stage Zone Models" in Sec. 11.6).

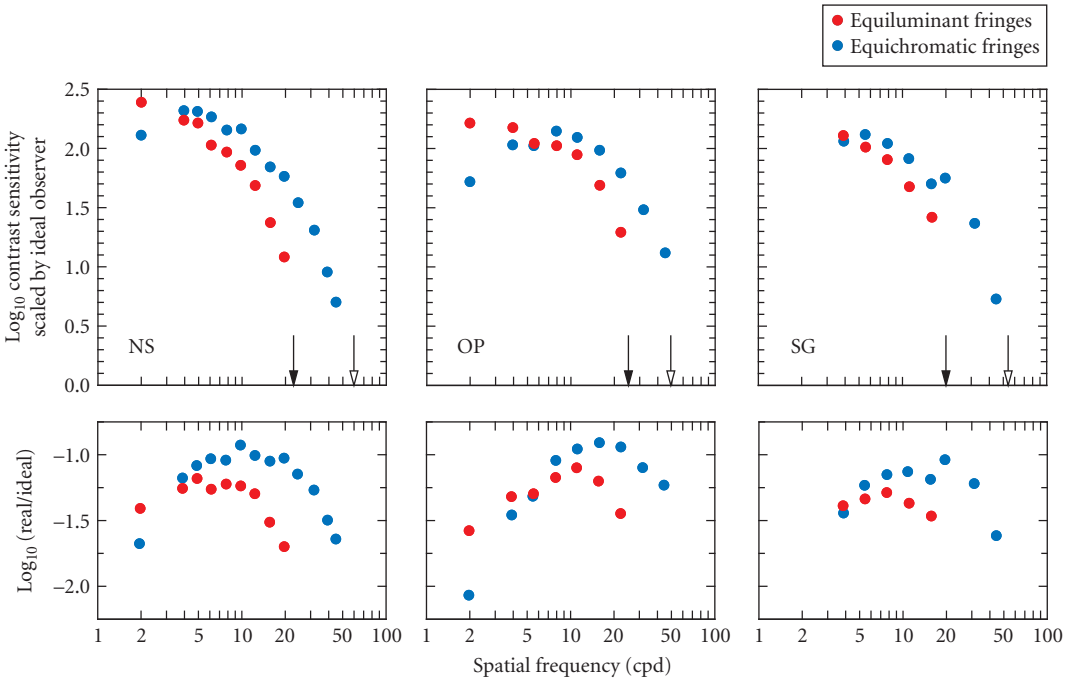


**FIGURE 22** Spatial equiluminant and equichromatic contrast sensitivity functions. Top panels: Foveal CSFs for equiluminant (red circles) and equichromatic (blue circles) interference fringes for three observers. Filled and open arrows represent the foveal resolution limit for the equiluminant and the equichromatic stimuli, respectively. Bottom panels: The ratio of the ideal to the real observer's contrast sensitivity for detecting equiluminant (red circles) and equichromatic (blue circles) stimuli. (*Based on Figure 9 of Ref. 199.*)

Poirson and Wandell[167] measured spatial CSFs along the two cardinal directions and along intermediate directions in color space; that is, they effectively measured threshold contours for a series of grating spatial frequencies. They fitted the contours with an ellipsoidal model, but added a constraint of pattern-color separability; that is, they assumed that the effect of pattern operated independently in each of three second-site mechanisms. This constraint resolves the mechanism ambiguity inherent in fitting ellipsoidal contours to the individual data, and allowed Poirson and Wandell to estimate the sensitivities of three underlying mechanisms by jointly analyzing the contours across spatial frequency. They found two opponent and one nonopponent mechanisms, with sensitivities consistent with the cardinal mechanisms, L+M, L–M, and S–(L+M) (see Fig. 6 of Ref. 167).

We next consider results obtained using the field method.

## Field Sensitivities

*Stiles' π-Mechanisms* Stiles used the field sensitivity method to define the spectral sensitivities of the $\pi$-mechanisms, which are illustrated in Fig. 23. The tabulated field sensitivities can be found in Table 2 (7.4.3) of Ref. 53 and Table B of Ref. 33. The field sensitivities are the reciprocals of the field radiances (in log quanta $s^{-1}$ $deg^{-2}$) required to raise the threshold of each isolated $\pi$-mechanism by one log unit above its absolute threshold. The tabulated data are average data for four subjects: three females aged 20 to 30 and one male aged 51.

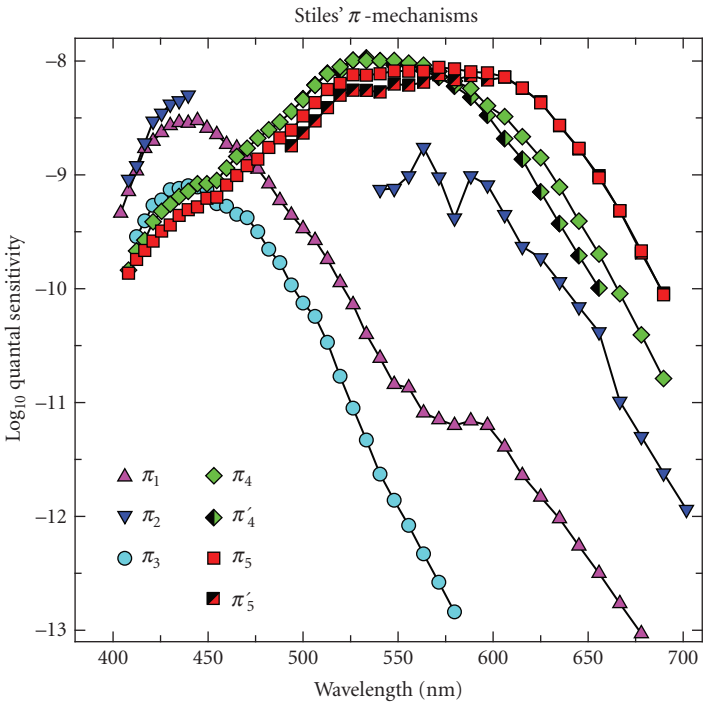


**FIGURE 23** Stiles' $\pi$-mechanisms. Field spectral sensitivities of the seven photopic $\pi$-mechanisms: $\pi_1$ (purple triangles), $\pi_2$ (dark blue inverted triangles), $\pi_3$ (light blue circles), $\pi_4$ (green diamonds), $\pi'_4$ (green half-filled diamonds), $\pi_5$ (red squares), $\pi'_5$ (red half-filled squares). The field sensitivities are the reciprocals of the field radiances (in log quanta $s^{-1}$ $deg^{-2}$) required to raise the threshold of each "isolated" $\pi$-mechanism by one log unit above its absolute threshold. The results were averaged across four subjects: three females aged 20 to 30 and one male aged 51. Details of the experimental conditions can be found on p. 12 of Stiles' book.[33] (*Data from Table 2(7.4.3) of Wyszecki and Stiles.*[53])

Through field sensitivity measurements, and measurements of threshold versus background radiance for many combinations of target and background wavelength, Stiles identified seven photopic $\pi$-mechanisms: three predominately S-cone mechanisms ($\pi_1$, $\pi_2$, and $\pi_3$), two M-cone ($\pi_4$ and $\pi_4'$), and two L-cone ($\pi_5$ and $\pi_5'$). Although it has been variously suggested that some of the $\pi$-mechanisms might correspond to cone mechanisms,[97,201–203] it is now clear that all reflect some form of postreceptoral cone interaction. The surfeit of $\pi$-mechanisms and their lack of obvious correspondence to cone mechanisms or simple postreceptoral mechanisms led to the demise of Stiles' model. Its usefulness, however, was prolonged in the work of several investigators, who used failures of Stiles' model as a way of investigating and understanding the properties of chromatic mechanisms (see "Field Additivity" in this section). But, as noted in the parallel discussion in the context of test sensitivity, the potential ongoing value of the $\pi$-mechanism field sensitivities is that they provide an empirical database that may be used to constrain current models.

***Achromatic Detection and Chromatic Adaptation*** Achromatic spectral sensitivity (or luminous efficiency) is strongly dependent on chromatic adaptation.[63,64,142,204–210] Figure 24*a* shows the changes in luminous efficiency caused by changing background field wavelength from 430 to 670 nm and Fig. 24*b* shows the changes caused by mixing 478- and 577-nm adapting fields in different luminance

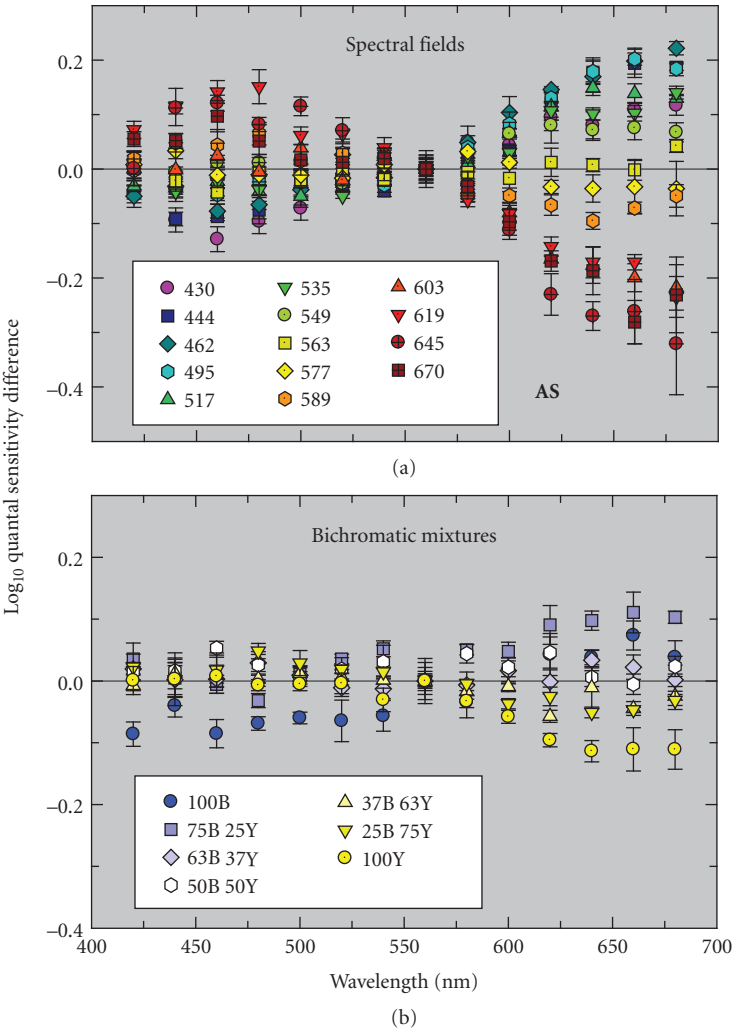


**FIGURE 24** Dependence of luminous efficiency on chromatic adaptation. Changes in quantal luminous efficiency caused by changes in adapting field chromaticity plotted relative to the mean luminous efficiency. Data from Observer S1 of Stockman, Jägle, Pirzer and Sharpe.[129] Measurements were made using 25-Hz heterochromatic flicker photometry (HFP) on 1000-td backgrounds. (*a*) HFP changes on fourteen 1000-td spectral adapting fields from 430 to 670 nm and (*b*) changes on seven 1000 td bichromatic, 478(B) + 577(Y)-nm adapting field mixtures that varied from 100 percent B to 100 percent Y.

ratios. These changes are consistent with selective adaptation reducing L-cone sensitivity relative to M on longer wavelength fields, and reducing M-cone sensitivity relative to L on shorter wavelength fields. Between about 535 and 603 nm the selective changes are roughly consistent with Weber's law ($\Delta I/I$ = constant). Consequently, plotted in cone contrast space, the sensitivity contour for the achromatic mechanism should remain of constant slope between field wavelengths of 535 and 603 nm, *unlike* the example shown in Fig. 8*b*. For background wavelengths shorter than 535 nm,

on the other hand, the changes in spectral sensitivity are consistent with a relative loss of M-cone sensitivity in excess of that implied by Weber's law (for details, see Ref. 129). This is consistent with other evidence that also shows that the luminance contribution of the L- or M-cone type more sensitive to a given chromatic field can be suppressed by more than Weber's law implies.[63,64,142] Such supra-Weber suppression, illustrated in Fig. 8*b* for the L-cone case, causes the luminance sensitivity contours in cone contrast space to rotate away from the axis of the more suppressed cone.

*Multiple cone inputs* There is now good psychophysical evidence that the standard model of the luminance channel as an additive channel with just fast L- and M-cone inputs (referred to here as *+fL+fM*) is incomplete. According to this model, pairs of sinusoidally alternating lights that are "luminance-equated" and detected solely by the luminance channel should appear perfectly steady or nulled whatever their chromaticities (equating alternating lights to produce a null is known as heterochromatic flicker photometry or HFP). And, indeed, such nulls are generally possible, but sometimes only if moderate to large phase delays are introduced between the pairs of flickering lights.[184,211–215] Moreover, these large phase delays are often accompanied by substantial frequency-dependent changes in the spectral sensitivity of flicker detection and modulation sensitivity.[216–218] From the phase delays and sensitivity changes, it is possible to infer that, in addition to the faster *+fM+fL* signals, sluggish *+sM–sL*, *+sL–sM*, and *–sS* signals also contribute to the luminance-signal nulls in a way that depends on adapting chromaticity and luminance.[94,215–223]

Figure 25 shows examples of large phase delays that are found for M- and L-cone-detected flickering lights on four increasingly intense 658 nm fields. In these plots, 0° means that the two lights cancelled when they were physically in opposite phase (i.e., when they were alternated), while ± 180° means that they cancelled when they were actually in the same phase. The differences between the plotted M- and L-cone phase delays therefore show the delays between the M- and L-cone signals introduced *within* the visual system. As can be seen, some of the phase delays are substantial even at moderately high temporal frequencies, particularly for the M-cone signals. Such delays are inconsistent with the standard model of luminance, which, except for phase differences caused by the selective adaptation of the L cones by the long-wavelength field, predicts that no phase adjustments should be required. Notice also the abrupt changes in phase *between* intensity levels 3 and 4.

The continuous lines in Fig. 25 are fits of a vector model, in which it was assumed that sluggish and fast signals both contribute to the resultant M- and L-cone signals, but in different ratios depending on the cone type and intensity level. At levels 1 to 3, the dominant slow and fast signals are *+sL–sM* and *+fL+fM*, respectively, as illustrated in the lower neural circuit diagram of Fig. 25, whereas at level 4 they are *–sL+sM* and *+fL+fM*, as illustrated in the upper neural circuit diagram. According to the model, the polarities of the both the slow M- and the slow L-cone signals reverse between levels 3 and 4.

Note that although the sluggish signals *+sM–sL* and *+sL–sM* are spectrally opponent, they produce an achromatic percept that can be flicker photometrically cancelled with luminance flicker, rather than producing an R/G chromatic percept.

***Chromatic Adaptation and the Sloan Notch*** Thornton and Pugh[107] measured test spectral sensitivity functions on fields of 560, 580, and 600 nm using a target that strongly favors chromatic detection. As illustrated in Fig. 17*a*, they found that the local minimum in spectral sensitivity, or Sloan notch, coincides with the field wavelength (i.e., it occurs when the target and background wavelengths are the same; i.e., homochromatic). As discussed in subsection "Sensitivity to Spectral Lights" in Sec. 11.5, the notch is thought to correspond to the target wavelength that produces a minimum or null in the L–M chromatic channel, so that the less-sensitive, achromatic channel takes over detection. For the notch to occur at the homochromatic target wavelength means that adaptation to the field has shifted the zero crossing or null in the cone-opponent mechanism to the field wavelength. Such a shift is consistent with reciprocal (von Kries) adaptation occurring independently in both the M and the L cones. This type of adaptation is plausible given that Weber's law behavior for detection will have been reached on the fairly intense fields used by Thornton and Pugh.[33] If first-site adaptation had fallen short of the proportionality implied by Weber's Law, then the Sloan notch would not have shifted as far as the homochromatic target wavelength.

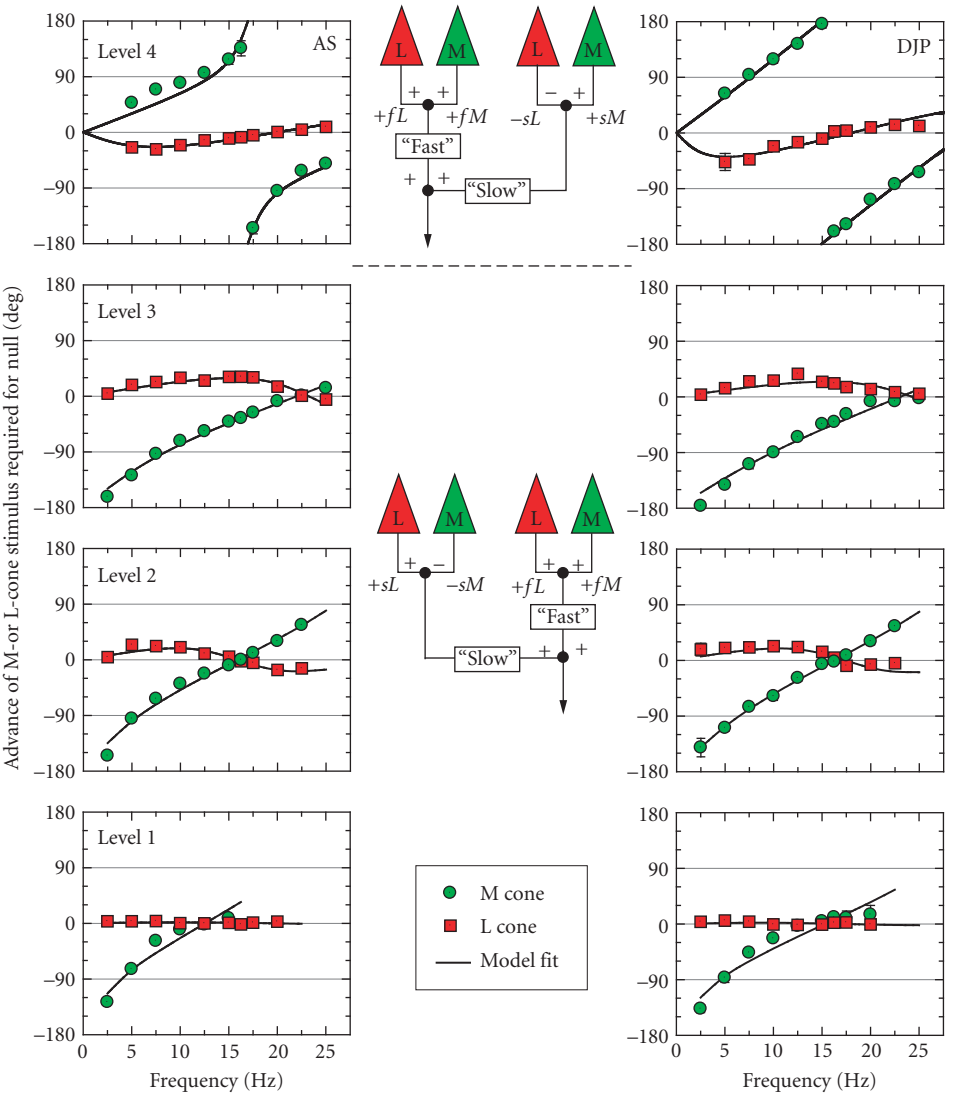


**FIGURE 25** Large phase delays in the "luminance" channel. Phase advances of M-cone (green circles) or L-cone (red squares) stimuli required to flicker-photometrically null a 656-nm target for observers AS (left panels) and DJP (right panels) measured on 658-nm backgrounds of 8.93 (*Level 1*), 10.16 (*Level 2*), 11.18 (*Level 3*), or 12.50 (*Level 4*) $\log_{10}$ quanta $s^{-1}$ $deg^{-2}$. The M-cone stimuli were alternating pairs of L-cone-equated 540 and 650 nm targets; and the L-cone stimuli were pairs of M-cone-equated 650- and 550-nm targets. The continuous lines are fits of a model in which the L- and M-cone signals are assumed to be the resultant of a fast signal (*f*) and a delayed slow signal (*s*) of the same or opposite sign. The predominant signals at each level are indicated by the wiring diagrams in the central insets (see Ref. 223).

As noted in Sec. 11.3, the idea that the zero or null point of an opponent second site always corresponds to the background field wavelength is due to von Kries adaptation is clearly an oversimplification. Were that the case, chromatic detection contours measured in cone contrast units would be independent of field wavelength, which they clearly are not (see subsection "Detection Contours and Field Adaptation" in Sec. 11.5). Similarly, chromatic sensitivity would be independent of field chromaticity at intensities at which Weber's law had been reached, which is also not the case in field additivity experiments (see next). In general, if first-site adaptation was precisely inversely proportional to the amount of background excitation, second-site opponent desensitization would play little or no role in adaptation to steady fields. It would, of course, still play an important role in contrast adaptation; that is, in adaptation to excursions around the mean adapting level.

***Field Additivity*** By using mainly spectral backgrounds (but sometimes with fixed-wavelength auxiliary backgrounds), Stiles restricted his measurements to the spectrum locus of color space. Some of the most revealing failures of his model, however, occur in the interior volume of color space when two spectral backgrounds are added together in different intensity ratios. Given the expectation in Stiles' model that $\pi$-mechanisms should behave univariantly, bichromatic field mixtures should raise the threshold of a $\pi$-mechanism simply in accordance with the total quantum catch generated by those fields in that mechanism. For a linear mechanism, the effects of mixed fields, in other words, should be additive whenever only a single $\pi$-mechanism is involved. However, failures of field additivity can be subadditive, the mixed fields have less than the expected effect, or superadditive, when they have more than the expected effect. Subadditivity is an indication of opponency, and cases of subadditivity are thus another way that field experiments provide evidence of opponency.

Arguably the most interesting failures of field additivity occur under conditions that isolate Stiles' S-cone mechanisms, $\pi_1$ and $\pi_3$, as illustrated in Fig. 26. On a blue, 476-nm background, the threshold for a 425 nm target rises faster than Weber's law predicts (leftmost data set, dashed vs continuous lines), this is superadditivity and is consistent with S-cone saturation.[224,225] However, when a yellow, 590-nm background is added to the blue background, additivity typically fails. For lower 476-nm radiances (open circles, dashed vs continuous lines), superadditivity is found again,[226] whereas for higher 476-nm radiances (open and filled squares, open triangles) subadditivity is found.[227,228] Comparable failures of field additivity are found for the L-cone mechanism or $\pi_5$,[55,188] but less clearly for the M-cone mechanisms or $\pi_4$.[188,196,229,230]

***First- and Second-Site Adaptation*** Pugh and Mollon[231] developed a model to account for the failures of field additivity and other "anomalies" in the S-cone pathway, which has been influential. They assumed that the S-cone signal can be attenuated by gain controls at two sites. Gain at the first site is cone-specific, being controlled in the case of $\pi_1$ and $\pi_3$ solely by excitation in the S cones. By contrast, gain at the cone-opponent second-site is controlled by the net difference between signals generated by the S cones and those generated by the two other cone types. Excursions at the second site either in the S-cone direction or in the L+M-cone direction reduce the gain of that site, and thus attenuate the transmitted S-cone signal. Sensitivity at the second site is assumed to be greatest when the S-cone and the L+M-cone signals are balanced. Superadditivity occurs when attenuation at the first and second sites work together, for example on a blue spectral background. Subadditivity occurs when the addition of a background restores the balance at the second site, for example when a yellow background is added to a blue one. The original version of the Pugh and Mollon[231] model is formalized in their Eqs. (1) to (3). Another version of the model in which the second-site "gain" is implemented as a bipolar static nonlinearity (see Fig. 6 of Ref. 227) is illustrated in Fig. 27. The nonlinearity is a sigmoidal function that compresses the response and thus reduces sensitivity if the input is polarized either in the +S or –(L+M) direction or in the L+M or –S direction. The presence of a compressive nonlinearity in the output of mechanisms is now generally accepted as an important extension of the basic model. Such nonlinearities form a critical piece of models that aim to account for discrimination as well as detection data (see subsection "Pedestal Experiments" in Sec. 11.5).

There is an inconsistency in the Pugh and Mollon scheme for steady-state adaptation. In order for first-site adaptation to be consistent with Weber's law ($\Delta I/I$ = constant), sensitivity adjustment is assumed to be reciprocal—any increase in background radiance is compensated for by a reciprocal

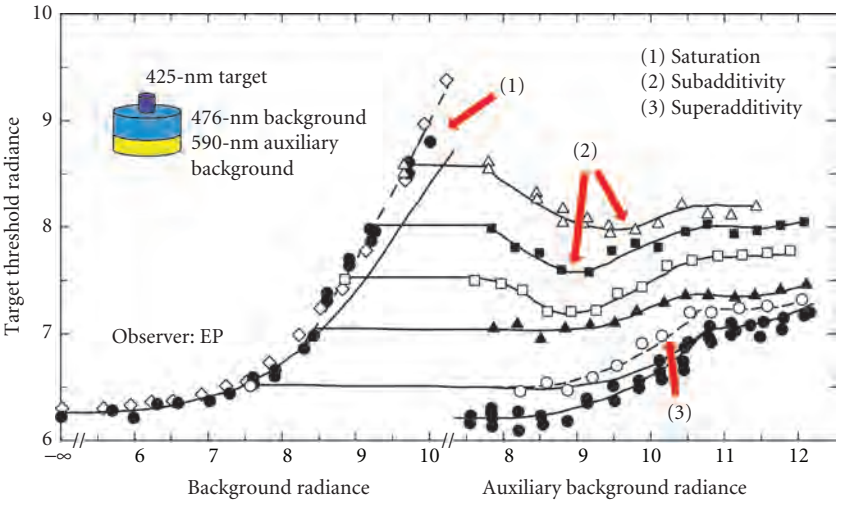


**FIGURE 26** Field additivity failures. S-cone threshold data replotted from Fig. 1A of Pugh and Larimer.[228] The data are increment thresholds for a 425 nm, 200-ms duration, 1° diameter foveal target presented in the centre of 476-nm fields (filled circles and open diamonds, left curves), 590-nm fields (filled circles, right curves), and various bichromatic mixtures of the two. (A 590-nm field of at least 8.0 $\log_{10}$ quanta $s^{-1}$ $deg^{-2}$ was always added to the 476-nm field.) In the bichromatic mixture experiments a series of increasingly intense 590-nm fields, the intensities of which are indicated along the abscissa on the right, were added to a fixed intensity 476-nm field, the intensity of which corresponds to the abscissa associated with the dashed curve at target threshold radiance values corresponding to the data points at the lowest auxiliary background radiances. The shape of solid curves associated with the filled circles and open diamonds on the left and with the filled circles on the right is the standard Stiles threshold-versus-increment (tvi) template shape. The data provide examples of saturation (1), when the threshold elevation grows faster than Weber's law,[224,225] subadditivity (2), when the threshold elevation of the bichromatic mixture falls short of the additivity prediction,[227] and superadditivity (3), when the threshold elevation exceeds the additivity prediction.[226] Figure design based on Figs. 1A and 2 of Pugh and Larimer.[228] Units of radiance are log quanta $sec^{-1}$ $deg^{-2}$.

decrease in gain. Consequently, the signal that leaves the first site (and potentially reaches the second site) should be independent of background radiance (see also "First-Site Adaptation" in Sec. 11.3). However, for the Pugh and Mollon model (and comparable models of first- and second-site adaptation) to work requires that the cone signals reaching the second site continue to grow with background radiance. To achieve this in their original model, they decrease the S-cone gain at the second site in proportion to the background radiance raised to the power $n$ (where $n$ is 0.71, 0.75, or 0.82 depending on the subject) rather than in proportion to the background radiance as at the first site ($n = 1$). Thus, the S-cone signal at the input to the second site continues to grow with background radiance, even though the signal at the output of the first site is constant. This scheme requires that the cone signal at second site somehow bypasses first-site adaptation, perhaps depending on signals at the border of the field[89] or on higher temporal frequency components, which are not subject to Weber's law.[52]

A now mainly historical issue is how much adaptation occurs at the cone photoreceptors. Although some evidence has suggested that relatively little adaptation occurs within photoreceptors until close to bleaching levels,[232,233] other compelling evidence suggests that significant adaptation occurs at much lower levels.[46–48] Measures of adaptation in monkey horizontal cells show that light adaptation is well advanced at or before the first synapse in the visual pathway, and begins at levels as low as 15 td.[234,235] Moreover, psychophysically, local adaptation has been demonstrated to occur with the resolution of single cones.[236–238] The available evidence supports a receptoral site of cone adaptation.

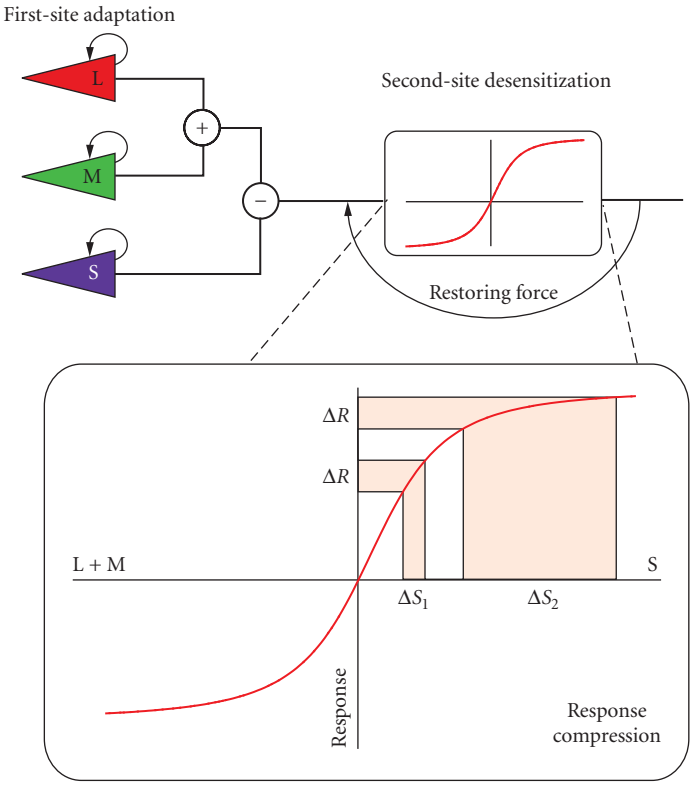


**FIGURE 27** Pugh and Mollon cone-opponent model. Version of the Pugh and Mollon model[231] in which the cone-opponent, second-site desensitization is implemented at a bipolar static nonlinearity.[227] The nonlinearity is a sigmoidal function that compresses the response as the input is polarized either in the +S [or –(L+M)] direction or in the L+M or (–S) direction. The effect of the nonlinearity can be understood by assuming that the system needs a criterion change in response ($\Delta R$) in order for a change in the input to be detected. At smaller excursions along the +S direction, a smaller change in the S-cone signal, $\Delta S_1$, is required to produce the criterion response than the change in signal, $\Delta S_2$, required at greater excursions. Sensitivity should be greatest when the polarization is balanced, and the system is in the middle of its response range.

***Detection Contours and Field Adaptation*** Stromeyer, Cole, and Kronauer[61] measured cone contrasts in the L,M-cone plane (the plane defined by the $\Delta L/L$ and $\Delta M/M$ cone contrast axes, which includes chromatic L–M and achromatic L+M excursions) on spectral green, yellow, and red adapting backgrounds. Changing background wavelength moved the parallel chromatic contours for the detection of 200-ms flashes either outward (reducing sensitivity) or inward (increasing sensitivity). In general, background field wavelength strongly affects chromatic detection with sensitivity being maximal on yellow fields, declining slightly on green fields, and declining strongly on red fields. Since the slopes of the contours in contrast space are unaffected by these changes, the results again show that chromatic adaptation does not alter the relative weights of the M- and L-cone contrast inputs to the chromatic mechanism, but does change the sensitivity of the chromatically opponent second site. These data should be compared with the predictions shown in Fig. 8*a*. S-cone stimulation did not affect the L–M chromatic detection contours.[61]

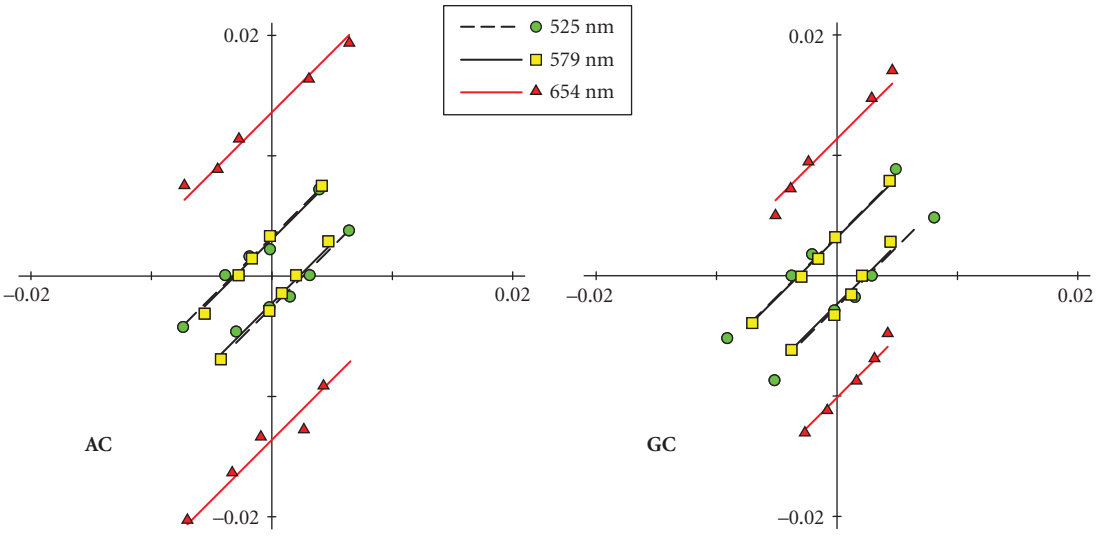


**FIGURE 28** Second-site desensitization of L–M by steady fields. L–M detection contours in cone contrast space for two subjects measured by Chaparro, Stromeyer, Chen, and Kronauer[62] on 3000-td fields of 525 nm (green circles), 579 nm (yellow squares), and 654 nm (red triangles) replotted from their Fig. 4. $\Delta M/M$ is plotted along the ordinate and $\Delta L/L$ along the abscissa. The straight contours fitted to thresholds have slopes of 1, consistent with detection by an L–M mechanism with equal and opposite L- and M-cone contrast weights. Constant relative L- and M-cone weights are a characteristic of von Kries first-site adaptation. The displacement of the contour from the origin on the 654 nm field is characteristic of second-site adaptation.

Figure 28 shows a clear example of the effect of changing the background wavelength of 3000 td fields from 525 to 579 to 654 nm from Fig. 4 of Ref. 62. Consistent with Stromeyer, Cole, and Kronauer,[61] the L–M chromatic detection contours have positive unity slopes, and move outward from the origin as the wavelength lengthens to 654 nm.

The relation between these detection contours and spectral sensitivity data is nicely illustrated by replotting the spectral sensitivity data as cone contrasts. Figure 17*b*, shows the spectral sensitivity data of Thornton and Pugh[107] replotted in cone contrast space by Eskew, McLellan, and Giulianini.[89] The replotted spectral sensitivity data have the same characteristics as the detection contours shown in Fig. 28.

*Habituation or Contrast Adaptation Experiments* The extent of second-site desensitization produced by steady backgrounds is fundamentally limited by first-site adaptation. A natural extension of the field sensitivity method is to temporally modulate the chromaticity or luminance of the background around a mean level, so partially "bypassing" all but the most rapid effects of first-site adaptation and enhancing the effects of second-site desensitization. Moreover, if the spectral properties of the postreceptoral detection mechanisms are known, one mechanism can be selectively desensitized by adapting (or habituating) to modulations along a cardinal axis, which are invisible or "silent" to the other mechanisms (see Ref. 239 for a review of silent substitution methods and their origins).

In an influential paper, Krauskopf, Williams, and Heeley[14] used habituation (the loss of sensitivity following prolonged exposure, in this case, to a temporally varying adapting stimulus) to investigate the properties of what they referred to as the "cardinal mechanisms" (see also Ref. 240). They used a 50 td, 2° diameter field made up of 632.5-, 514.5-, and 441.6-nm laser primaries. Following habituation to 1-Hz sinusoidal modulations (a 30-s initial habituation, then 5-s top-ups between test presentations) that were either chromatic (in the L–M, or S directions at equiluminance), or achromatic (L+M+S), or intermediate between these three directions, the detection sensitivity for Gaussian target pulses ($\sigma = 250$ ms) was measured in various directions of color space.

Figure 29 shows the results for observer DRW. The red circles show the losses of sensitivity and the black circles the increase in sensitivity following habituation to stimuli modulated in the directions of the orange arrows shown in all panels. These results should be compared with the predictions shown in Fig. 11. In their original paper, Krauskopf, Williams, and Heeley[14] concluded that their results showed that habituation occurred independently along each of the three cardinal mechanism axes: L–M, S, and L+M. Thus, the sensitivity losses to habituation along one axis were mainly confined to targets modulated along the same axis, whereas the losses to habituation along axes intermediate to the cardinal ones involved losses in both mechanisms.

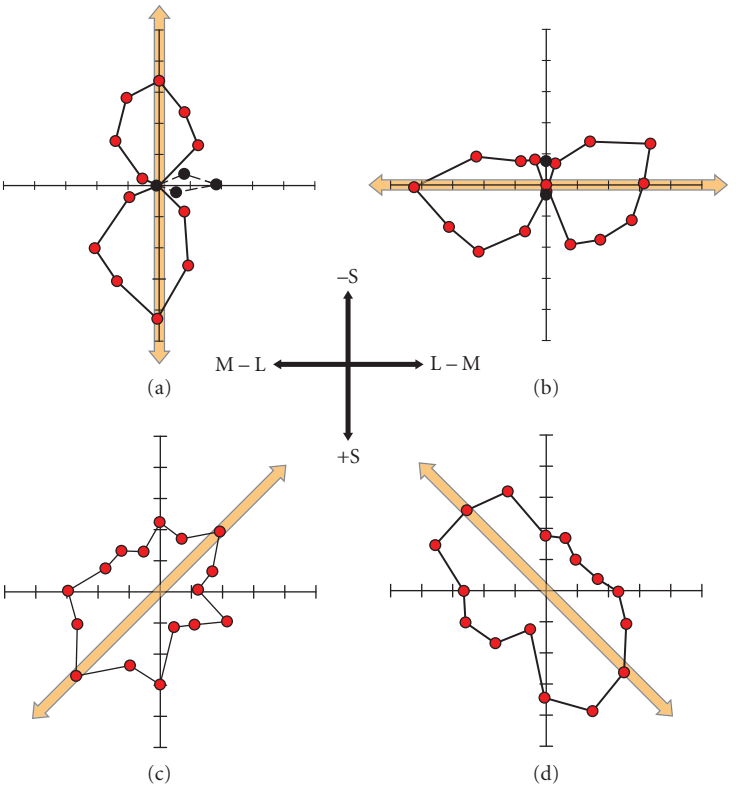


**FIGURE 29** Habituation. Data from Fig. 6 of Krauskopf, Williams, and Heeley[14] plotted in the canonical format shown in Fig. 11. These data are for stimuli that silence the L+M mechanism and reveal the properties of the L–M and S–(L+M) mechanisms plotted in a color space in which the horizontal axis corresponds to stimuli that only stimulate the L–M mechanism and the vertical axis corresponds to stimuli that only stimulate the S–(L+M) mechanism (by modulating S). (*a*) and (*b*) Results for habituation stimuli oriented along the horizontal and vertical axes, respectively. (*c*) and (*d*) Threshold changes for habituation stimuli along intermediate directions. The pattern of results is in qualitative agreement with the predictions developed in Figs. 9 to 11, and provides evidence for second-site adaptation in two opponent-discrimination mechanisms. The red circles plot increases in threshold following habituation, whereas the black circles plot cases where threshold was slightly decreased, rather than increased, by habituation.

Three years later, after a more rigorous analysis using Fourier methods, Krauskopf, Williams, Mandler, and Brown[241] concluded instead that the same data showed that habituation could desensitize multiple "higher-order" mechanisms tuned to intermediate directions in the equiluminant plane between the L–M and S cardinal directions. Yet, in terms of the magnitude of the selective losses, those along the intermediate axes are very much second-order effects compared with those found along the cardinal L–M or S axes. These second-order effects are not particularly compelling evidence for the existence of higher-order mechanisms, because they might also be due to more mundane causes, such as the visual distortion of the habituating stimuli or low-level mechanism interactions. The strong conclusion that can be drawn from the habituating experiments is that selective losses are largest when the habituating stimuli are modulated along the S, L–M, or L+M+S cardinal axes. The evidence for higher-order mechanisms along intermediate axes is secondary. Other workers have suggested that instead of there being multiple mechanisms, the cardinal mechanisms adapt to decorrelate the input signals so that their mechanism vectors rotate.[242–244]

*Noise-Masking Experiments* Another field method used to investigate visual mechanisms is the introduction of masking noise to raise detection threshold. The spectral properties of the underlying mechanisms can then be investigated by varying either the chromaticity and/or luminance of the target (which, if the noise is held constant, is strictly speaking a test method) or by varying the chromaticity and/or luminance of the noise. As with habituating stimuli, the noise stimuli can be fashioned to excite one or other receptoral or postreceptoral mechanism. However, whereas habituation is assumed to have little effect at the first site, noise masking can potentially raise thresholds at both the first and the second sites. Although it is possible to selectively excite different first-stage cone mechanisms by modulating the noise along cone-isolating vectors or to selectively excite different second-stage color-discrimination mechanisms by modulating the noise along cardinal vectors, each noise stimulus inevitably excites both first- and second-stage mechanisms. As described in section "Sites of Limiting Noise" in Sec. 11.3 with respect to internal noise (see Figs. 12 and 13), changing the balance of noise at the first and second sites has the potential of rotating the detection contours in color space. Consequently, the discovery of detection contours for some noise vectors that do not align with the assumed low-level mechanism axes does not necessarily imply the existence of high-order mechanisms.

Gegenfurtner and Kiper[245] measured thresholds for a 1.2-cpd Gabor patch ($\sigma = 0.8°$ in space and 170 ms in time) in the presence of noise modulated in different directions around white in the L,M plane of DKL space. The target was either modulated in the L–M or L+M+S directions or in an intermediate direction along which the target color appeared to change between bright red and dark green. For all three directions masking was maximal when the noise was in the target direction, and minimal when it was in the orthogonal direction, even if the target direction did not lie along a cardinal axis. These findings suggested to the authors that there must be multiple mechanisms, some tuned to axes other than the cardinal ones.

The mechanisms derived by Gegenfurtner and Kiper, however, combined cone inputs nonlinearly. In a linear mechanism, the effectiveness of the noise should depend on the cosine between the cardinal direction and the noise direction, but Gegenfurtner and Kiper[245] found mechanisms that were more narrowly tuned. Curiously, when square rather than Gabor patches were used, evidence for multiple mechanisms was not found.

The central findings of Gegenfurtner and Kiper have been contradicted in other papers, some of which used comparable techniques. Sankeralli and Mullen[246] found evidence for only three mechanisms in $\Delta L/L$, $\Delta M/M$, $\Delta S/S$ cone contrast space using a 1-cpd semi-Gabor patch ($\sigma = 1.4°$ vertically, and 4° horizontally with sharp edges in space, and $\sigma = 170$ ms in time). Mechanism tuning was found to be linear in cone contrast units with a cosine relationship between the noise effectiveness and the angle between the mechanism and noise vectors. Giulianini and Eskew[175] working in the $\Delta L/L$, $\Delta M/M$ cone contrast plane using 200-ms circular Gaussian blobs ($\sigma = 1°$) or horizontal Gabor patches (1 cpd, $\sigma = 1°$) similarly found evidence for only two mechanisms in that plane. Their results were consistent with a linear L–M mechanism with equal cone contrast weights, and a linear L+M mechanism with greater L-than M-cone weights.

Some of Giulianini and Eskew's[175] results from their Fig. 5 are shown in Fig. 20, for noise masks in the chromatic direction (Fig. 20*a* and *c*) and in the M-cone direction (Fig. 20*b* and *d*). Their interpretation

of the data is shown by the solid contours in Fig. 20*a* and *b*. Their model is consistent with detection by two mechanisms with roughly constant L–M contours across the two noise directions, but L+M contours that rotate slightly away from the M-cone axis in the presence of M-cone noise. However, as our elliptical fits in Fig. 20*c* and *d* show, other interpretations of their data are also plausible; most of the data in the presence of chromatic and M-cone noise can be described by ellipses, but the major axes of the ellipses do not align with the noise directions.

Subsequently, Eskew, Newton, and Giulianini[179] extended these measurements to include S-cone modulations in the equiluminant plane, and again found no evidence for higher-order mechanisms in detection or near-threshold discrimination tasks. Some of their results are shown in Fig. 21. These data seem more consistent with a rounded parallelogram than an ellipse. All three studies just described, in contradiction to Gegenfurtner and Kiper,[245] found that the directions at which noise masking was maximal more closely aligned with the expected mechanism directions than with the noise directions. However, see also Hansen and Gegenfurtner.[247]

In a related study, D'Zmura and Knoblauch[248] did find evidence for multiple mechanisms within the equiluminant plane of DKL space. They used "sectored" noise made up of noise centered on the signal direction combined with noise of various strengths in the orthogonal direction. Contrast thresholds for "yellow," "orange," "red," and "violet" signals ($\sigma = 2.4°$ in space and 160 ms in time) were independent of the strength of the orthogonal noise, which suggests the existence of linear broad-band mechanisms tuned to each of the signal directions (for which the orthogonal direction is a null direction). Like Gegenfurtner and Kiper[245] multiple mechanisms were found, but they were broadly rather than narrowly tuned. D'Zmura and Knoblauch[248] argued that narrow tuning can result from off-axis looking in which subjects switch among multiple linear broad-band detection channels to reduce the noise and maximize the detectability of the signal.

An important caveat about D'Zmura and Knoblauch's experiments is that they used the 1924 $V(\lambda)$ function to equate luminance (see p. 3118 of Ref. 248). Because $V(\lambda)$ substantially underestimates luminous efficiency at short wavelengths, modulations of their blue phosphor will produce a luminance signal in their nominally equiluminant plane, which could complicate the interpretation of their results. For example, nominally S-cone modulations might have superimposed and cancelling L+M modulations, and some signal directions might be luminance-detected (and therefore artifactually independent of chromatic noise in the orthogonal direction). Nonetheless, Monaci et al.[249] using a related technique, but a better definition of luminous efficiency, came to the same conclusion.

Most recently, Giulianini and Eskew[250] used noise masking to investigate the properties of the S–(L+M) mechanism, and, in particular, whether or not the mechanism responds linearly to noises in different directions of cone contrast space. Though the effects of noise on the L–M mechanism are linear, for both polarities of the S–(L+M) mechanism (i.e., for +S and –S detection) its effects are nonlinear.[250]

## Chromatic Discrimination

***Basic Experiments*** Chromatic discrimination is the ability to distinguish the difference between two test lights that differ in chromaticity. The prototypical set of chromatic discrimination data are the discrimination ellipses of MacAdam[251] originally plotted as CIE *x,y* chromaticity coordinates, and thus in a color space that is not especially conducive to understanding the underlying mechanisms. These ellipses were determined from the variability of repeated color matches made at 25 different reference chromaticities in the CIE color space. Le Grand[252] reanalyzed MacAdam's data and found that much of the variability between the ellipses could be accounted for by considering variability along the tritan (S) dimension and along the cone-opponent (L–M) dimension. Interpretation of MacAdam's data is complicated by the fact that each ellipse was measured for a different state of adaptation, namely that determined by the mean match whose variability was being assessed.

Boynton and Kambe[253] made a series of discrimination measurements in the equiluminant plane along the important S and L–M color directions. They found that discrimination along the S axis depended on only S-cone excitation level; specifically that $\Delta S/S+S_0 = \text{constant}$, where $S$ is the background excitation and $S_0$ is an "eigengrau" or "darklight" term. At high S-cone excitation levels, as $S_0$ becomes less significant, Weber's law holds (i.e., $\Delta S/S$ is approximately constant).[254–256] A similar

conclusion was reached by Rodieck[257] in his reanalysis of MacAdam's[251] data (see Figs. XXIII-10 and XXIII-11 of Ref. 257). When plotted in a normalized cone excitation diagram, chromaticity ellipses for individual subjects have similar shapes regardless of the reference chromaticity.[258]

*Chromatic Discrimination Near Detection Threshold* Under conditions that isolate the chromatic mechanisms, near-threshold lights can be indistinguishable over fairly extended spectral or chromaticity ranges. On a white background using 0.75° diameter, 500-ms duration test discs, Mullen and Kulikowski[197] found that there were four indistinguishable wavelength ranges that corresponded to the threshold lights appearing orange (above 585 nm), pale yellow (566–585 nm), green (c. 490– 566 nm), and blue (c. 456–490 nm), and that there was weaker evidence for a fifth range that appeared violet (< c. 456 nm). Importantly, too, these boundaries were independent of the wavelength *differences* between pairs of lights, which suggests that each mechanism is univariant. These results suggest the existence of four or five distinct unipolar mechanisms at threshold.[197] Unlike the bipolar mechanisms (L–M) and S–(L+M), a unipolar mechanism responds with only positive sign. The bipolar (L–M) mechanism, for example, may be thought of as consisting of two unipolar mechanisms |L–M| and |M–L|, each of which is half-wave rectified (see "Unipolar versus Bipolar Chromatic Mechanisms" in Sec. 11.6).

Eskew, Newton, and Giulianini[179] looked at discrimination between near-threshold Gabor patches modulated in various directions in the equiluminant plane. Noise masking was used to desensitize the more sensitive L–M mechanism and thus reveal more of the S-cone mechanism, and perhaps higher-order mechanisms. Despite the presence of noise they found evidence for only four color regions within which lights were indiscriminable. These regions corresponded to detection by the four poles of the classical cone-opponent mechanisms |L–M|, |M–L|, |S–(L+M)|, and |(L+M)–S|. Some of their results are shown in Fig. 21. The four colors shown in the three outer arcs of the figure correspond to the four regions within which lights were indiscriminable. The data in each semicircular polar plot (filled squares) show the discriminability of a given chromatic vector from the standard vector shown by the arrow. The open circles are model predictions (see legend). There is no evidence here for higher-order color mechanisms. In a later abstract, Eskew, Wang, and Richters[259] reported evidence also from threshold level discrimination measurements for a fifth unipolar mechanism, which from hue-scaling measurements they identified as generating a "purple" hue percept (with the other four mechanisms generating blue, green, yellow, and red percepts).

Thus, the work of both Mullen and Kulikowski[197] and Eskew et al.[179,259] may be consistent with five threshold-level color mechanisms. By contrast, Krauskopf et al.[241] found evidence for multiple mechanisms. They measured the detection and discrimination of lights that were 90° apart in the equiluminant DKL plane and modulated either along cardinal or intermediate axes. No difference was found between data from the cardinal and noncardinal axes, which should not be the case if only cardinal mechanisms mediate discrimination. The authors argued that stimuli 90° apart modulated along the two cardinal axes should always be discriminable at threshold, because they are always detected by different cardinal mechanisms. In contrast, stimuli 90° apart modulated along intermediate axes will only be discriminable if they are detected by different cardinal mechanisms, which will not always be the case. Care is required with arguments of this sort, because angles between stimuli are not preserved across color space transformations (i.e., they depend on the choice of axes for the space and also on the scaling of the axes relative to each). More secure are conclusions based on an explicit model of the detection and discrimination process. Note that this caveat applies not just here but also to many studies that rely on intuitions about the angular spacing of stimuli relative to each other.

Clearly, colors that are substantially suprathreshold and stimulate more than one color mechanism should be distinguishable. However, the range of suprathreshold univariance can be surprisingly large. Calkins, Thornton, and Pugh[111] made chromatic discrimination and detection measurements in the red-green range from 530 to 670 nm both at threshold and at levels up to 8 times threshold. Measurements were made with single trough-to-trough periods of a 2-Hz raised-cosine presented on a yellow field of 6700 td and 578 nm. The observers' responses were functionally monochromatic either for wavelengths below the Sloan notch (between 530 and 560 nm) or for wavelengths above the Sloan notch (between 600 and 670 nm); that is, any two wavelengths within each range were indistinguishable at some relative intensity. The action spectra for indiscriminability above threshold

and for detection at threshold were consistent with an L–M opponent mechanism. Discrimination for pairs of wavelengths either side of the Sloan notch was very good, and between stimuli near the notch and stimuli further away from the notch was also good. The good discriminability near the notch is consistent with a diminution of |L–M| as the signals become balanced and with the intrusion of another mechanism, which between 575 and 610 nm has a spectral sensitivity comparable with the photopic luminosity function [although whether or not this corresponds to luminance or the L+M lobe of S–(L+M) is unclear]. For full details, see Ref. 111.

The results reviewed in this section are especially important because they suggest that each color mechanism is not only univariant, but behaves like a "labeled line." As Calkins et al. note on their p. 2365 "Phenomenologically speaking, the discrimination judgments [in the monochromatic regions] are based upon variation in perceptual brightness."

***Pedestal Experiments*** Discrimination experiments, sometimes called "pedestal experiments" can be used to investigate the properties of mechanisms over a range of contrasts both above and below the normal detection threshold. In a typical pedestal experiment, an observer is presented with two identical but brief "pedestal" stimuli, separated either in space or in time, upon one of which a test stimulus is superimposed. The observer's task is to discriminate in which spatial or temporal interval the test stimulus occurred. By presenting the test and pedestal stimuli to the same mechanism (sometimes called the "uncrossed" condition), it is possible to investigate the properties of chromatic and luminance mechanisms separately. By presenting the test and pedestal stimuli to different mechanisms (sometimes called the "crossed" condition), it is possible to investigate interactions between them. The presentation of the pedestals causes a rapid shift away from the mean adapting state. The transient signals produced by these shifts will be affected by instantaneous or rapid adaptation mechanisms, such as changes in the response that depend on static transducer functions, but not by more sluggish adaptation mechanisms.

When pedestal and test stimuli are both uncrossed and of the *same* sign, the discrimination of the test stimulus typically follows a "dipper" function as the pedestal contrast is increased. As the pedestal contrast is raised from below its contrast threshold, the threshold for detecting the test stimulus falls by a factor of about two or three, reaching a minimum just above the pedestal threshold, after which further increases in pedestal contrast hurts the detection of the test.[260–265] Facilitation has been explained by supposing there is a transducer (input-output) function that accelerates at lower contrasts, thus causing the difference in output generated by the pedestal and test-plus-pedestal to increase with pedestal contrast (e.g., Refs. 263, 266). Alternatively, it has been explained by supposing that the pedestal, because it is a copy of the test, reduces detection uncertainty.[267] The dipper function is found both for uncrossed luminance and uncrossed chromatic stimuli, and has similar characteristics for the two mechanisms.[169,268,269] When pedestals and test stimuli are uncrossed but of the *opposite* sign, increases in pedestal contrast first raise threshold—consistent with subthreshold cancellation between the pedestal and test. As the pedestal approaches its own threshold, however, discrimination threshold abruptly decreases, after which further increases in pedestal contrast hurt detection of the test for both uncrossed luminance and uncrossed chromatic conditions.[169] The increase followed by decrease in threshold has been referred to as a "bumper" function.[270] The dipper and bumper functions found under uncrossed conditions show clear evidence of subthreshold summation or cancellation. Figure 30*a* shows examples of the dipper (upper right and lower left quadrants) and bumper functions (upper left and lower right quadrants) for uncrossed L–M chromatic pedestals and targets from Cole, Stromeyer, and Kronauer.[169]

Presenting the pedestals and test stimuli to different mechanisms in the crossed conditions is a potentially powerful way of investigating how the luminance and chromatic mechanisms interact. For example, if the two mechanisms interact before the hypothesized accelerating transducer, then the crossed and uncrossed dipper and bumper functions should be comparable and should also show evidence for subthreshold interactions. If the chromatic and luminance mechanisms are largely independent until later stages of visual processing, then subthreshold effects should be absent, but given the uncertainty model suprathreshold facilitation might still be expected.

The results obtained with crossed test and pedestal stimuli, however, remain somewhat equivocal. Luminance square-wave gratings or spots have been shown to facilitate chromatic discrimination.[194,271]

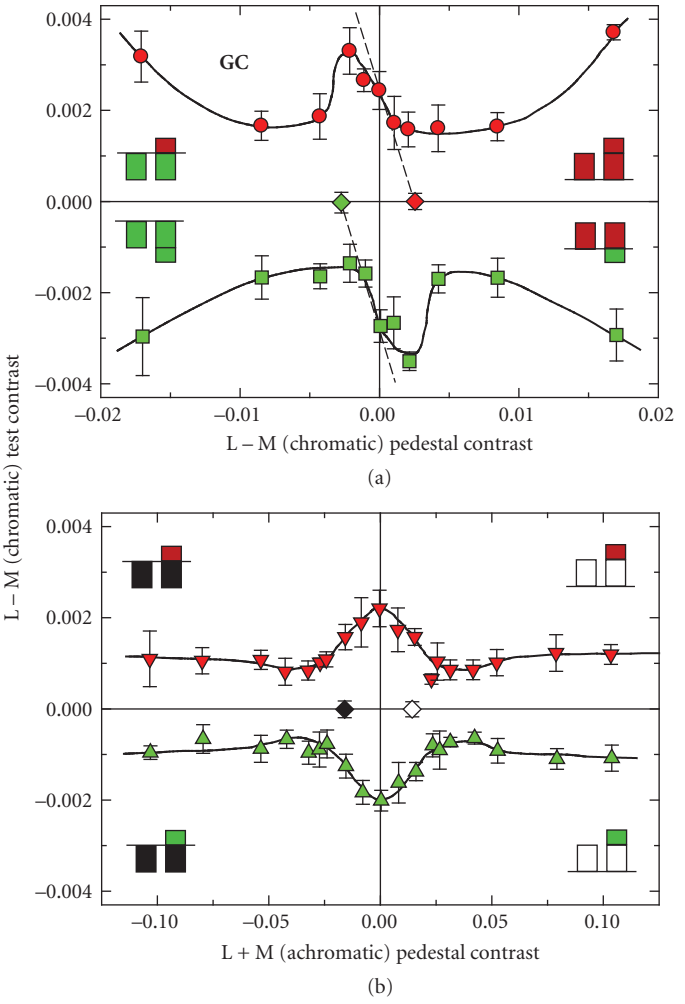


**FIGURE 30** Pedestal effects. (*a*) Detection of chromatic L–M tests on chromatic L–M pedestals. As indicated by the icons in each quadrant, the data points are the thresholds for detecting red chromatic targets (red circles) on either red (upper right quadrant) or green (upper left quadrant) chromatic pedestals, or for detecting green chromatic targets (green squares) on either red (lower right quadrant) or green (lower left quadrant) pedestals. The diamonds show the thresholds for detecting the red (red diamond) or green (green diamond) chromatic pedestals alone. The dashed lines show predictions that the discrimination of the presence of the test depends only on the intensity of the test plus the pedestal (which implies that pedestal alone is ineffectual). (*b*) Detection of chromatic L–M tests on achromatic L+M pedestals. As indicated by the icons, the data are the thresholds for detecting red chromatic targets (red inverted triangles) on incremental (upper right quadrant) or decremental (upper left quadrant) luminance pedestals, or for detecting green chromatic targets (green triangles) on incremental (lower right quadrant) or decremental (lower left quadrant) luminance pedestals. The diamonds show the thresholds for detecting the incremental (open diamond) or decremental (filled diamond) luminance pedestals alone. (*Data replotted from Figs. 4 and 5 of Cole, Stromeyer, and Kronauer.*[169] *Design of the figure based on Fig. 18.10 of Eskew, McLellan, and Giulianini.*[89])

Using sine-wave gratings, De Valois and Switkes[265] and Switkes, Bradley, and De Valois[268] found that crossed facilitation and masking was asymmetric: for luminance pedestals and chromatic tests they found facilitation and no masking, but for chromatic pedestals and luminance tests they found no facilitation and strong masking. This curious asymmetry has not always been replicated in subsequent measurements. Using spots, Cole, Stromeyer, and Kronauer[169] obtained equivalent results for crossed luminance pedestals and chromatic tests and for crossed chromatic pedestals and luminance tests. They found in both cases that increasing the contrast of the crossed pedestal had little effect on test threshold until the pedestal approached or exceeded its own threshold by a factor of two or more, and that further increases in pedestal contrast had little or no masking effect.[169] Figure 30*b* shows examples of their crossed luminance and chromatic results. Similarly, Mullen, and Losada[269] found facilitation for both types of crossed pedestals and tests when the pedestal was suprathreshold, but unlike Cole, Stromeyer, and Kronauer[169] they found crossed masking for higher pedestal contrasts. Chen, Foley, and Brainard,[272] however, obtained results that were more consistent with De Valois and Switkes[265] and Switkes, Bradley, and De Valois.[268] They used spatial Gabors (1 cpd, 1° standard deviation) with a Gaussian temporal presentation (40-ms standard deviation, 160-ms total duration), and investigated the effects of targets and pedestals presented in various directions of color space. They found masking for all target-pedestal pairs and facilitation for most target-pedestal pairs. The exceptions were that (1) equiluminant pedestals did not facilitate luminance targets, and (2) tritan (blue/yellow) pedestals facilitated only tritan targets.

So, what does all this mean? The fact that the crossed facilitation, when it is found, occurs mostly with suprathreshold pedestals[169,268,269] suggests that the interaction occurs after the stages that limit the thresholds in the chromatic and luminance mechanisms. This is surprising, given that center-surround L–M neurons respond to both chromatic and luminance gratings (see subsection "Multiplexing Chromatic and Achromatic Signals" in Sec. 11.5). This early independence is supported by findings with gratings that the crossed facilitation is independent of the spatial phase of the gratings.[268,269] However, the facilitation is not found with crossed dichoptic pedestals and tests. The finding that crossed facilitation survives if the luminance pedestal is replaced with a thin ring[169] suggests that it might be due to uncertainty reduction. However, yes-no psychometric functions and receiver operating characteristics show clearly that the facilitation of chromatic detection by luminance contours is inconsistent with the uncertainty model.[177] To explain their results, Chen, Foley, and Brainard[273] presented a model made up of three postreceptoral channels with separate excitatory inputs (producing facilitation), but each with divisive inhibition aggregated from all channels (producing masking).

Krauskopf and Gegenfurtner[255] performed a series of experiments in which chromatic discrimination was measured after an abrupt change in chromaticity away from an equal-energy-white adapting light (see also Refs. 274, 275). The change in chromaticity was effected by simultaneously presenting four 36-min diameter discs for 1 s. Three of the discs were of the same chromaticity, but the fourth was slightly offset from the others. The observer's task was to identify which disc was different. The task can be thought of as the presentation of three stimuli defined by a "pedestal" color vector from the white point with the fourth stimulus being defined by the vector sum of the pedestal vector plus a "test" vector.[89] The experiments were carried out in the DKL equiluminant plane at a luminance of 37 cd/m$^2$. The discrimination of a test vector along one of the cardinal axes was found to deteriorate if the pedestal vector was along the same axis, but was relatively unaffected if the pedestal vector was along the other axis. Color discrimination, therefore, depended primarily on the L–M and S–(L+M) mechanisms nominally isolated by modulations along the cardinal axes.[255] A more detailed determination of the shapes of chromatic discrimination ellipses for pedestal and test vectors along 16 color directions was also consistent with discrimination being determined by the cardinal mechanisms, but there was also evidence for another mechanism orientated along a blue-green to orange axis, from 135 to 315° in the DKL space.[255] This might reflect the existence of a higher-level mechanism, but it might also be consistent with other explanations. Maintaining the phosphors at 37 cd/m$^2$ [a photometric measure defined by the discredited CIE $V(\lambda)$ function that underestimates luminous efficiency in the blue and violet] results in modulation of the blue phosphor at nominal "equiluminance" producing a luminance (L+M) axis close to the blue-green axis. The effect of such a signal is hard to predict, but could affect the sensitivity of the S–(L+M) mechanism by

cancelling S, or it could be detected by L+M. Another possibility is that the evidence for an additional mechanism might instead reflect a small S-cone contribution to L–M, which would rotate the L–M mechanism axis.[89]

## Color Appearance and Color Opponency

When viewed in isolation (i.e., in the "aperture" mode), monochromatic lights have characteristic color appearances. Across the visible spectrum hues vary from violet through blue, blue-green or cyan, green, yellow-green, yellow, orange, and red.[276] Yet, however compelling these colors might seem, they are private perceptions. Consequently, to investigate them, we must move away from the safer and more objective psychophysical realms of color matching, color detection, and color discrimination, and rely instead on observers' introspections about their perceptual experiences (see Ref. 277 for a related discussion of "Class A" and "Class B" observations). Experiments that depend upon introspection are an anathema to some psychophysicists, yet they represent one of the few methods of gaining insights into how color is processed beyond the early stages of the visual system. As long as the limitations of the techniques are recognized, such experiments can be revealing. In addition, it is of interest to understand color appearance per se, and to do so requires the use of subjective methods in which observers report their experience.

Physiological measurements of the spectral properties of neurons in the retina and LGN are generally inconsistent with the spectral properties of color-appearance mechanisms, which suggests that color appearance is likely to be determined by cortical processes (see, e.g., Ref. 18). Relative to the input at the photoreceptors, the relevant neural signals that eventually determine color appearance will have undergone several transformations, likely to be both linear and nonlinear, before they reach the cortex. Despite this many models of color appearance are based on the assumption that appearance can be accounted for by mechanisms that linearly combine cone inputs (see Sec. 11.4). As we will see later, this is at best an approximation, at least for some aspects of color appearance. One reason for the failures of linearity may be that the suprathreshold test stimuli used to probe appearance are often adapting stimuli that intrude significantly on the measurements. That is, unlike in detection experiments where near-threshold tests can reasonably be assumed not to perturb the adapted state of the visual system very much, nonlinear adaptive processes cannot be ignored even for nominally steady-state color-appearance measurements, except perhaps under some contrived experimental conditions (see subsection "Linearity of Color-Opponent Mechanisms" in Sec. 11.5).

*Opponent-Colors Theory* Color appearance is often conceptualized in terms of Hering's opponent-color theory; that is, in terms of the perceptual opposition of red and green (R/G), blue and yellow (B/Y), and dark and light. In many versions of the model, the opponent mechanisms are assumed, either explicitly or implicitly, to combine their inputs from cones in a linear fashion.[11,12,18,19,29,76,278–282] Stage 3 of Fig. 4 represents a version of the linear model derived by the simple combinations of cone-opponent mechanisms (see subsection "Three-Stage Zone Models" in Sec. 11.6 for details).

The assumption of linearity constrains and simplifies the predicted properties of the color-opponent mechanisms. For example, under this assumption each opponent mechanism is completely characterized by its spectral response. As a function of wavelength, the R/G opponent mechanism responds R at both short and long wavelengths, corresponding to the red constituent in the appearance of both short- and long-wavelength lights, and responds G at middle wavelengths. The B/Y mechanism responds B at shorter wavelengths and Y at longer wavelengths. Each response (R, G, Y, or B) is univariant, and the responses of opposed poles (R vs. G, and B vs. Y) are mutually exclusive. The colors of lights detected solely by the same pole of a given mechanism cannot be distinguished at threshold, but lights detected by different poles can. In the model, color appearance depends on the relative outputs of the color-opponent appearance mechanisms. The individual mechanisms signal one opponent color or the other (e.g., redness or greenness) in different strengths, or a null.

The wavelength at which the opponent response of a mechanism changes polarity is a zero crossing for that mechanism, at which its response falls to zero. These zero crossings correspond to the unique hues. Unique blue and yellow are the two zero crossings for the R/G mechanism, and unique green and red are the two zero crossings for the Y/B mechanism. Unique red does not appear in plots

of valence against wavelength because it is extra-spectral (i.e., it has no monochromatic metamer and can only be produced by a mixture of spectral lights). Another extra-spectral color is white, which corresponds to an "equilibrium color" for *both* the R/G and B/Y mechanisms. A property of opponent-color mechanisms is that both the R/G and the Y/B mechanisms do not respond to a suitably chosen broadband white stimulus (such as an equal energy white). Thus, the sum of the outputs of the positive and negative lobes of each mechanism in response to such stimuli should be zero.

Tests of the assumptions of linearity of opponent-colors mechanisms are discussed below (see subsection "Linearity of Color-Opponent Mechanisms" in Sec. 11.5). See also Hurvich[283] for more details of opponent colors theory.

***Spectral Properties of Color-Opponent Mechanisms*** Several techniques have been used to investigate the spectral properties of the color-opponent mechanisms. Most rely on the assumption that opponent-color mechanisms can be nulled or silenced by lights or combinations of lights that balance opposing sensations. The null may be achieved experimentally by equating two lights so that their combination appears to be in equilibrium (see section "Appearance Test Measurements and Opponency" in Sec. 11.4). A closely related alternative is to find single spectral lights that appear to be in equilibrium for a particular mechanism (e.g., that appear neither red nor green, or neither blue nor yellow). Another related technique is hue scaling, in which lights are scaled according to how blue, green, yellow, or red they appear. Thus, lights that are rated 100 percent blue, green, yellow, or red are equilibrium or unique hues.

*Hue scaling* Despite the variety of color terms that could be used to describe the colors of lights, observers require only four—red, yellow, green, and blue—to describe most aspects of color appearance.[6,7] Other colors such as orange can be described as reddish-yellow, cyan as bluish-green, purple as reddish-blue, and so on. The need for just four color terms is consistent with opponent-colors theory. By asking observers to scale how blue, green, yellow, and blue spectral lights appear, hue scaling can be used to estimate the spectral response curves of the opponent mechanisms.[21,284–286] A cyan, for example, might be described as 50-percent green, 50-percent blue, and an orange as 60-percent red and 40-percent yellow. Figure 31 shows hue scaling data obtained by De Valois et al.,[21] who instead of using spectral lights used equiluminant modulations in DKL space, the implications of which are discussed below. Hue-scaling results have been reported to be consistent with hue-cancellation valence functions,[286] but inconsistencies have also been reported.[287]

*Color-opponent response or valence functions* As introduced in section "Appearance Test Measurements and Opponency," the phenomenological color-opponency theory of Hering[6] was given a more quantitative basis by the hue-cancellation technique.[279,280,288] Jameson and Hurvich (see Fig. 14 for some of their data) determined the amount of particular standard lights that had to be added to a spectral test light in order to cancel the perception of either redness, greenness, blueness, or yellowness that was apparent in the test light, and so produced "valence" functions. Figure 32 shows additional R/G valence data from Ingling and Tsou[12] and B/Y valence data from Werner and Wooten.[286] Individual lobes of the curves show the amounts of red, green, blue, or yellow light required to cancel the perception of its opposing color in the test light. The zero crossings are the "unique" colors of blue, green, and yellow.

These types of judgments are, of course, highly subjective because the observer must abstract a particular color quality from color sensations that vary in more than one perceptual dimension. In valence settings, the color of the lights at equilibrium depends on the wavelength of the spectral test light. Lights that are in red/green equilibrium vary along a blue-achromatic-yellow color dimension, while those in yellow/blue equilibrium vary along a red-achromatic-green color dimension. To reduce the need for the observer to decide when a light is close enough to the neutral point to accept the adjustment, some authors have used techniques in which the observer judges simply whether a presented light appears, for example, reddish or greenish, to establish the neutral points of each mechanism.[289]

*Unique hues and equilibrium colors* The equilibrium points of the R/G color opponent mechanism correspond to the unique blue and unique yellow hues that appear neither red nor green,

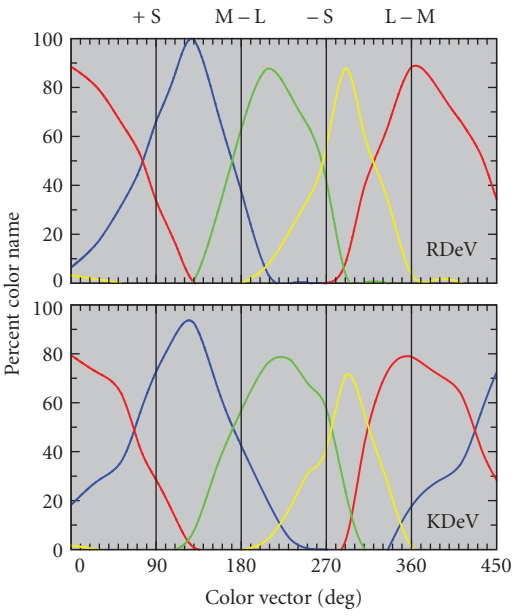


**FIGURE 31** Hue scaling. Data replotted from Fig. 3 (Observers: RDeV and KDeV) of De Valois, De Valois, Switkes, and Mahon.[21] The data show the percentage of times that a stimulus with a given color vector in the equiluminant plane of DKL space was called red (red lines), yellow (yellow lines), green (green lines), or blue (blue lines). The vertical lines indicate the cardinal axes at 90/450° (+S), 180° (M–L), 270° (–S), and 0/360° (L–M). With the exception perhaps of the red function for RDeV, the other hue naming functions do not align with the cardinal axes.

whereas those of the B/Y mechanism correspond to the unique green and unique red hues that appear neither blue nor yellow. These hues are "unique" in the sense that they appear phenomenologically unmixed.[290]

Measurements of the spectral positions of the unique hues have been made in several studies.[281,290–296] Kuehni[297] provides a useful summary of the unique hue settings from 10 relatively recent studies. For unique yellow, the mean and standard deviation after weighting by the number of observers in each study are 577.8 and 2.9 nm, respectively; for unique green, 527.2 and 14.9 nm; and for unique blue, 476.8 and 5.2 nm. Studies that generate colors either on monitors[22,289,298] or in print,[299,300] and therefore use desaturated, nonspectral colors, are not necessarily comparable with the results obtained using spectral lights, since perceived hue depends upon saturation.[301] The mean unique yellow, green, and blue wavelengths taken from Table of Kuehni[297] *excluding* those obtained by extrapolation from desaturated, nonspectral equilibrium lights are 576.3, 514.8, and 478.0 nm, respectively. Although unique hues show sizable individual differences, the settings within observers are generally quite precise.[302,303] Dimmick and Hubbard[290] review historical estimates.

Dimmick and Hubbard[290] reported, nearly 70 years ago, that unique blue and yellow and unique red and green are not complementaries (see also Ref. 304). By extending unique hue settings to include nonspectral colors it is possible to determine the equilibrium vectors of the opponent mechanisms in two dimensions or the equilibrium planes in three dimensions. Valberg[305] determined unique blues, greens, yellows, and reds as a function of saturation. Although not commented on in the original paper, two important features of his results were that (1) the unique red and green vectors plotted

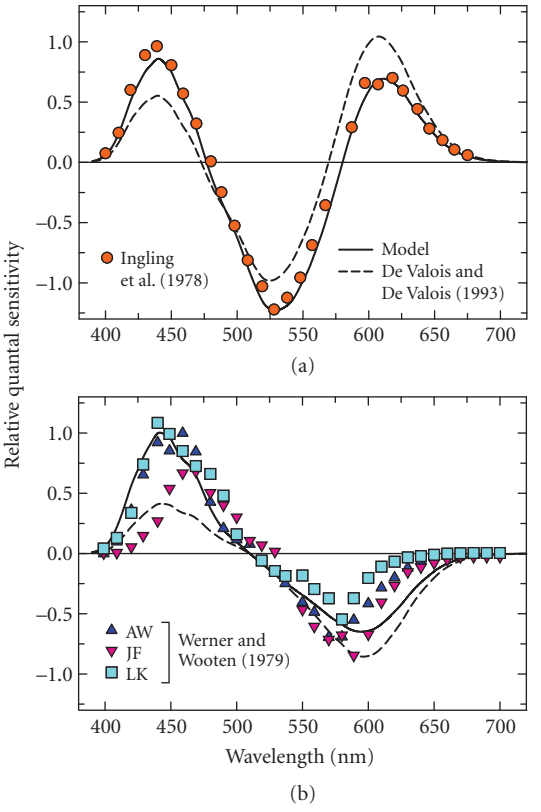


**FIGURE 32** Color valence data. (*a*) R/G valence data (red circles) replotted from Fig. 2A of Ingling, Russell, Rea, and Tsou.[314] (*b*) B/Y valence data for observers AW (dark blue triangles), JF (purple inverted triangles) and LK (light blue squares) replotted from Fig. 9 of Werner and Wooten.[286] The continuous lines are the spectral sensitivity predictions of Stage 3 of the Müller-zone model outlined in the text (see section "Three-Stage Zone Models" in Sec. 11.6). Each set of valence data has been scaled to best fit the spectral sensitivity predictions. For comparison, the spectral sensitivity predictions of the model proposed by De Valois and De Valois[18] are also shown as dashed lines, in each case scaled to best fit the Müller-zone model predictions.

in a CIE *x,y* chromaticity diagram were not colinear, and (2) unique yellow and blue vectors, though continuous through the white point, were slightly curved. Burns et al.[16] in a comparable experiment confirmed that the unique green and red vectors were not colinear, and that the unique blue vector was curved, but found that the unique yellow and green vectors were roughly straight.

Chichilnisky and Wandell[289] located equilibrium boundary planes by presenting stimuli varying in both intensity and chromaticity on various backgrounds, and then asking subjects to classify them into red-green, blue-yellow, and white-black opponent-color categories. They found that the opponent-color classification boundaries were not coplanar. Wuerger, Atkinson, and Cropper[22] determined the null planes for the four unique hues using a hue-selection task in which subjects selected the equilibrium hue from an array of colors. They concluded that unique green and unique red planes in a space defined by the color monitor phosphors were not coplanar, consistent with the previous findings, but

that unique blue and unique yellow could form a single plane. However, they did not try to fit their data with curved surfaces, as might be suggested by previous work.

In summary, unique red and green are not colinear in two-dimensional color space or coplanar in three, and the unique blue "vector" or "plane" is curved. As we discuss below, failures of colinearity or coplanarity imply that either a bipolar color-opponent mechanism is not a single mechanism or it is a single but nonlinear mechanism, while curved vectors and planes imply failures of additivity within single mechanisms.

## Linearity of Color-Opponent Mechanisms

*Tests of linearity* For the spectral sensitivities of color-opponent mechanisms to be generalizable implicitly or explicitly, the color-opponent mechanisms must be linear and additive. This assumption is made in many accounts of zero crossings and/or in descriptions of valence functions as linear combinations of the cone fundamentals.[11,18,19,24,29,76,278,279,306–308]

Larimer, Krantz, and Cicerone[307,309] specifically tested whether the equilibrium colors behaved additively under dark adapted conditions. They tested two predictions of additivity: (1) that equilibrium colors should be intensity-invariant (the so-called "scalar invariance law"), and (2) that mixtures of equilibrium hues should also be in equilibrium ("the additivity law"). Another consequence of these predictions is that the chromatic response or valence function should be a linear combination of the cone fundamentals.[75] For R/G opponency, Larimer, Krantz, and Cicerone[307] found that the spectral position of the blue and yellow equilibrium hues were intensity-invariant over a range of 1 to 2 log units, and that mixtures of red/green equilibrium hues remained in red/green equilibrium. These results suggest that R/G color opponency is additive. Additivity for the R/G mechanism has also been reported in other studies[310,311] and is consistent with the R/G valence functions being linear combinations of the cone spectral sensitivities.[12,286,312]

Several studies, however, suggest that linearity fails for the R/G mechanism. The curvilinear unique blue vector[16,305] implies that mixtures of lights that individually appear unique blue and therefore in R/G equilibrium will not be in equilibrium when they are mixed—as is required for additivity. Similarly, the nonplanar red-green color categories[289] also imply failures of additivity. Ayama, Kaiser, and Nakatsue[313] carried out an additivity test for red valence and found that while additivity was found for some pairs of wavelength within separate R valence lobes (400 paired with 440 nm and 610 paired with 680 nm) failures were found between lobes (400 paired with 680 nm) for 3 out of 4 observers. Ingling et al.[314] found that the short-wavelength shape of the R valence lobe was dependent on the technique used to measure it. If the redness of the violet light was assessed by matching rather than by cancellation, the estimate of redness was as much as 30 times less. Ingling, Barley, and Ghani[287] analyzed previous R/G hue cancellation and hue-scaling data and found them to be inconsistent with the linear model.

By contrast, most evidence suggests that the B/Y color-opponent mechanism is nonlinear. Larimer, Krantz, and Cicerone[309] found that equilibrium green was approximately intensity-invariant, but that equilibrium red was not, becoming more bluish-red as the target intensity was increased. Moreover, although mixtures of B/Y equilibrium hues remained in equilibrium as their overall intensity changed, the equilibria showed an intensity-dependence. Other results also suggest that B/Y color opponency is nonlinear. The unique green and red vectors are not colinear in two dimensions of color space[16,305] and the unique green and unique red planes are not coplanar.[22,289] These failures of colinearity and coplanarity suggest that the B and the Y valence function have different spectral sensitivities, but the same neutral or balance point. The failure of additivity is consistent with the fact that the B/Y valence functions cannot be described by a linear combination of the cone fundamentals; instead some form of nonlinearity must be introduced.[286,309] Elzinga and de Weert[315] found failures of intensity-invariance for equilibrium mixtures and attributed the failures to a nonlinear (power) transform of the S-cone input. Ayama and Ikeda[316] found additivity failures for combinations of several wavelength pairs. Ingling, Barley, and Ghani[287] found that previous B/Y hue cancellation and hue-scaling data were inconsistent with the linear model. Knoblauch and Shevell[317] found that the B/Y nonlinearity might be related to the signs of the cone signals changing with luminance.

Interestingly, the B/Y mechanism behaves linearly in protanopes and deuteranopes, which suggests that the nonlinearity might depend in some way on L–M.[318,319]

*Why linearity?* This question of whether color-opponent mechanisms are linear or nonlinear was originally formulated when it was still considered plausible that cone signals somehow fed directly into color-opponent channels without modification. Given our current knowledge of receptoral adaptation and postreceptoral circuitry, that hope now seems somewhat optimistic. Receptoral adaptation is an essentially nonlinear process, so that unless the adaptive states of all three cone types are held approximately constant (or they somehow change together as perhaps in the case of invariant hues), linearity will fail.

Tests that have found linearity have used elaborate experimental strategies to avoid the effects of adaptation. Larimer, Krantz, and Cicerone,[307,309] for example, used dark-adapted conditions and presented the stimuli for only 1 second once every 21 seconds. This protracted procedure succeeded in achieving additivity in the case of the red/green equilibrium experiments but not in the case of the blue/yellow ones.

It would be a mistake to conclude from results like these that color opponency and color appearance are, in general, additive with respect to the cone inputs. Experiments like those of Larimer, Krantz, and Cicerone[307,309] demonstrate additivity, but only under very specific conditions. While the results are important, because they provide information about the properties of the "isolated" postreceptoral mechanisms, they are not necessarily relevant to natural viewing conditions under which the mechanisms may well behave nonlinearly with respect to the cone inputs.

***Bezold-Brücke Effect and Invariant Hues*** Hue depends upon light intensity. Although a linear explanation of such hue changes has been suggested (see, e.g., Fig. 4 on p.74 of Hurvich[283]), it now seems clear that these changes reflect underlying nonlinearities in the visual response. These nonlinearities arise in part because the cone outputs are nonlinear functions of intensity, but they may also reflect inherent nonlinearities within the color-appearance mechanisms themselves and the way in which they combine cone signals. The dependence of hue on intensity is revealed clearly by the Bezold-Brücke effect,[320,321] which is illustrated in Fig. 33 using prototypical data from Purdy.[322] As the intensity of a spectral light is increased, those with wavelengths shorter than 500-nm shift in appearance toward that of an invariant blue hue of approximately 474 nm, while those with wavelengths

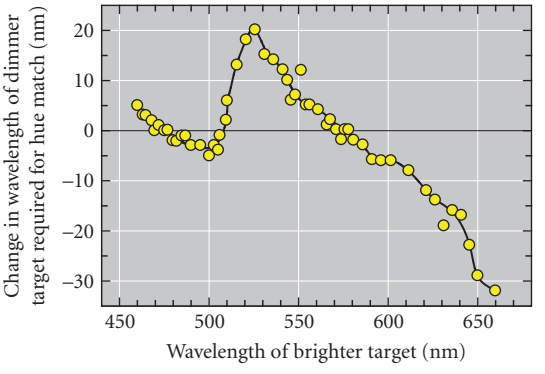


**FIGURE 33** Bezold-Brücke effect. Data replotted from Fig. 1 of Purdy[322] illustrating the changes in apparent hue as the light level increases, a phenomenon known as the Bezold-Brücke hue shift. The graph shows the change in the wavelength of a 100-td target from that of the 1000-td target required to match the hue of the 1000-td target plotted as a function of the wavelength of the more intense target.

longer than about 520 nm shift in appearance toward that of the invariant yellow of approximately 571 nm. Intermediate spectral colors shift to an invariant green of approximately 506 nm.

The invariant hues are usually assumed to coincide with the unique hues of color-opponent theory,[283] yet when the coincidence is tested, small discrepancies are found in some[284,322,323] but not all[307,309] studies (see also Ref. 296). Although invariant hues are often interpreted as being the zero crossings of cone-opponent mechanisms,[136] they are also consistent with models that incorporate just receptor adaptation.[323,324] As Vos[323] pointed out, if hue invariance and unique hues reflect different underlying processes, their approximate agreement may serve an important purpose.

*Color Appearance and Chromatic Adaptation* In the Bezold-Brücke effect, the level of adaptation is varied by increasing or decreasing the intensity of spectral lights of fixed wavelength. Under such conditions, as noted in the previous section, the appearances of some wavelengths are invariant with intensity. If, however, the state of chromatic adaptation is varied by superimposing the spectral lights on a chromatic background, their color appearance will change. In general, the appearances of targets superimposed on an adapting background move away from the appearance of the adapting wavelength. Thus, a target that appears yellow when viewed alone will appear reddish if superimposed on a middle-wavelength adapting background or greenish if superimposed on a long-wavelength one.[325–327] Similarly, the appearance of a superimposed target of the *same* wavelength as the adapting background will move toward the appearance of the equilibrium yellow hue. Indeed, on intense adapting fields of 560, 580, and 600 nm, Thornton and Pugh[107] showed that the spectral position of equilibrium yellow for a superimposed target coincided with the adapting field wavelength. However, this agreement breaks down on longer wavelength fields. Long-wavelength flashes presented on long-wavelength fields appear red, not equilibrium yellow.[65,328,329]

Historically, changes in color appearance with adaptation were thought to be consistent with von Kries adaptation,[330] in which the gain of each photoreceptor is attenuated in proportion to the background adaptation. However, von Kries adaptation cannot completely account for the changes in color appearance[77,331–333] (but see Ref. 334). In particular, asymmetric color matches, in which targets presented on different adapting backgrounds are adjusted to match in hue, do not survive proportional changes in overall intensity—as they should if the von Kries coefficient law holds.[335]

Jameson and Hurvich[336] proposed that the adapting field alters color appearance in two ways. First, by changing the cone sensitivities in accordance with von Kries adaptation, and second by an additive contribution to the appearance of the incremental mixture. For example, a red background tends to make an incremental target appear greener because it selectively adapts the L- cones, but it also tends to make it appear redder because it adds to the target. Color-appearance models of this sort remain in vogue (see Ref. 337). Figure 15 shows a case where a model with both gain control at the cones and an additive term accounts for much but not all of the variance in an asymmetric matching data set.

The details of this two-stage theory have been contentious, despite the fact that all authors are in essential agreement that much of the effect of the background is removed from the admixed background and test. Walraven,[325,338] using 1.5° diameter targets superimposed on 7° diameter backgrounds, determined the equilibrium mixtures of incremental 540 and 660 nm targets on various 660 nm backgrounds. He found that the equilibria were consistent with von Kries adaptation produced by the background, but that the color appearance of the background was completely discounted, so that it made no additive contribution to the appearance of the incremental target. By contrast, Shevell, using thin annuli or transiently presented 150-ms targets that were contiguous with the background, found that the background is not discounted completely and instead makes a small additive contribution to the target.[326,327,339] Walraven[338] suggested that Shevell's results reflected the fact that his conditions hindered the easy separation of the incremental target from the background. Yet, later workers came to similar conclusions as Shevell.[340–342] However, although the background is not entirely discounted, its additive contribution to color appearance is much less than would be expected from its physical admixture.[327,343] Thus, a discounting mechanism must be playing some role. Indeed, the failure of complete discounting is small compared to the magnitude of the additive term, so that the failure is very much a second-order effect.

*Color Appearance and Chromatic Detection and Discrimination* Several attempts have been made to link explicitly the cone-opponent effects evident in field sensitivity and field adaptation detection experiments with changes in color appearance measured under the same conditions.

On a white, xenon field, Thornton and Pugh[164] showed that the L–M cone-opponent detection implied by the Sloan notch is consistent with the suprathreshold color opponency implied by red-green hue equilibria. Thus, the wavelength of the notch, which is assumed to occur when the L–M cone-opponent signals are equal, coincided with an R/G equilibrium hue. A comparable convergence was found for 430- and 570-nm mixtures and the suprathreshold yellow-blue equilibrium locus.

S-cone thresholds on bichromatic mixtures of spectral blue and yellow fields are subadditive (see Fig. 26). According to the Pugh and Mollon[231] cone-opponent model, the greatest sensitization should occur when the opposing signals at the second site are in balance; that is, when the S- and L+M-cone signals are equal and opposite. In an attempt to link these cone-opponent effects to the color opponency of Hering, two groups have suggested that the background mixture that yields the lowest threshold, which is therefore the balance point of the cone-opponent at the second site, should also be the mixture that is in blue-yellow equilibrium (i.e., the mixture that appears neither yellow nor blue).

Pugh and Larimer[228] investigated the detection sensitivity of $\pi_1/\pi_3$ on field mixtures that appeared to be in yellow-blue equilibrium. They reasoned that if such mixtures are also null stimuli for the cone-opponent S–(L+M) second site, then detection sensitivity should depend only on first-site adaptation. Their results were consistent with their hypothesis, since field mixtures in yellow-blue equilibrium never produced superadditivity, a characteristic assumed to be due to second-site adaptation (see "Field Additivity" in Sec. 11.5). However, Polden and Mollon[227] looked specifically at the relationship between the maximum sensitization and the contribution of the longer wavelength component of the field mixture and found that it approximately followed a $V(\lambda)$ spectral sensitivity. By contrast, the comparable equilibrium hue settings for long-wavelength fields fell much more steeply with wavelength for fields longer than 590 nm, implying that different underlying spectral sensitivities operate in the two cases.

Rinner and Gegenfurtner[344] looked at the time course of adaptation for color appearance and discrimination and identified three processes with half lives of less than 10 ms, 40 to 70 ms, and 20 s. The slow and intermediate adaptation processes were common to color appearance and discrimination, but the fast process affected only color appearance. However, in an extensive study, Hillis and Brainard[78] compared the effects of chromatic adaptation on color discrimination and asymmetric color matching. Pedestal discrimination measurements made as a function of pedestal intensity on five different chromatic backgrounds were used to estimate the response-intensity curves on each background. These response-intensity curves were then used to predict pairs of light that should match on different pairs of backgrounds. The agreement they found between the predicted asymmetric matches and measured ones suggests that color appearance and discriminability on different uniform backgrounds are controlled by the same underlying mechanism.[78] A follow-up study reached the same conclusion about the effect of habituation on "unstructured" spatiotemporal contrast,[82] although this study did not probe performance with test stimuli likely to tap purported higher-order chromatic mechanisms.

Overall, the results of these experiments are somewhat equivocal, but the majority of experiments find some correspondence between the effects of adaptation on color detection and discrimination on the one hand, and its effects on color appearance on the other. Given, however, that the discrimination and appearance processes have very different spectral sensitivities, this correspondence must break down under some conditions of chromatic adaptation, at least if the signals that control the adaptation of mechanisms depend strongly on the output of those same mechanisms. Of note here is that Hillis and Brainard did find clear dissociations of the effect of adaptation on discrimination and on appearance when the stimuli contained sufficient spatial structure to be perceived as illuminated surfaces.[345] Elucidation of the nature of this dissociation awaits further investigation.

*Color Appearance and Habituation* The results of Webster and Mollon[32,79] were used as an example in subsection "Appearance Field Measurements and Second-Site Adaptation" in Sec. 11.4. Briefly, they

found that contrast adaptation produced changes in appearance that were selective for the habituating axis whether that axis was in the equiluminant plane or not. This finding is a potentially important difference between the effects of habituation on color appearance and its effects on detection, since only the appearance data provides clear evidence for higher-order mechanisms that are sensitive to both chromatic and luminance modulations. The detection data measured after habituation suggest that the chromatic and luminance mechanisms behave independently.[241] Determining conclusively whether this comparison across studies reflects a dissociation between habituation effects on thresholds and appearance, or instead represents a difference between the processing of near-threshold and suprathreshold test stimuli, could be resolved by applying the logic developed by Hillis and Brainard[78,82] to data collected for the full set of stimulus conditions studied by Webster and Mollon.[32,79]

Webster and Mollon[32,79] suggested two models that might account for their data. In the first, they replaced the three color mechanisms tuned to the three cardinal directions of color space with many mechanisms with tuning that varied according to a Gaussian distribution around each of the three cardinal directions. They found that they could account for the individual data by varying the standard deviations of the Gaussian distributions. In the second, they assumed that there were just three mechanisms, but that their tuning could be modified by adaptation. With adaptation, inhibition was assumed to build up between the mechanisms to decorrelate the input signals and reduce redundancy (see also Refs. 242–244). These models can also be applied to chromatic detection data.

***Luminance and Brightness*** Brightness matching functions are broader than luminous efficiency functions measured using techniques such as HFP or MDB that produce additive results (see subsection "Sensitivity to Spectral Lights" in Sec. 11.5) and are thought to measure the sensitivity of the luminance channel.[115,118,122,346]

Figure 34 shows examples of a brightness matching function measured by direct brightness matching (red line) and luminous efficiency measured by flicker photometry (black line) replotted from Wagner and Boynton.[122] The brightness matching function is relatively more sensitive in the blue and orange spectral regions and slightly less sensitive in the yellow. These differences are usually attributed to a chromatic contribution to brightness but not to luminance.[11,122,347]

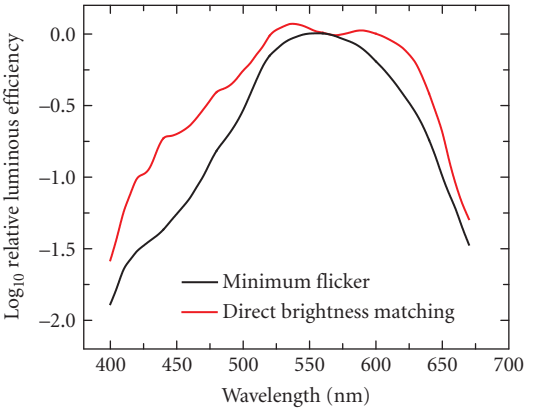


**FIGURE 34** Luminous efficiency and brightness. Mean matching data for three subjects replotted from Figs. 6 and 8 of Wagner and Boynton[122] obtained either using flicker photometry (black line) or using direct brightness matching (red line). The discrepancies are consistent with a chromatic contribution to brightness matching but not to flicker photometric matching.[120,122]

## Mechanisms of Color Constancy

The literature on mechanisms of color appearance is closely tied to a phenomenon known as "color constancy." The need for color constancy stems from two observations. First, our normal use of color appearance is to associate colors with objects. Second, the stimulus reflected to the eye from a fixed object depends not only on the object's intrinsic reflectance properties but also on the spectrum of the illumination. When the illuminant changes, so does the spectrum of the reflected light. If the visual system did not compensate for this change to stabilize the appearance of objects, it would not be possible to use color appearance as a reliable guide to object properties.

Empirically, color constancy is studied in much the same way as color appearance, using techniques of asymmetric matching, hue cancellation, or hue scaling. Papers published under the rubric of color constancy, however, have tended to employ stimulus conditions designed to model scenes consisting of illuminated objects and to emphasize context changes induced by manipulating the illuminant, rather than the simpler test-stimuli-on-background configurations favored for working out mechanistic accounts of color appearance.[348–353] The evidence supports the empirical generalization that when the illuminant is varied in a manner typical of the variations that occur in the natural environment, the visual system adapts to compensate for the physical change in reflected light, and thus to stabilize color appearance. That is, constancy in the face of naturally occurring illumination changes is good.[352,353] At the same time, it is important to note that constancy is not perfect: objects do not appear exactly the same across illumination changes. Moreover, other scene manipulations, such as those that change the reflectance of objects near the one of interest, also affect color appearance, even in rich scenes.[354] Figure 1 shows examples of this latter type of effect for simple stimulus configurations; these may be regarded as failures of constancy. Several recent reviews treat empirical studies of color constancy in more detail.[355–357]

Considerable theoretical attention has been devoted to modeling human color constancy. Much of this work is in the computational tradition, in which the theorist starts not with experimental data but rather by asking how constancy could in principle be achieved (or approximated), given the information about object reflectance properties that is available in the retinal image.[358–363]

With a few exceptions, work in the computational tradition does not connect explicitly with the mechanistic account of processing that we have developed in this chapter. Rather the work seeks to elucidate the sources of information in an image that could contribute to constancy. This is then used both to guide experiments[354] as well as in models whose purpose is to explicitly predict color appearance.[364–367] A particular promise of this approach is that it generalizes naturally as scene complexity increases, allowing (for example) predictions of the effects of manipulations in complex three-dimensional scenes using the principles developed for simpler scene configurations.[368–370]

A limitation of computational models is that they do not, in and of themselves, provide much insight about how neural mechanisms might act to provide constancy. Not surprisingly, then, there is also an important line of theoretical work that attempts to understand constancy in terms of the action of the first- and second-site mechanisms of adaptation that we have reviewed in this chapter.

Land's retinex theory[371–374] may be understood as a computational model that incorporates first-site cone-specific gain control to stabilize the representation of object color. Several authors have shown that for natural illuminant changes, such first-site gain control provides excellent, although not perfect, compensation for the effect of illumination changes on the light reflected from natural objects as long as the gains are set correctly for the scene illumination.[375–378] Moreover, asymmetric matching data from experiments conducted using rich, naturalistic stimuli are well fit by postulating first-site gain control.[352] Webster and Mollon[379] (see also Ref. 380) extended this general line of thinking by showing that following first-site cone-specific adaptation with a second-site process that is sensitive to image contrast can improve the degree of compensation for the physical effect of illuminant changes. As we have reviewed in subsections "Appearance Field Measurements and Second Site Adaptation" in Sec. 11.4 and "Color Appearance and Habituation" in Sec. 11.5, it has also been established that contrast adaptation affects color appearance,[32,79,379,381] which provides a connection between human performance and the observation that contrast adaptation can help achieve color constancy.

A number of authors[382–384] have emphasized that it is clarifying, in the context of understanding constancy and more generally adaptation, to distinguish two questions. First, what parameters of visual processing (e.g., first-site gains, subtractive terms, second-site gains) are affected by contextual factors. That is, what can adapt? Second, what are the particular contextual features that act to set each of the adaptable parameters? Our understanding of these aspects is less developed. For example, it is not obvious how theories based on data obtained with spatially uniform adapting fields should be generalized to predict the adapted state for image contexts that have rich spatial and temporal structure. Simple hypotheses for generalization include the idea that a weighted average of the cone coordinates of the image might play the role of the uniform field, as might the most luminous image region. Ideas of this sort are implicit, for example, in Land's retinex theory. Explicit tests of hypotheses of this nature for rich scenes, however, have not revealed simple scene statistics sufficient to predict the visual system's state of adaptation.[354] Indeed, understanding what image statistics are used by the visual system to achieve constancy, and connecting the extraction of these statistics explicitly to mechanistic sites of adaptation is a primary focus of current research on constancy. In this regard, the computational work may provide critical guidance, as at the heart of each computational theory is an analysis of where in the retinal image the most valuable information about the illumination may be found. Zaidi[385] and Golz and MacLeod,[386] for example, translate analyses of image statistics that carry information about the illuminant into mechanistic terms.

## Color and Contours

In the natural world, differently colored regions are usually delimited by contours across which there is also a luminance difference. If the luminance difference is removed, the contour becomes indistinct, and it becomes more difficult to discriminate the chromatic differences between the two regions. For example, Boynton, Hayhoe, and MacLeod[387] showed that color discrimination is severely impaired if the difference between two regions is dependent on only the S cones, and Eskew and Boynton[388] showed that the contour remains indistinct even for chromaticity differences up to twice threshold. For two regions separated by a border defined by S cones (i.e., if the regions are tritan pairs), "melting" of the border[389] and "chromatic diffusion" between the regions[388] have been reported.

Figure 35*a* shows two examples of chromatic regions filling in an area bordered by a luminance contour. These are versions of the "Boynton illusion" (see p. 287 of Ref. 15 and http://www.yorku.ca/eye/boynton.htm). The yellow areas, which are discriminated from the white background mainly by S cones, appear to fill-in the black borders as you move further away from the figure. The filling-in illustrates the tendency of luminance contours to constrain the spatial extent of signals mediated by the chromatic pathways.

Figure 35*b* shows four examples of a related illusion, which is known as the watercolor illusion or effect.[390–392] If an area is delineated by a darker outer chromatic contour flanked by a brighter inner chromatic contour, then the brighter color spreads faintly into the inner area.[393] This faint coloration resembles a "watercolor" wash.

*The "Gap" Effect and Luminance Pedestals* The gap effect is a well-known phenomenon described by Boynton, Hayhoe, and MacLeod.[387] A small gap introduced between two juxtaposed test fields improves their discriminability if the fields differ only in S-cone excitation, impairs it if they differ only in luminance, and can result in a small improvement if they differ only in L- and M-cone excitation at constant luminance (i.e., in L–M excitation).[387,394] The small gap that separates the tritan pair and improves discriminability can be produced either by a luminance difference or by an L–M chromatic difference.[395]

The improvement in chromatic discriminability caused by gaps can be related to the improvement in chromatic sensitivity when a luminance pedestal or contour is coincident with the chromatic stimulus[169,177,194,269,271,272]—the so-called "crossed" pedestal facilitation described above (see subsection "Pedestal Experiments" in Sec. 11.5). Moreover, as also noted above, the crossed facilitation survives if the luminance pedestal is replaced by a thin ring[169] (see also Ref. 177). Montag[394] compared the gap

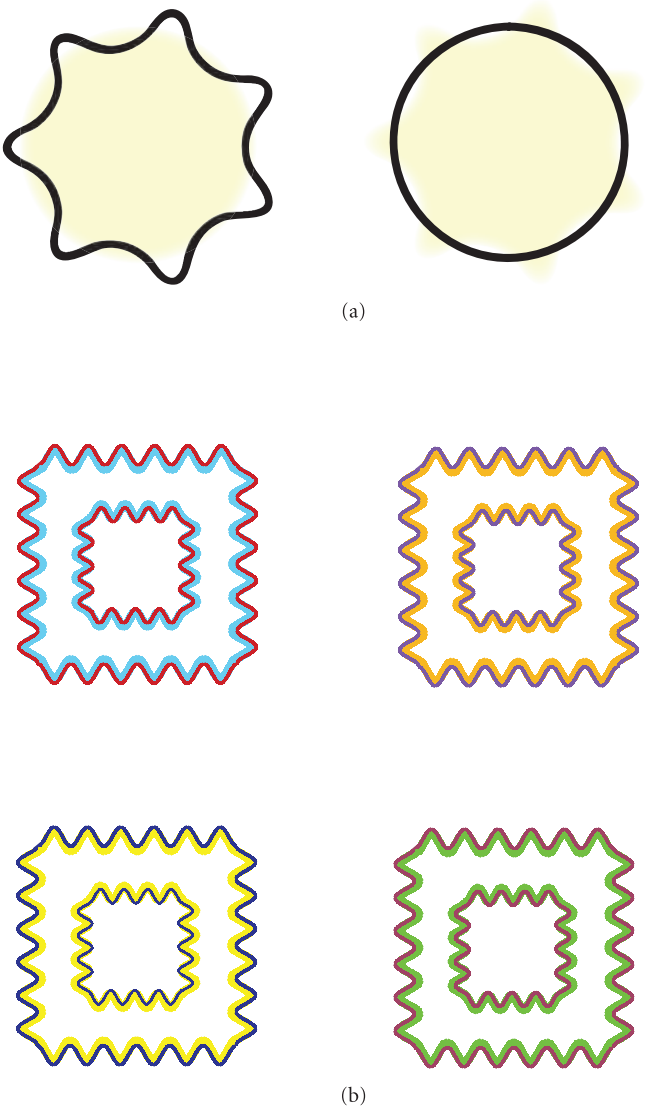

**FIGURE 35** Boynton and watercolor illusions. (*a*) Two examples of the Boynton illusion. In the left picture, a star-shaped black outline is superimposed on a circular yellow area, while in the right picture a circular black outline is superimposed on a star-shaped yellow area. As you move away from the picture, the yellow areas appear to fill the black outlines. These are variations of an illusion attributed to Robert M. Boynton by Peter Kaiser, see: http://www.yorku.ca/eye/boynton.htm. (*b*) Four examples of the watercolor illusion.[390–392] Each square is outlined by a pair of juxtaposed sinuous contours. The similar colors of the inner contour of each larger square and the outer contour of each smaller square fill in the intervening space with a faint color (which looks like a watercolor wash). Inspired by a version of the watercolor illusion designed by Akiyoshi Kitaoka, see: http://www.psy.ritsumei.ac.jp/~akitaoka/watercolorillusionsamples.jpg.

effect with facilitation produced by adding thin lines of the same orientation to gratings at half-cycle intervals. He found that the detection of S-cone gratings was facilitated by placing dark lines at the midpoints between the peaks and troughs of the gratings (i.e., where the luminance of the grating is equal to the mean luminance of the stimulus—zero crossings of the spatially varying factor in the stimulus), but that the facilitation declined to zero as the lines were moved toward the peaks and troughs. A comparable but smaller effect was found for equiluminant L- and M-cone modulated gratings, while the detection of luminance gratings was always impaired. Montag suggested that the gap effect and pedestal enhancement may be complementary effects.[394] Indeed, Gowdy, Stromeyer, and Kronauer[396] reported that the facilitation of L–M detection by luminance pedestals is markedly enhanced if the luminance grating is square-wave rather than sinusoidal. They argued that the square-wave produces an abrupt border across which the L–M mechanism is somehow able to compare chromatic differences.

*Color Appearance and Stabilized Borders* The importance of contours on color appearance is made clear in experiments in which the retinal image is partially or wholly stabilized. When the retinal image is wholly stabilized, the color and brightness of the stimulus fades until it is no longer seen.[397] The color appearance of partially stabilized images in which stabilized and unstabilized borders are combined can be entirely independent of the local quantal absorptions. Krauskopf[398] found that when the border between a disc and a surrounding annulus is stabilized, and the outer border of the annulus unstabilized, the disc "disappears" and its color is filled in by the color of the annulus. When, for example, the border between a green, 529-nm annulus, and an orange, 640-nm disc, is stabilized, the disc appears green. These changes are not restricted to the stabilized disc. Unstabilized targets presented on stabilized discs also change their color appearance as the color of the disc fills in to the color of the annulus.[399] For example, if the annulus is yellow and the stabilized disc is either red or green, both discs fill in to take on the yellow color of the annulus. Unstabilized yellow targets presented in the center of the stabilized discs, however, take on the color appearance complementary to actual color of the disc, so that the yellow target on a green disc appears red, and the yellow target on a red disc appears green. Such changes are consistent with the local contrast signals at the target edges determining the filled-in appearance of the yellow target (see Experiment 4 of Ref. 400).

It has also been reported that stabilized boundaries can produce colors that appear reddish-green and yellowish-blue, and so violate the predictions of the opponent-colors theory that opposed colors (red and green, or yellow and blue) cannot be perceived simultaneously. These "forbidden colors" were produced by presenting two vertical stripes side-by-side, with their common border stabilized, but their outer borders unstabilized. When the juxtaposed stripes were red and green, most observers reported that the merged stripes appeared reddish-green or greenish-red, and when the stripes were blue and yellow most observers reported that they appeared bluish-yellow[401] (see Experiment 3 of Ref. 400). Forbidden colors were also reported by some subjects in another study, but only when the stripes were equiluminant.[402]

The results obtained using stabilized and unstabilized borders add to the view that color appearance need not be a local retinal phenomenon. A crucial question, then, is whether the changes in color appearance caused by image stabilization also influence phenomena that are ostensibly more low-level, and thus more likely to be local, such as detection. Two experiments have addressed this question. Nerger, Piantanida, and Larimer[403] found that when a red disk was surrounded by a yellow annulus, stabilizing the edge between the two fields on the retina caused the yellow to fill in, making the disk appear yellow too. This filling-in affected the color appearance of small tests added to the disk, but it did not affect their increment threshold. The results for S-cone flicker detection, somewhat surprisingly, suggest that filling-in can change S-cone flicker sensitivity. Previously, Wisowaty and Boynton,[404] using flickering tritan pairs to isolate the S-cone response, had found that yellow background adaptation reduces the S-cone modulation sensitivity compared to no background adaptation. Piantanida[405] showed that the reduction in S-cone flicker sensitivity caused by a yellow field could also be caused by a dark field that only appeared yellow because its outer border with a yellow annulus was stabilized. In a related experiment, Piantanida and Larimer,[400] compared S-cone modulation sensitivities on yellow and green fields, and found that the S-cone modulation sensitivity was

lower on the yellow field. Again, this sensitivity difference depended upon the field appearance rather than upon its spectral content. Thus, the reduced sensitivity was found not only on the yellow field but also on a green field that appeared yellow because its border with a surrounding yellow annulus was stabilized. Similarly, the increased sensitivity was found not only on the green field but also on a yellow field that appeared green because its border with a surrounding green annulus was stabilized. The differences between studies may indicate that different sites of limiting noise act to limit detection in the different tasks.

*Contours and Aftereffects* Daw[406] showed that the saliency of colored after-images depended upon the presence of an aligned monochrome image. Thus, adaptation to a colored image produces a clear afterimage if the after-image is aligned with a monochrome image with the same contours, but produces a poor after-image if the two are misaligned. Figure 36 demonstrates this effect.

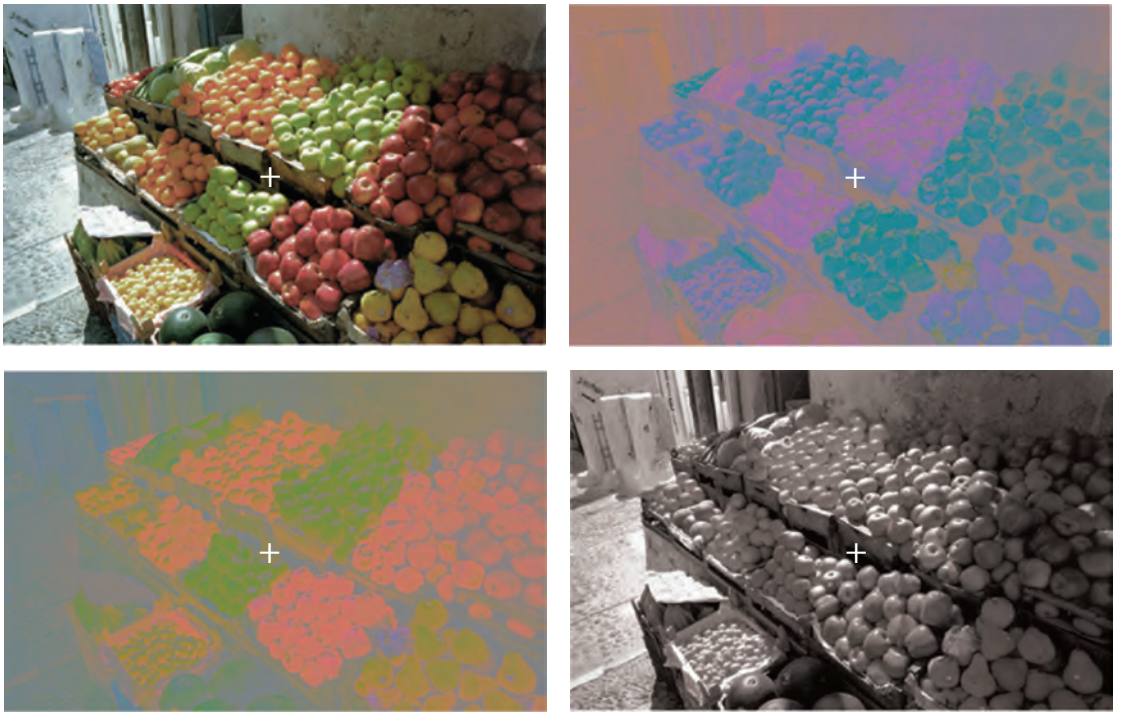

**FIGURE 36** Color and contour. Four different images of a fruit stall are shown. The full color image (top left) has been decomposed into its chromatic (bottom left) and luminance components (bottom right). The image on the top right is the complementary or inverse of the chromatic image. Notice that the details of the image are much better preserved in the luminance image than in the chromatic image. The chromatic information, although important for object discrimination and identification, is secondary to the perception of form. Color fills-in the picture delineated by the luminance information. This can be demonstrated by fixating the cross in the center of the complementary chromatic image (top right) for several seconds, and then diverting your gaze quickly to the cross in the center of the luminance image (bottom right). You should see a correctly colored version of the picture. Notice that if you shift your gaze slightly, so that the after-image no longer aligns precisely with the luminance image, the color disappears. You can also try adapting to the chromatic image (bottom left) and repeating the experiment. The effects are stronger with projected CRT versions of the images and successive presentation, which can be seen at http://www.cvrl.org. Color scene after Fig. 1.14A of Sharpe et al.[477] from an original by Minolta Corp. A version of this aftereffect demonstration was first described in 1962 by Nigel Daw.[406] Other examples of this illusion along with instructions about how to produce comparable images can be found at: http ://www.johnsadowski.com/color_illusion_tutorial.html.

Impressive demonstrations of the influence of contours on after-images have recently been produced by van Lier and Vergeer[407] and van Lier, Vergeer, and Anstis.[408] Their demonstrations show that colored stimuli can produce different after-image colors at the same retinal location, depending on the positioning of contours presented with the after-image. In one version, observers adapt to a plaid pattern made up of blue, green, orange, and purple squares, and then view, together with the after-image, either horizontal or vertical contours aligned with the borders of the squares. The color of the after-image changes with the orientation of the contours, because the "mean" after-image along the horizontal rows and along the vertical columns is different, thanks to the arrangement of the adapting squares in the plaid. The demonstration can be seen at: http://www-psy.ucsd.edu/~sanstis/SAai.html.

*McCollough Effect* The McCollough effect is a well-known orientation-contingent color after-effect.[409] After prolonged viewing of colored "adapting" gratings of, say, vertical or horizontal orientation, neutral, black-and-white test gratings of the same orientation take on the complimentary hue of the adapting grating. For example, following adaptation to red horizontal and green vertical gratings, horizontal and vertical black-and-white gratings appear, respectively, slightly greenish and reddish (see Fig. 37).

The McCollough effect can persist undiminished for many days provided that test gratings are not viewed.[410] This prolonged effect is distinct from colored afterimages, such as the effect demonstrated in the previous subsection, which decline relatively quickly. Vul, Krizay, and MacLeod[411] have recently identified two processes in the generation of the McCollough effect. The first process behaves like a leaky integrator, and produces an effect that declines exponentially with a time constant of roughly 30 s. The second process behaves like a perfect integrator, and produces an effect that shows no decay.[411] Several lines of evidence suggest that the McCollough effect is generated relatively early in the visual pathway. First, the McCollough effect exhibits little interocular transfer.[409,412,413] Second, it can by produced by alternating red-striped and green-striped adapting patterns at rates as high as 50 Hz, frequencies at which the colored patterns cannot be consciously perceived.[414] Third, it is dependent on the spectral content of the inducing stimuli, not their color appearance.[415] These findings suggest that the "adaptation" has an effect that occurs at a relatively early visual site that precedes binocularity, is able to respond high-frequency flicker, and retains some veridical information about the spectral content of lights. However, the contingency of the McCollough effect on grating orientation suggests that the site cannot be earlier than primary visual cortex, V1, where orientation selectivity is first clearly established.[416,417] There is an extensive literature on the McCollough effect (e.g., Refs. 418–423).

*Multiplexing Chromatic and Achromatic Signals* Information about color and contour may be transmitted—at least in part—by the same postreceptoral pathways. The ways in which these mixed signals are demultiplexed may give rise to some of the color and border phenomena described in the previous subsections. The evidence for the color-luminance multiplexing comes mainly from knowledge of the spatial properties of neuronal receptive fields in the early visual pathway. Cone-opponent, center-surround mechanisms that are also spatially opponent encode not only chromatic information, which is dependent upon the difference between the spectral sensitivities of their center and surround, but also "achromatic" information, which is dependent on the sum of their spectral sensitivities. For color, the center and surround behave synergistically producing a low-pass response to spatial variations in chromaticity, but for luminance they behave antagonistically producing a more band-pass response to spatial variations in luminance.[149–151] This type of multiplexing can, in principle, apply to any mechanism that is both chromatically and spatially opponent, but it is most often considered in the context of P-cells or midget ganglion cells, which make up as much as 80 percent of the primate ganglion cell population.[424] These cells are chromatically opponent with opposed L- and M-cone inputs,[36] but also respond to spatial differences in luminance.[425,426] In the fovea, they may be chromatically opponent simply by virtue of having single L- or M-cone centers [427,428] and mixed surrounds.[429–431] How segregated the L- and M-cone inputs are to P-cell surrounds and to P-cell centers in the periphery remains controversial.[432–440]

The multiplexing of color and luminance signals may just be an unwanted and unused artifact of having both spatial and chromatic opponency in P-cells. Indeed, Rodieck[441] has argued that the L–M

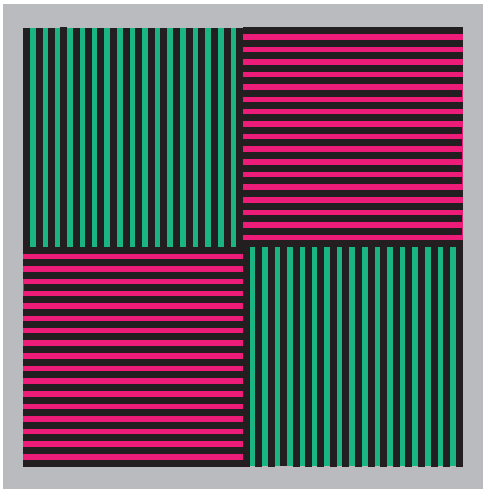

(a)

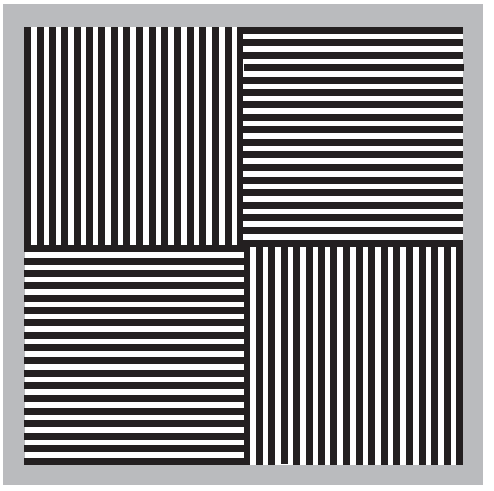

(b)

**FIGURE 37** McCollough effect. View the upper colored image (*a*) for several minutes letting your gaze fall on different colored areas for several seconds at a time. Look next at the lower monochrome image (*b*).

opponent system is mediated instead by a population of so-called Type II cells with coincident centers and surrounds, which are chromatically but not spatially opponent. For the multiplexing of color and luminance signals in cells with concentric center-surrounds to be unambiguously useful to later visual stages, the signals must be decoded. Several decoding strategies have been suggested, most of which depend on the chromatic signal being spatially low-pass filtered by the center-surround interaction, and the luminance signal being spatially band-pass filtered. Because of this filtering, signals between adjacent mechanisms will, in general, change slowly if the signals are chromatic and rapidly if they are achromatic. Thus, the chromatic and luminance signals can be decoded by spatially

low-pass or band-pass filtering, respectively, across adjacent mechanisms.[149,150] In such a scheme, low spatial-frequency luminance information and high spatial-frequency chromatic (edge) information is lost. The high-frequency luminance or edge information can be used both in "filling-in" the low spatial frequency luminance information, and to define missing chromatic edges. Several well-known visual illusions, such as the Craik-O'Brien-Cornsweet illusion (see Ref. 442), are consistent with filling-in, while others, such as the Boynton illusion (see Fig. 35*a*), are consistent with luminance edges defining chromatic borders.

Simple mechanisms for decoding the luminance and chromatic signals that difference or sum center-surround chromatically opponent neurons have been proposed.[153,443–445] Such mechanisms are, in fact, mathematically related to decoding using matched spatial filters.[445] In one version, spatially superimposed opponent cells with different cone inputs are either summed or differenced.[153] The band-pass luminance signal is decoded by summing +Lc–Ms and +Mc–Ls to give +(L+M)c–(L+M)s and by summing –Mc+Ls and –Lc+Ms to give –(L+M)c+(L+M)s, both of which are also bandpass and, in principle, achromatic (where c = center, s = surround). The low-pass chromatic signal is decoded by differencing +Lc–Ms and –Mc+Ls to give (+L–M)c,s and by differencing –Lc+Ms and +Mc–Ls to give (+M–L)c,s, both of which have spatially coincident centers and surrounds. These combination schemes are illustrated in Fig. 38. As Kingdom and Mullen[446] point out, superimposed centers with

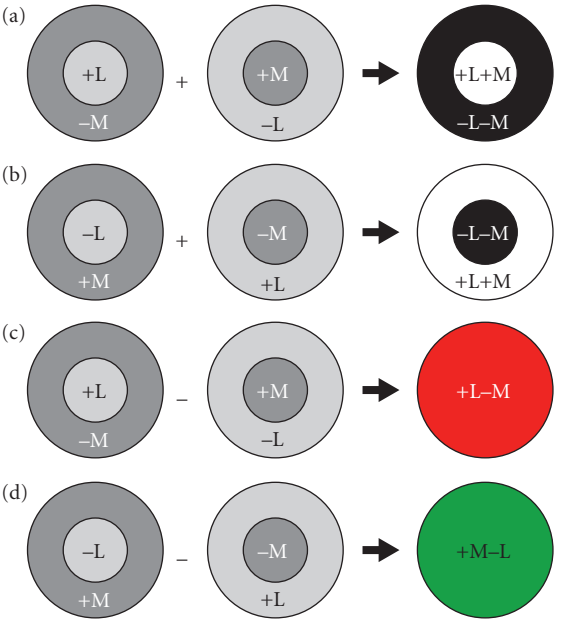


**FIGURE 38** Double-duty L–M center-surround opponency. Achromatic and chromatic information can be demultiplexed from LM-cone-opponent center-surround mechanisms by summing or differencing different types of mechanisms. Spatially opponent On and Off center achromatic mechanisms can be produced by summing, respectively, either (*a*) L and M On-center mechanisms, or (*b*) L and M Off-center mechanisms. Spatially nonopponent L–M and M–L chromatic mechanisms can be produced by differencing, respectively, either (*c*) L and M On-center mechanisms, or (*d*) L and M Off-center mechanisms. See Fig. 24 of Lennie and D'Zmura[478] and Fig. 2 of Kingdom and Mullen.[446]

different cone inputs must be spatially offset, simply because two cones cannot occupy the same space. They found that such offsets produce significant crosstalk between the decoded luminance and chromatic outputs. However, this problem is mitigated somewhat by the blurring of the image by the eye's optics, and, in the case of chromatic detection, by neural blurring (see Fig. 7 of Ref. 200).

In another version of the decoding mechanism, De Valois and De Valois[18] added S-cone inputs to generate spectral sensitivities more consistent with opponent-colors theory (see subsection "Spectral Properties of Color-Opponent Mechanisms" in Sec. 11.5). Billock,[445] by contrast, opposed P-cells of the same sign in both the center and surround, thus directly generating double-opponent cells. This can be achieved by differencing (e.g., +L–M in the center differenced from +L–M in the surround) or by summing (e.g., +L–M in the center summed with –L+M in the surround).

The importance of multiplexing in spatially and chromatically opponent mechanisms, and, in particular, in P-cells, remains controversial. Clearly, the P-cells, which make up 80 percent of the ganglion cells and have small receptive fields, must be important for spatial, achromatic vision, but their importance for color vision, while likely, is not yet firmly established. Speculative arguments have been based on the phylogenetically recent duplication of the M/L-cone photopigment gene, which is thought to have occurred about 30 to 40 million years ago after the divergence of Old and New World primates.[447] The typical argument is that the color opponency in P-cells is parasitic on an "ancient" system that before the duplication detected only luminance contrast.[448] However, this raises the possibility that the "decoding" of color information might be done simply to remove it and so improve image fidelity rather than to provide a color signal.

Many psychophysical experiments have attempted to elucidate the properties of the P-cells by employing equiluminant stimuli.[449] The idea is that these stimuli silence the M-cells and thus reveal the properties of the P-cells. If we accept this logic, there is still, of course, an important limitation to these experiments: they do not, by their design, provide any information about how the P-cells respond to luminance modulation. Thus, these experiments can provide only a partial characterization of the P-cells' response.

## 11.6 CONCLUSIONS

In Sections 11.3 and 11.4, we introduced basic mechanistic models for color discrimination and color appearance. Section 11.5 reviewed evidence that both supports the basic model and indicates areas where it is deficient. Here we summarize what we see as the current state of mechanistic models of color vision.

### Low-Level and Higher-Order Color-Discrimination Mechanisms

Test methods provide clear evidence for the existence of three low-level "cardinal" postreceptoral mechanisms: L–M, S–(L+M), and L+M in detection and discrimination experiments (see subsection "Test Sensitivities" in Sec. 11.5). This simple picture is complicated by evidence that L–M and L+M may have small S-cone inputs (see subsection "Sensitivity to Different Directions of Color Space" in Sec. 11.5), but nevertheless the weight of the evidence suggests that just three bipolar cardinal mechanisms (or six unipolar mechanisms—see next section "Unipolar versus Bipolar Chromatic Mechanisms") are sufficient to understand the preponderance of the data. Consistent with the existence of cardinal mechanisms, near-threshold color-discrimination experiments, with one exception,[241] require only four or five unipolar detection mechanisms.[179,197,260] Field methods (see subsection "Field Sensitivities" in Sec. 11.5) also confirm the importance of the three cardinal mechanisms. This agreement across methods provides strong psychophysical evidence for the independent existence of these mechanisms.

Test methods provide little or no evidence for the existence of "higher-order" (or noncardinal) mechanisms. Evidence for higher-order mechanisms comes almost entirely from field methods carried

out mainly in the DKL equiluminance plane using detection and habituation,[241] detection and noise masking,[245,248,450] discrimination and habituation,[241,255] texture segmentation and noise,[451] and image segmentation and noise.[452] In contrast, three experiments using detection and noise carried out with stimuli specified in cone contrast space found little or no evidence for higher-order mechanisms.[175,179,246]

In principal, the choice of space should not influence the results. However, the choice of space used to represent the data does tend to affect the ensemble of stimuli studied, in the sense that stimuli that uniformly sample color directions when they are represented in one space do not necessarily do so when they are represented in another. Another concern is that experiments carried out at nominal equiluminance are liable to luminance artifacts, since the elimination of luminance signals is, in practice, difficult to achieve. Aside from limits on calibration precision or inaccuracies introduced by the assumption that the 1924 CIE $V(\lambda)$ function (i.e., candelas/m$^2$) defines equiluminance, a recurring difficulty in producing truly equiluminant stimuli is that the luminance spectral sensitivity varies not only with chromatic adaptation and experimental task, but also shows large individual differences (see subsection "Luminance" in Sec. 11.5). Moreover, the luminance channel almost certainly has cone-opponent inputs (see Fig. 25). Finally, even when the luminance mechanism is silenced, the low-level L–M mechanism may have a small S-cone input, which will rotate the mechanism axis away from the cardinal axis.

These concerns notwithstanding, the results of field methods also suffer from an inherent ambiguity. Just because noise masking or habituation alters the detection spectral sensitivity does not necessarily reveal transitions between multiple higher-order mechanisms. Such changes can also result if the simple model used to characterize mechanisms fails to capture, for example, low-level interactions and nonlinearities. Indeed, Zaidi and Shapiro[243] have suggested that such "failures" might actually be an adaptive orthogonalization among cardinal mechanisms that reduces sensitivity to the adapting stimulus and improves sensitivity to the orthogonal direction. Moreover, noise masking can produce rotated detection contours by changing the balance of noise at the first and second sites (see subsection "Sites of Limiting Noise" in Sec. 11.3) without the need to invoke high-order mechanisms.

Of course, it would be absurd to suppose that higher-order color mechanisms do not exist in some form. They are clearly found in more "cognitive" experiments such as Stroop or reverse-Stroop experiments, which show clearly the effects of color categorization (e.g., Ref. 453). The central question with respect to color discrimination, however, is how such mechanisms can be revealed and investigated psychophysically using conventional threshold techniques. For example, if the site of limiting noise precedes higher-order mechanisms for most stimulus conditions, this may not be possible. In that case, the study of higher-order mechanisms will require the use of appearance or other experimental tasks in addition to knowledge of the input characteristics.

On the other hand, some discrimination tasks do provide clear evidence for higher-order mechanisms. Zaidi and Halevy[454] showed that the discrimination thresholds for an excursion in color space away from a background, the chromaticity of which was modulated at 0.46 Hz along a circle in the DKL equiluminant-color plane, depended on the direction of the background color change. Discrimination was consistently worse if the excursion was in the same direction as the background color change, than if it was in the opposite direction. Since this effect was independent of the actual background chromaticity, the effect is inconsistent with there being a limited number of cardinal mechanisms. More generally, Flanagan, Cavanagh, and Favreau[31] used the tilt after-effect to investigate the spectral properties of the orientation-selective mechanisms thought to underlie the after-effect. They found that the orientation-selectivity occurs independently in each of the three cardinal mechanisms, but they also found evidence for secondary orientation-selective mechanisms at other directions in color space. In addition, they found evidence for another orientation-selective mechanism that was nonselective for color directions in any color direction. Other experiments that suggest high-order mechanisms include visual search,[455] color appearance,[32,79,456] and the motion coherence of plaid patterns.[457] A unified understanding of when and why higher-order mechanisms are revealed experimentally remains an important question for the field.

## Unipolar versus Bipolar Chromatic Mechanisms

The strong implication that cone-opponent and color-opponent mechanisms may be unipolar rather than bipolar came first from physiology. The inhibitory range of LGN opponent cells

(i.e., the extent of decreases in firing rate from the resting or spontaneous level) is seldom more than 10 to 20 impulses per second, compared with an excitatory range of several hundred (i.e., the extent of increases in firing rate from the resting level).[458] Consequently, cells of both polarities (i.e., L–M and M–L) are required in a push-pull relationship to encode fully both poles of a cone-opponent response. By the cortex, the low spontaneous firing rates of cortical neurons makes cells effectively half-wave rectifiers, because they cannot encode inhibitory responses.[459,460] Thus, the bipolar L–M, M–L, S–(L+M), and (L+M)–S cone-opponent mechanisms must become unipolar |L–M|, |M–L|, |S–(L+M)|, and |(L+M)–S| cone-opponent mechanisms, while the bipolar R/G and B/Y mechanism become unipolar R, G, B, and Y mechanisms.

Behavioral evidence for unipolar mechanisms at the cone-opponent level is sparse in the case of the L–M mechanism, because the opposite polarity L–M and M–L detection mechanisms have similar cone weights (see subsection "Detection contours in the L, M Plane" in Sec. 11.5), so in many ways they behave like a unitary bipolar mechanism.[34] Nevertheless, there is some evidence that the |L–M| and |M–L| poles behave differently. In particular, habituations to sawtooth chromaticity modulations can selectively elevate thresholds for |L–M| or |M–L| targets.[14,461] Sankeralli and Mullen[462] raised detection threshold using unipolar masking noise and found that masking was most evident when the test and noise had the same polarity (thus, |L–M| noise selectively masks an |L–M| test, and |M–L| noise selectively masks an |M–L| test). Other evidence suggests that |L–M| and |M–L| are separate mechanisms at the fovea.[396,463] Evidence for separate mechanisms is also apparent in the peripheral retina, where the |L–M| mechanism predominates.[176,178,464]

There is better evidence for the existence of unipolar S-cone mechanisms. Sawtooth chromaticity modulations selectively elevate thresholds for |S–(L+M)| or |(L+M)–S| targets,[14,461] as do unipolar |S–(L+M)| or |(L+M)–S| masks.[462] Other evidence shows that (1) the spatial summation for S-cone incremental and decremental flashes differs,[465] (2) the longer wavelength field sensitivity for transient tritanopia is different for incremental and decremental flashes, which indicates different L- and M-cone inputs for the two S cone polarities,[466] and (3) habituation or transient adapting flashes have differential effects on S increment and S decrement thresholds.[467,468] There is also ample physiological and anatomical evidence that S-cone ON and OFF pathways are distinct (e.g., Ref. 2). For a recent review, see Ref. 34.

Eskew[34] takes the more philosophical stance that a psychophysical mechanism should be defined as a univariant mechanism, the output of which is a "labeled line."[469,470] This means that a bipolar cone-opponent mechanism cannot by definition be a unitary mechanism, since it can exist in two discriminable states (positive and negative).

## Discrepancies between Color-Discrimination and Color-Appearance Mechanisms

Much evidence indicates that color-discrimination and color-appearance mechanisms are distinct, at least given the linking hypotheses currently used to connect mechanism properties to performance.[14,16–22] As with color-discrimination mechanisms, much color appearance data may be accounted for by postulating three postreceptoral mechanisms. But the detailed properties of these mechanisms differ from those of the color-discrimination mechanisms.

In general, excitation of single cone-opponent mechanisms along cardinal directions does not give rise to the perceptions expected of isolated color-opponent mechanisms. Thus, the modulation of L–M around white produces a red/magenta to cyan color variation, whereas modulation of S around white produces a purple to yellow/green modulation.[31,32]

In specific tests of the relationship between color-discrimination and color-appearance mechanisms, unique hues, which correspond to the null vector of color-appearance mechanisms (see subsection "Spectral Properties of Color-Opponent Mechanisms" in Sec. 11.5), have been compared with the null vectors of color-discrimination mechanisms. Webster et al.[298] plotted pairs of unique colors of different saturation in DKL space. They found that only the unique red pair aligned with one of the cone-opponent axes, the L–M axis. The blue and yellow pair aligned roughly along an intermediate axis, but the green pair was not colinear with the red pair. Thus, unique blue and yellow, in particular,

must reflect the joint activity of L–M and S–(L+M). Chichilnisky and Wandell[289] and Wuerger, Atkinson, and Cropper[22] found that their four unique hue planes did not correspond to the null planes of color-discrimination mechanisms. Using a hue-naming technique, De Valois et al.[21] found that hue names are also not easily related to modulations of color-discrimination mechanisms (see Fig. 31).

The inconsistencies between color-discrimination and color-appearance mechanisms strongly suggest that the two are fundamentally different. But can they be considered to be mechanisms at different levels of a common serial processing stream or are they even more distinct? And if they do act serially, how might they be related? The simplified three-stage zone model described in the next section suggests that they could be parts of a common serial process and, at least for R/G, very simply related.

## Three-Stage Zone Models

As noted in the Introduction (see section "The Mechanistic Approach" in Sec. 11.2), linear three-stage Müller zone models,[23] in which the second stage is roughly cone-opponent and the third stage color-opponent, have been proposed by Judd[24] and more recently by Guth[29] and De Valois, and De Valois.[18]

The De Valois and De Valois[18] three-stage zone model is an interesting example based on physiological and anatomical assumptions about the relative numerosity of cone inputs to center-surround-opponent neurons. In their indiscriminate-surround model, neurons are assumed to have single cone inputs to their centers and mixed cone inputs to their surrounds (in the ratio of 10L:5M:S). Consequently, both the L–M and M–L cone-opponent stages have −S inputs, as a result of which the third color-opponent stage with an S input to R/G is arguably not needed (see Guth[471] and De Valois and De Valois[472]). [The dangers of assuming that cone weights can be simply related to relative cone numerosity were discussed before in the context of luminous efficiency (see subsection "Luminance" in Sec. 11.5).] The spectral sensitivities of the De Valois and De Valois[18] third-stage color-opponent mechanisms are shown in Fig. 32, as dashed black lines. Despite their physiologically based approach, the De Valois and De Valois[18] zone model inevitably derives from earlier psychophysical models, partly because there are only a limited number of ways in which the cone fundamentals can be linearly combined to produce plausible cone-opponent and color-opponent spectral sensitivities. As well as three-stage models, there are also many examples of two-stage models, in which the second stage is designed to account either for color-discrimination or for color-appearance data in isolation.[8–13,15]

As an exercise, we next provide an illustrative example of a linear three-stage zone model based on a few very simple assumptions about the signal transformations at each stage. Our goal was to see if we could derive plausible estimates of the zero crossings of opponent-colors theory without resorting to speculative physiological models or psychophysical data fitting.

*First zone* At the first stage, we assume the Stockman and Sharpe[28] cone fundamentals: $\bar{l}(\lambda)$, $\bar{m}(\lambda)$, and $\bar{s}(\lambda)$, the spectral sensitivities of which are labelled Stage 1 in Fig. 4. These functions are normalized to unity peak.

*Second zone* At the second stage, we assume classical cone opponency. In the case of L–M (and M–L), we assign equal cone weights, thus yielding $\bar{l}(\lambda)-\bar{m}(\lambda)$, and its opposite-signed pair $\bar{m}(\lambda)-\bar{l}(\lambda)$. This is consistent with the evidence from psychophysical detection experiments for equal L- and M-cone contrast weights into L–M (see subsection "Sensitivity to Different Directions of Color Space" in Sec. 11.5). Note that the zero crossing of this cone-opponent L–M mechanism is 549 nm, which is far from unique yellow. For the zero crossing to be near the 580 nm—the unique yellow assumed at the next stage—the relative M:L cone weight would have to be increased from 1 to 1.55 (see, e.g., Fig. 7.4 of Ref. 15).

In the case of S–(L+M) and (L+M)–S, we assign half the weight to M as to L (in accordance with many other models) and then scale both by 0.69 to give equal weights (in terms of peak spectral sensitivity) to S and L+0.5M, thus yielding $\bar{s}(\lambda)-0.69[\bar{l}(\lambda)+0.5\bar{m}(\lambda)]$ and its opposite signed pair $0.69[\bar{l}(\lambda)+0.5\bar{m}(\lambda)]-\bar{s}(\lambda)$. The zero crossing of this mechanism is 486 nm, which is closer to unique blue (a zero crossing of R/G) than to unique green (a zero crossing of Y/B). For a *linear* Y/B to have a zero crossing near unique green, the B pole must have a contribution from M or L. The cone weights

into the cone-opponent mechanisms assumed at the second level are consistent with psychophysical measurements of color detection and discrimination estimates (e.g., Table 18.1 of Ref. 89).

The spectral sensitivities of the cone-opponent pairs are labelled Stage 2 in Fig. 4. (The L–M sensitivities have also been scaled by 2.55 in accordance with the proposals for the next stage.)

*Third zone* At the third stage, we sum the outputs of the second-stage mechanisms (or equivalently oppose ones of different signs), to give four color-opponent mechanisms (see also Refs. 29 and 18). The L–M cone-opponent input to the third stage is weighted by 2.55, so that R/G is zero for an equal-quantum white light, thus:

Red [L–M summed with S–(L+M)]

$$2.55[\bar{l}(\lambda)-\bar{m}(\lambda)]+(\bar{s}(\lambda)-0.69[\bar{l}(\lambda)+0.5\bar{m}(\lambda)])=1.86\bar{l}(\lambda)-2.90\bar{m}(\lambda)+\bar{s}(\lambda)$$

$$\text{(bipolar) or } |1.86\bar{l}(\lambda)-2.90\bar{m}(\lambda)+\bar{s}(\lambda)|\text{(unipolar)}$$

Green [M–L and (L+M)–S summed]

$$2.55[\bar{m}(\lambda)-\bar{l}(\lambda)]+(0.69[\bar{l}(\lambda)+0.5\bar{m}(\lambda)]-\bar{s}(\lambda))=-1.86\bar{l}(\lambda)+2.90\bar{m}(\lambda)-\bar{s}(\lambda)$$

$$\text{(bipolar) or } |-1.86\bar{l}(\lambda)+2.90\bar{m}(\lambda)-\bar{s}(\lambda)|\text{(unipolar)}$$

R/G is required to be zero for an equal-quantal white, because otherwise, according to opponent-colors theory, such whites would appear colored (see Ref. 283). Initially, we used the same weights for the cone-opponent inputs to B/Y and Y/B, thus:

Blue [M–L summed with S–(L+M)]

$$2.55[\bar{m}(\lambda)-\bar{l}(\lambda)]+(\bar{s}(\lambda)-0.69[\bar{l}(\lambda)+0.5\bar{m}(\lambda)])=-3.24\bar{l}(\lambda)+2.21\bar{m}(\lambda)+\bar{s}(\lambda)$$

$$\text{(bipolar) or } |-3.24\bar{l}(\lambda)+2.21\bar{m}(\lambda)+\bar{s}(\lambda)|\text{(unipolar)}$$

Yellow [L–M summed with (L+M)–S]

$$2.55[\bar{l}(\lambda)-\bar{m}(\lambda)]+(0.69[\bar{l}(\lambda)+0.5\bar{m}(\lambda)]-\bar{s}(\lambda))=3.24\bar{l}(\lambda)-2.21\bar{m}(\lambda)-\bar{s}(\lambda)$$

$$\text{(bipolar) or } |3.24\bar{l}(\lambda)-2.21\bar{m}(\lambda)-\bar{s}(\lambda)|\text{(unipolar)}$$

The spectral sensitivities of the color-opponent mechanisms are labelled Stage 3 in Fig. 4. The R/G mechanism yields reasonable estimates of unique blue (477 nm) and unique yellow (580 nm), and the B/Y mechanism yields a reasonable estimate of unique green (504 nm).

One potential problem, however, is that the opposing poles of B/Y and Y/B are unbalanced (as they also are in the De Valois and De Valois model), so that B/Y and Y/B will produce a nonzero response to an equal-quantum white. Given that Y > B, the white field would be expected to appear yellowish. This imbalance can be corrected by decreasing the relative contributions of Y perhaps after the half-wave rectification of B/Y into unipolar B and Y mechanisms. Alternatively, it can be corrected by decreasing the weights of the L- and M-cone inputs into B/Y and into Y/B. For this illustrative example, we choose the latter correction and accordingly scale the weights of the L- and M-inputs into Y/B by 0.34 to give a zero response to white, so that:

Blue [M–L summed with S–(L+M)] becomes

$$-1.10\bar{l}(\lambda)+0.75\bar{m}(\lambda)+\bar{s}(\lambda)\text{(bipolar) or } |-1.10\bar{l}(\lambda)+0.75\bar{m}(\lambda)+\bar{s}(\lambda)|\text{ (unipolar)}$$

Yellow [L–M summed with (L+M) –S] becomes

$$1.10\bar{l}(\lambda)-0.75\bar{m}(\lambda)-\bar{s}(\lambda)\text{(bipolar) or } |1.10\bar{l}(\lambda)-0.75\bar{m}(\lambda)-\bar{s}(\lambda)|\text{(unipolar)}$$

The spectral sensitivities of the Y/B and B/Y color-opponent pair are shown in the lower right panel of Fig. 4 as dashed lines. The correction shifts unique green to 510 nm. Such post hoc adjustments are inevitably somewhat speculative, however. Moreover, given that B/Y is clearly nonlinear (see subsection "Linearity of Color-Opponent Mechanisms" in Sec. 11.5), any mechanism that adjusts the balance of B/Y is also likely to be nonlinear.

Nonetheless, this example demonstrates that plausible estimates of the zero crossings of third-stage color opponency can be generated by making a few very simple assumptions about the transformations at the cone-opponent and color-opponent stages. But, how close are the R/G and B/Y spectral sensitivities to color-appearance data at wavelengths removed from the zero crossings? Figure 32 compares the R/G and B/Y spectral sensitivities with color valence data. Figure 32*a* shows as red circles R/G valence data from Ingling et al.[314] scaled to best (least-squares) fit the R/G spectral sensitivity. As can be seen, the agreement between R/G and the valence data is remarkably good. Figure 32*b*, shows B/Y valence data for three subjects (AW, JF, and LK, dark blue triangles, purple inverted triangles, and light blue squares, respectively) from Werner and Wooten[286] each scaled to best (least-squares) fit B/Y. Consistent with their own failed attempts to find linear combinations of cone fundamentals to describe their B/Y valence data,[286] our B/Y spectral sensitivity agrees only approximately with the data for AW and LK, and poorly with the data for JF.

Also shown in Fig. 32 are the spectral sensitivities of R/G and B/Y color-opponent mechanisms proposed by De Valois and De Valois[18] scaled to best fit our functions. Their R/G and B/Y functions agree poorly with our functions and with the valence data. In contrast, our R/G spectral sensitivity agrees well with the proposal by Ingling et al.,[314] which was based on the valence data shown in Fig. 32*a* (see also Ref. 12).

In summary, simple assumptions about signal transformations at the second and third stages yield a reasonable estimate of the spectral sensitivity of the R/G color-opponent mechanism. Perhaps, then, the R/G mechanism does reflect a cortical summing of the chromatic responses of double-duty L–M center-surround neurons and S–(L+M) neurons as has been suggested before.[18,29] In contrast, the B/Y mechanism cannot be accounted for so simply, and may reflect much more complex nonlinear transformations (see subsection "Linearity of Color-Opponent Mechanisms" in Sec. 11.5). These differences between R/G and B/Y could be linked to the idea that the R/G mechanism represents the opportunistic use of an existing or perhaps slightly modified neural process following the relatively recent emergence of separate L- and M-cone photopigment genes,[447] whereas the B/Y mechanism is some more ancient neural process.[448]

Figure 39 shows a speculative "wiring" diagram of the three-stage Müller zone model.

## Final Remarks

Although the three-stage zone model provides a way to integrate the separate two-stage models required for discrimination and for appearance, it is important to note several limitations.

First, as formulated, it does not account for the nonlinearities in unique hue and hue-scaling judgments described in "Linearity of Color-Opponent Mechanisms" in Sec. 11.5. It is possible that explicitly incorporating nonlinearities in the contrast-response functions of each stage could remedy this, but this remains an open question.

Second, the model as outlined just above is for a single state of adaptation. We know that adaptive processes act at both the first and second stages and, with the three-stage models, the effects of these would be expected to propagate to the third stage and thus affect both discrimination and appearance in a common fashion. Although some data, reviewed in "Color Appearance and Chromatic Detection and Discrimination" in Sec. 11.5, suggest that this is the case, further investigation on this point is required. In addition, test on pedestal data for crossed conditions suggest that somewhere in the processing chain there may be additional cross mechanism adaptive effects. Such effects have also been suggested to play a role in appearance data.[381]

Third, the model as formulated does not explicitly account for effects of the temporal and spatial structure of the stimuli. These components could certainly be added, but whether this can be done in a parsimonious fashion that does justice to the empirical phenomena is not clear. If our mechanistic understanding of color vision is to be applied to natural viewing, then its extension to handle the

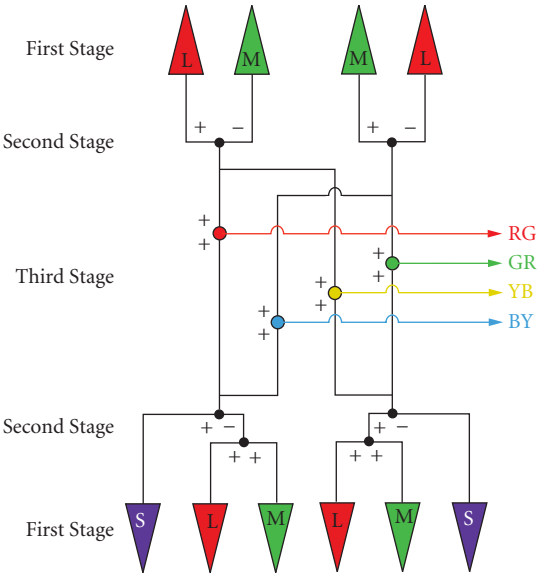


**FIGURE 39** Three-stage Müller zone model. *First stage:* L-, M-, and S-cone photoreceptors (top and bottom). *Second stage:* L–M and M–L cone opponency (top) and S–(L+M) and (L+M)–S cone opponency (bottom). *Third stage:* Color opponency (center) is achieved by summing the various cone-opponent second-stage outputs.

complexity of natural retinal stimulation must be a high priority. At the same time, this is a daunting problem because of the explosion in stimulus parameters and the difficulties in controlling them adequately that occur when arbitrary spatiotemporal patterns are considered for both test and field.

Finally, we do not know whether models of this sort can provide a unified account of data across a wider range of tasks than simple threshold and appearance judgments.

Despite these unknowns and limitations, the type of three-stage model described here provides a framework for moving forward. It remains to be seen whether a model of this type will eventually provide a unified account of a wide range data, or whether what will be required, as was the case with Stiles' $\pi$-mechanism model which preceded it, is a reconceptualization of the nature of the psychophysical mechanisms and/or the linking hypotheses that connect them to behavioral data.

## 11.7 ACKNOWLEDGMENTS

The first author acknowledges a significant intellectual debt to Rhea Eskew not only for his writings on this subject, but also for the many discussions over many years about color detection and discrimination. He also acknowledges the support of Sabine Apitz, his wife, without whom this chapter could not have been written; and the financial support of the Wellcome Trust, the BBSRC, and Fight for Sight. The second author acknowledges the support of NIH R01 EY10016. The authors are grateful to Bruce Henning for helpful discussions, proofreading and help with Fig. 20, and Caterina Ripamonti for help with Fig. 16. They also thank Rhea Eskew, Bruce Henning, Ken Knoblauch, and Caterina Ripamonti for helpful comments on the manuscript.

## 11.8 REFERENCES


1. K. R. Gegenfurtner and D. C. Kiper, "Color Vision," *Annual Review of Neuroscience* **26:**181–206(2003).
2. P. Lennie and J. A. Movshon, "Coding of Color and Form in the Geniculostriate Visual Pathway," *Journal of the Optical Society of America A* **10:**2013–2033 (2005).
3. S. G. Solomon and P. Lennie, "The Machinery of Colour Vision," *Nature Reviews Neuroscience* **8:**276–286 (2007).
4. T. Young, "On the Theory of Light and Colours," *Philosophical Transactions of the Royal Society of London* **92:**20–71 (1802).
5. H. von Helmholtz, *Handbuch der Physiologischen Optik*, Hamburg and Leipzig, Voss, 1867.
6. E. Hering, *Zur Lehre vom Lichtsinne. Sechs Mittheilungen an die Kaiserliche Akademie der Wissenschaften in Wien*, Carl Gerold's Sohn, Wien, 1878.
7. E. Hering, *Grundzüge der Lehre vom Lichtsinn,* Springer, Berlin, 1920.
8. L. M. Hurvich and D. Jameson, "An Opponent-Process Theory of Color Vision," *Psychological Review* **64:**384–404 (1957).
9. R. M. Boynton, "Theory of Color Vision," *Journal of the Optical Society of America* **50:**929–944 (1960).
10. P. L. Walraven, "On the Mechanisms of Colour Vision," Institute for Perception RVO-TNO, The Netherlands, 1962.
11. S. L. Guth and H. R. Lodge, "Heterochromatic Additivity, Foveal Spectral Sensitivity, and a New Color Model," *Journal of the Optical Society of America* **63:**450–462 (1973).
12. C. R. Ingling, Jr. and H. B.-P. Tsou, "Orthogonal Combination of the Three Visual Visual Channels," *Vision Research* **17:**1075–1082 (1977).
13. S. L. Guth, R. W. Massof, and T. Benzschawel, "Vector Model for Normal and Dichromatic color vision," *Journal of the Optical Society of America* **70:**197–212 (1980).
14. J. Krauskopf, D. R. Williams, and D. W. Heeley, "Cardinal Directions of Color Space," *Vision Research* **22:**1123–1131 (1982).
15. R. M. Boynton, *Human Color Vision,* Holt, Rinehart and Winston, New York, 1979.
16. S. A. Burns, A. E. Elsner, J. Pokorny, and V. C. Smith, "The Abney Effect: Chromaticity Coordinates of Unique and Other Constant Hues," *Vision Research* **24:**479–489(1984).
17. M. A. Webster and J. D. Mollon, "Contrast Adaptation Dissociates Different Measures of Luminous Efficiency," *Journal of the Optical Society of America A* **10:**1332–1340 (1993).
18. R. L. De Valois and K. K. De Valois, "A Multi-Stage Color Model," *Vision Research* **33:**1053–1065 (1993).
19. I. Abramov and J. Gordon, "Color Appearance: On Seeing Red-or Yellow, or Green, or Blue," *Annual Review of Psychology* **45:**451–485 (1994).
20. R. T. Eskew, Jr. and P. M. Kortick, "Hue Equilibria Compared with Chromatic Detection in 3D Cone Contrast Space," *Investigative Ophthalmology and Visual Science (supplement)* **35:**1555 (1994).
21. R. L. De Valois, K. K. De Valois, E. Switkes, and L. Mahon, "Hue Scaling of Isoluminant and Cone-Specific Lights," *Vision Research* **37:**885–897 (1997).
22. S. M. Wuerger, P. Atkinson, and S. Cropper, "The Cone Inputs to the Unique-Hue Mechanisms," *Vision Research* **45:**25–26 (2005).
23. G. E. Müller, "Über die Farbenempfindungen," *Zeitschrift für Psychologie und Physiologie der Sinnesorgane, Ergänzungsband* **17:**1–430 (1930).
24. D. B. Judd, "Response Functions for Types of Vision According to the Müller Theory, Research Paper RP1946," *Journal of Research of the National Bureau of Standards* **42:**356–371 (1949).
25. D. B. Judd, "Fundamental Studies of Color Vision from 1860 to 1960," *Proceedings of the National Academy of Science of the United States of America* **55:**1313–1330 (1966).
26. G. Svaetichin and E. F. MacNichol, Jr., "Retinal Mechanisms for Chromatic and Achromatic Vision," *Annals of the New York Academy of Sciences* **74:**385–404 (1959).
27. R. L. De Valois, I. Abramov, and G. H. Jacobs, "Analysis of Response Patterns of LGN Cells," *Journal of the Optical Society of America* **56:**966–977 (1966).

28. A. Stockman and L. T. Sharpe, "Spectral Sensitivities of the Middle- and Long-Wavelength Sensitive Cones Derived from Measurements in Observers of Known Genotype," *Vision Research* **40:**1711–1737 (2000).
29. S. L. Guth, "A Model for Color and Light Adaptation," *Journal of the Optical Society of America A* **8:**976–993 (1991).
30. H. Hofer, J. Carroll, J. Neitz, M. Neitz, and D. R. Williams, "Organization of the Human Trichromatic Cone Mosaic," *Journal of Neuroscience* **25:**9669–9679 (2005).
31. P. Flanagan, P. Cavanagh, and O. E. Favreau, "Independent Orientation-Selective Mechanisms for the Cardinal Directions of Colour Space," *Vision Research* **30:**769–778 (1990).
32. M. A. Webster and J. D. Mollon, "The Influence of Contrast Adaptation on Color Appearance," *Vision Research* **34:**1993–2020 (1994).
33. W. S. Stiles, *Mechanisms of Colour Vision,* Academic Press, London, 1978.
34. R. T. Eskew, Jr, "Chromatic Detection and Discrimination," in *The Senses: A Comprehensive Reference, Volume 2: Vision II,* T. D. Albright and R. H. Masland, eds., Academic Press Inc., San Diego, 2008, pp. 101–117.
35. D. A. Baylor, B. J. Nunn, and J. L. Schnapf, "The Photocurrent, Noise and Spectral Sensitivity of Rods of the Monkey Macaca Fascicularis," *Journal of Physiology* **357:**575–607 (1984).
36. A. M. Derrington, J. Krauskopf, and P. Lennie, "Chromatic Mechanisms in Lateral Geniculate Nucleus of Macaque," *Journal of Physiology* **357:**241–265 (1984).
37. A. M. Derrington and P. Lennie, "Spatial and Temporal Contrast Sensitivities of Neurones in the Lateral Geniculate Nucleus of Macaque," *Journal of Physiology* **357:**219–240 (1984).
38. N. Graham and D. C. Hood, "Modeling the Dynamics of Adaptation: the Merging of Two Traditions," *Vision Research* **32:**1373–1393 (1992).
39. D. C. Hood, "Lower-Level Visual Processing and Models of Light Adaptation," *Annual Review of Psychology* **49:**503–535 (1998).
40. W. S. Stiles, "The Directional Sensitivity of the Retina and the Spectral Sensitivity of the Rods and Cones," *Proceedings of the Royal Society of London. Series B: Biological Sciences* **B127:**64–105 (1939).
41. W. S. Stiles, "Incremental Thresholds and the Mechanisms of Colour Vision," *Documenta Ophthalmologica* **3:**138–163 (1949).
42. W. S. Stiles, "Further Studies of Visual Mechanisms by the Two-Colour Threshold Technique," *Coloquio sobre problemas opticos de la vision* **1:**65–103 (1953).
43. D. M. Green and J. A. Swets, *Signal Detection Theory and Psychophysics*, John Wiley & Sons, New York, 1966.
44. H. B. Barlow and W. R. Levick, "Threshold Setting by the Surround of Cat Retinal Ganglion Cells," *Journal of Physiology* **259:**737–757 (1976).
45. R. Shapley and C. Enroth-Cugell, "Visual Adaptation and Retinal Gain Controls," in *Progress in Retinal Research,* N. Osborne and G. Chader, eds., Pergamon Press, New York, 1984, pp. 263–346.
46. R. M. Boynton and D. N. Whitten, "Visual Adaptation in Monkey Cones: Recordings of Late Receptor Potentials," *Science* **170:**1423–1426 (1970).
47. J. M. Valeton and D. van Norren, "Light Adaptation of Primate Cones: An Analysis Based on Extracellular Data," *Vision Research* **23:**1539–1547 (1983).
48. D. A. Burkhardt, "Light Adaptation and Photopigment Bleaching in Cone Photoreceptors *in situ* in the Retina of the Turtle," *Journal of Neuroscience* **14:**1091–1105(1994).
49. V. Y. Arshavsky, T. D. Lamb, and E. N. Pugh, Jr., "G Proteins and Phototransduction," *Annual Review of Physiology* **64:**153–187 (2002).
50. R. D. Hamer, S. C. Nicholas, D. Tranchina, T. D. Lamb, and J. L. P. Jarvinen, "Toward a Unified Model of Vertebrate Rod Phototransduction," *Visual Neuroscience* **22:**417–436 (2005).
51. E. N. Pugh, Jr., S. Nikonov, and T. D. Lamb, "Molecular Mechanisms of Vertebrate Photoreceptor Light Adaptation," *Current Opinion in Neurobiology* **9:**410–418 (1999).
52. A. Stockman, M. Langendörfer, H. E. Smithson, and L. T. Sharpe, "Human Cone Light Adaptation: From Behavioral Measurements to Molecular Mechanisms," *Journal of Vision* **6:**1194–1213 (2006).
53. G. Wyszecki and W. S. Stiles, *Color Science: Concepts and Methods, Quantitative Data and Formulae*, 2nd ed., Wiley, New York, 1982.

54. C. Sigel and E. N. Pugh, Jr., "Stiles's $\pi_5$ Color Mechanism: Tests of Field Displacements and Field Additivity Properties," *Journal of the Optical Society of America* **70:**71–81 (1980).
55. B. A. Wandell and E. N. Pugh, Jr., "Detection of Long-Duration Incremental Flashes by a Chromatically Coded Pathway," *Vision Research* **20:**625–635 (1980).
56. E. H. Adelson, "Saturation and Adaptation in the Rod System," *Vision Research* **22:**1299–1312(1982).
57. W. S. Geisler, "Effects of Bleaching and Backgrounds on the Flash Response of the Cone System," *Journal of Physiology* **312:**413–434 (1981).
58. D. C. Hood and M. A. Finkelstein, "Sensitivity to Light," in *Handbook of Perception and Human Performance,* K. Boff, L. Kaufman and J. Thomas, eds., Wiley, New York, 1986, pp. 5-1–5-66.
59. M. M. Hayhoe, N. I. Benimof, and D. C. Hood, "The Time Course of Multiplicative and Subtractive Adaptation Processes," *Vision Research* **27:**1981–1996 (1987).
60. D. H. Kelly, "Effects of Sharp Edges in a Flickering Field," *Journal of the Optical Society of America* **49:**730–732 (1959).
61. C. F. Stromeyer, III, G. R. Cole, and R. E. Kronauer, "Second-Site Adaptation in the Red-Green Chromatic Pathways," *Vision Research* **25:**219–237 (1985).
62. A. Chaparro, C. F. Stromeyer, III, G. Chen, and R. E. Kronauer, "Human Cones Appear to Adapt at Low Light Levels: Measurements on the Red-Green Detection Mechanism," *Vision Research* **35:**3103–3118 (1995).
63. C. F. Stromeyer, III, G. R. Cole, and R. E. Kronauer, "Chromatic Suppression of Cone Inputs to the Luminance Flicker Mechanisms," *Vision Research* **27:**1113–1137 (1987).
64. A. Eisner and D. I. A. MacLeod, "Flicker Photometric Study of Chromatic Adaptation: Selective Suppression of Cone Inputs by Colored Backgrounds," *Journal of the Optical Society of America* **71:**705–718 (1981).
65. S. J. Ahn and D. I. A. MacLeod, "Link-Specific Adaptation in the Luminance and Chromatic Channels," *Vision Research* **33:**2271–2286 (1991).
66. Y. W. Lee, *Statistical Theory of Communication,* John Wiley & Sons, Inc., New York, 1968.
67. H. L. van Trees, *Detection, Estimation, and Modulation Theory*, Part I, Wiley, New York, 1968.
68. J. Nachmias, "Signal Detection Theory and its Applications to Problems in Vision," in *Visual Psychophysics, Handbook of Sensory Physiology,* Vol. VII/4, D. Jameson and L. H. Hurvich, eds., Springer-Verlag, Berlin, 1972, pp. 56–77.
69. C. H. Coombs, R. M. Dawes, and A. Tversky, *Mathematical Psychology,* Prentice-Hall, Englewood Cliff, New Jersey, 1970.
70. R. O. Duda, P. E. Hart, and D. G. Stork, *Pattern Classification and Scene Analysis,* 2nd ed., John Wiley & Sons, New York, 2001.
71. H. B. Barlow, "Retinal and Central Factors in Human Vision Limited by Noise," in *Vertebrate Photoreception,* B. B. P. Fatt, ed., Academic Press, London, 1977, pp. 337–358.
72. A. B. Watson, H. B. Barlow, and J. G. Robson, "What Does the Eye See Best?," *Nature* **31:**419–422 (1983).
73. W. S. Geisler, "Physical Limits of Acuity and Hyperacuity," *Journal of the Optical Society of America A* **1:**775–782 (1984).
74. W. S. Geisler, "Sequential Ideal-Observer Analysis of Visual Discriminations," *Psychological Review* **96:**267–314 (1989).
75. D. H. Krantz, "Color Measurement and Color Theory: I. Representation Theorem for Grassmann Structures," *Journal of Mathematical Psychology* **12:**283–303 (1975).
76. D. H. Krantz, "Color Measurement and Color Theory: II Opponent-Colors Theory," *Journal of Mathematical Psychology* **12:**304–327 (1975).
77. D. L. MacAdam, "Chromatic Adaptation," *Journal of the Optical Society* **46:**500–513 (1956).
78. J. M. Hillis and D. H. Brainard, "Do Common Mechanisms of Adaptation Mediate Color Discrimination and Appearance? Uniform Backgrounds," *Journal of the Optical Society America A* **22:**2090–2106 (2005).
79. M. A. Webster and J. D. Mollon, "Changes in Colour Appearance Following Post-Receptoral Adaptation," *Nature* **349:**235–238 (1991).
80. J. P. Moxley and S. L. Guth, "Hue Shifts Caused by Post-Receptor Adaptation," *Investigative Ophthalmology and Visual Science (supplement)* **20:**206 (1981).

81. S. L. Guth and J. P. Moxley, "Hue Shifts Following Differential Postreceptor Achromatic Adaptation," *Journal of the Optical Society of America* **72:**301–303 (1982).
82. J. M. Hillis and D. H. Brainard, "Do Common Mechanisms of Adaptation Mediate Color Discrimination and Appearance? Contrast Adaptation," *Journal of the Optical Society America A* **24:**2122–2133 (2007).
83. C. Noorlander, M. J. G. Heuts, and J. J. Koenderink, "Sensitivity to Spatiotemporal Combined Luminance and Chromaticity Contrast," *Journal of the Optical Society of America* **71:**453–459 (1981).
84. D. H. Kelly, "Flicker," in *Visual Psychophysics, Handbook of Sensory Physiology,* Vol. VII/4, D. Jameson and L. H. Hurvich, eds., Springer-Verlag, Berlin, 1972, pp. 273–302.
85. R. Luther, "Aus dem Gebiet der Farbreizmetrik," *Zeitschrift für technische Physik* **8:**540–558 (1927).
86. D. I. A. MacLeod and R. M. Boynton, "Chromaticity Diagram Showing Cone Excitation by Stimuli of Equal Luminance," *Journal of the Optical Society of America* **69:**1183–1186(1979).
87. D. H. Brainard, "Cone Contrast and Opponent Modulation Color Spaces," in *Human Color Vision*, P. K. Kaiser, and R. M. Boynton, eds., Optical Society of America, Washington, D.C., 1996, pp. 563–579.
88. K. Knoblauch, "Dual Bases in Dichromatic Color Space," in *Colour Vision Deficiencies XII,* B. Drum, ed., Kluwer Academic Publishers, Dordrecht, 1995, pp. 165–176.
89. R. T. Eskew, Jr., J. S. McLellan, and F. Giulianini, "Chromatic Detection and Discrimination," in *Color Vision: From Genes to Perception,* K. Gegenfurtner and L. T. Sharpe, eds., Cambridge University Press, Cambridge, 1999, pp. 345–368.
90. A. Stockman and L. T. Sharpe, "Cone Spectral Sensitivities and Color Matching," in *Color Vision: From Genes to Perception,* K. Gegenfurtner and L. T. Sharpe, eds., Cambridge University Press, Cambridge, 1999, pp. 53–87.
91. B. Drum, "Short-Wavelength Cones Contribute to Achromatic Sensitivity," *Vision Research* **23:**1433–1439 (1983).
92. A. Stockman, D. I. A. MacLeod, and D. D. DePriest, "An Inverted S-cone Input to the Luminance Channel: Evidence for Two Processes in S-cone Flicker Detection," *Investigative Ophthalmology and Visual Science (supplement)* **28:**92 (1987).
93. J. Lee and C. F. Stromeyer, III, "Contribution of Human Short-Wave Cones to Luminance and Motion Detection," *Journal of Physiology* **413:**563–593 (1989).
94. A. Stockman, D. I. A. MacLeod, and D. D. DePriest, "The Temporal Properties of the Human Short-Wave Photoreceptors and Their Associated Pathways," *Vision Research* **31:**189–208(1991).
95. W. S. Stiles, "Separation of the 'Blue' and 'Green' Mechanisms of Foveal Vision by Measurements of Increment Thresholds," *Proceedings of the Royal Society of London. Series B: Biological Sciences* **B 133:**418–434 (1946).
96. W. S. Stiles, "The Physical Interpretation of the Spectral Sensitivity Curve of the Eye," in *Transactions of the Optical Convention of the Worshipful Company of Spectacle Makers,* Spectacle Maker's Company, London, 1948, pp. 97–107.
97. W. S. Stiles, "Color Vision: the Approach Through Increment Threshold Sensitivity," *Proceedings of the National Academy of Science of the United States of America* **45:**100–114 (1959).
98. W. S. Stiles, "Foveal Threshold Sensitivity on Fields of Different Colors," *Science* **145:**1016–1018 (1964).
99. J. M. Enoch, "The Two-Color Threshold Technique of Stiles and Derived Component Color Mechanisms," in *Handbook of Sensory Physiology*, Vol. VII/4, D. Jameson and L. H. Hurvich, eds., Springer-Verlag, Berlin, 1972 pp. 537–567.
100. R. M. Boynton, M. Ikeda, and W. S. Stiles, "Interactions Among Chromatic Mechanisms as Inferred from Positive and Negative Increment Thresholds," *Vision Research* **4:**87–117 (1964).
101. P. E. King-Smith, "Visual Detection Analysed in Terms of Luminance and Chromatic Signals," *Nature* **255:**69–70 (1975).
102. P. E. King-Smith and D. Carden, "Luminance and Opponent-Color Contributions to Visual Detection and Adaptation and to Temporal and Spatial Integration," *Journal of the Optical Society of America* **66:**709–717 (1976).
103. B. A. Wandell and E. N. Pugh, Jr., "A Field Additive Pathway Detects Brief-Duration, Long-Wavelength Incremental Flashes," *Vision Research* **20:**613–624 (1980).

104. W. S. Stiles and B. H. Crawford, "The Liminal Brightness Increment as a Function of Wavelength for Different Conditions of the Foveal and Parafoveal Retina," *Proceedings of the Royal Society of London. Series B: Biological Sciences* **B113:**496–530 (1933).
105. H. G. Sperling and R. S. Harwerth, "Red-Green Cone Interactions in Increment-Threshold Spectral Sensitivity of Primates," *Science* **172:**180–184 (1971).
106. K. Kranda and P. E. King-Smith, "Detection of Colored Stimuli by Independent Linear Systems," *Vision Research* **19:**733–745 (1979).
107. J. E. Thornton and E. N. Pugh, Jr., "Red/Green Color Opponency at Detection Threshold," *Science* **219:**191–193 (1983).
108. M. Kalloniatis and H. G. Sperling, "The Spectral Sensitivity and Adaptation Characteristics of Cone Mechanisms Under White Light Adaptation," *Journal of the Optical Society of America A* **7:**1912–1928 (1990).
109. L. L. Sloan, "The Effect of Intensity of Light, State of Adaptation of the Eye, and Size of Photometric Field on the Visibility Curve," *Psychological Monographs* **38:**1–87 (1928).
110. C. R. Ingling, Jr., "A Tetrachromatic Hypothesis for Human Color Vision," *Vision Research* **9:**1131–1148 (1969).
111. D. J. Calkins, J. E. Thornton, and E. N. Pugh, Jr., "Monochromatism Determined at a Long-Wavelength/Middle-Wavelength Cone-Antagonistic Locus," *Vision Research* **13:**2349–2367 (1992).
112. W. d. W. Abney and E. R. Festing, "Colour Photometry," *Philosophical Transactions of the Royal Society of London* **177:**423–456 (1886).
113. W. d. W. Abney, *Researches in Colour Vision*, Longmans, Green, London, 1913.
114. H. E. Ives, "Studies in the Photometry of Lights of Different Colours. I. Spectral Luminosity Curves Obtained by the Equality of Brightness Photometer and Flicker Photometer under Similar Conditions," *Philosophical Magazine Series 6* **24:**149–188 (1912).
115. W. W. Coblentz and W. B. Emerson, "Relative Sensibility of the Average Eye to Light of Different Color and Some Practical Applications," *Bulletin of the Bureau of Standards* **14:**167–236(1918).
116. E. P. Hyde, W. E. Forsythe, and F. E. Cady, "The Visibility of Radiation," *Astrophysical Journal*, **48:**65–83 (1918).
117. K. S. Gibson and E. P. T. Tyndall, "Visibility of Radiant Energy," *Scientific Papers of the Bureau of Standards* **19:**131–191(1923).
118. A. Dresler, "The Non-Additivity of Heterochromatic Brightness," *Transactions of the Illuminating Engineering Society* **18:**141–165 (1953).
119. R. M. Boynton and P. Kaiser, "Vision: The Additivity Law Made to Work for Heterochromatic Photometry with Bipartite Fields," *Science* **161:**366–368 (1968).
120. S. L. Guth, N. V. Donley, and R. T. Marrocco, "On Luminance Additivity and Related Topics," *Vision Research* **9:**537–575 (1969).
121. Y. Le Grand, "Spectral Luminosity," in *Visual Psychophysics, Handbook of Sensory Physiology*, Vol. VII/4, D. Jameson and L. H. Hurvich, eds., Springer-Verlag, Berlin, 1972, pp. 413–433.
122. G. Wagner and R. M. Boynton, "Comparison of Four Methods of Heterochromatic Photometry," *Journal of the Optical Society of America* **62:**1508–1515 (1972).
123. J. Pokorny, V. C. Smith, and M. Lutze, "Heterochromatic Modulation Photometry," *Journal of the Optical Society of America A* **6:**1618–1623 (1989).
124. P. Lennie, J. Pokorny, and V. C. Smith, "Luminance," *Journal of the Optical Society of America A* **10:**1283–1293 (1993).
125. V. C. Smith, and J. Pokorny, "Spectral Sensitivity of the Foveal Cone Photopigments between 400 and 500 nm," *Vision Research* **15:**161–171 (1975).
126. D. B. Judd, "Report of U.S. Secretariat Committee on Colorimetry and Artificial Daylight," in *Proceedings of the Twelfth Session of the CIE, Stockholm,* Bureau Central de la CIE, Paris, 1951, pp. 1–60.
127. J. J. Vos, "Colorimetric and Photometric Properties of a 2-deg Fundamental Observer," *Color Research and Application* **3:**125–128 (1978).
128. L. T. Sharpe, A. Stockman, W. Jagla, and H. Jägle, "A Luminous Efficiency Function, $V^*(\lambda)$, for Daylight Adaptation," *Journal of Vision* **5:**948–968 (2005).

129. A. Stockman, H. Jägle, M. Pirzer, and L. T. Sharpe, "The Dependence of Luminous Efficiency on Chromatic Adaptation," *Journal of Vision* **8**(16):1, 1–26 (2008).

130. CIE, *Fundamental Chromaticity Diagram with Physiological Axes—Part 1. Technical Report 170-1*, Central Bureau of the Commission Internationale de l' Éclairage, Vienna, 2007.

131. H. De Vries, "Luminosity Curves of Trichromats," *Nature* **157:**736–737 (1946).

132. H. De Vries, "The Heredity of the Relative Numbers of Red and Green Receptors in the Human Eye," *Genetica* **24:**199–212 (1948).

133. R. A. Crone, "Spectral Sensitivity in Color-Defective Subjects and Heterozygous Carriers," *American Journal of Ophthalmology* **48:**231–238 (1959).

134. W. A. H. Rushton and H. D. Baker, "Red/Green Sensitivity in Normal Vision," *Vision Research* **4:**75–85 (1964).

135. A. Adam, "Foveal Red-Green Ratios of Normals, Colorblinds and Heterozygotes," *Proceedings Tel-Hashomer Hospital: Tel-Aviv* **8:**2–6 (1969).

136. J. J. Vos and P. L. Walraven, "On the Derivation of the Foveal Receptor Primaries," *Vision Research* **11:**799–818 (1971).

137. M. Lutze, N. J. Cox, V. C. Smith, and J. Pokorny, "Genetic Studies of Variation in Rayleigh and Photometric Matches in Normal Trichromats," *Vision Research* **30:**149–162(1990).

138. R. L. P. Vimal, V. C. Smith, J. Pokorny, and S. K. Shevell, "Foveal Cone Thresholds," *Vision Research* **29:**61–78 (1989).

139. J. Kremers, H. P. N. Scholl, H. Knau, T. T. J. M. Berendschot, and L. T. Sharpe, "L/M-Cone Ratios in Human Trichromats Assessed by Psychophysics, Electroretinography and Retinal Densitometry," *Journal of the Optical Society of America A* **17:**517–526 (2000).

140. K. R. Dobkins, A. Thiele, and T. D. Albright, "Comparisons of Red-Green Equiluminance Points in Humans and Macaques: Evidence for Different L:M Cone Ratios between Species," *Journal of the Optical Society of America A* **17:**545–556 (2000).

141. K. L. Gunther, and K. R. Dobkins, "Individual Differences in Chromatic (red/green) Contrast Sensitivity are Constrained by the Relative Numbers of L- versus M-cones in the Eye," *Vision Research* **42:**1367–1378 (2002).

142. A. Stockman, D. I. A. MacLeod, and J. A. Vivien, "Isolation of the Middle- and Long-Wavelength Sensitive Cones in Normal Trichromats," *Journal of the Optical Society of America A* **10:**2471–2490 (1993).

143. J. Carroll, C. McMahon, M. Neitz, and J. Neitz, "Flicker-Photometric Electroretinogram Estimates of L:M Cone Photoreceptor Ratio in Men with Photopigment Spectra Derived from Genetics," *Journal of the Optical Society of America A* **17:**499–509 (2000).

144. J. Carroll, J. Neitz, and M. Neitz, "Estimates of L:M Cone Ratio from ERG Flicker Photometry and Genetics," *Journal of Vision* **2:**531–542 (2002).

145. M. F. Wesner, J. Pokorny, S. K. Shevell, and V. C. Smith, "Foveal Cone Detection Statistics in Color-Normals and Dichromats," *Vision Research* **31:**1021–1037 (1991).

146. D. H. Brainard, A. Roorda, Y. Yamauchi, J. B. Calderone, A. Metha, M. Neitz, J. Neitz, D. R. Williams, and G. H. Jacobs, "Functional Consequences of the Relative Numbers of L and M Cones," *Journal of the Optical Society of America A* **17:**607–614 (2000).

147. J. Albrecht, H. Jägle, D. C. Hood, and L. T. Sharpe, "The Multifocal Electroretinogram (mfERG) and Cone Isolating Stimuli: Variation in L- and M-cone driven signals across the Retina," *Journal of Vision* **2:**543–558 (2002).

148. L. T. Sharpe, E. de Luca, T. Hansen, H. Jägle, and K. Gegenfurtner, "Advantages and Disadvantages of Human Dichromacy," *Journal of Vision* **6:**213–223 (2006).

149. C. R. Ingling, Jr., and E. Martinez-Uriegas, "The Relationship between Spectral Sensitivity and Spatial Sensitivity for the Primate r-g X-Channel," *Vision Research* **23:**1495–1500(1983).

150. C. R. Ingling, Jr. and E. Martinez, "The Spatio-Chromatic Signal of the r-g Channels," in *Colour Vision: Physiology and Psychophysics*, J. D. Mollon and L. T. Sharpe, eds., Academic Press, London, 1983, pp. 433–444.

151. C. R. Ingling, Jr. and E. Martinez-Uriegas, "The Spatiotemporal Properties of the R-G X-cell Channel," *Vision Research* **25:**33–38 (1985).

152. C. R. Ingling, Jr. and H. B.-P. Tsou, "Spectral Sensitivity for Flicker and Acuity Criteria," *Journal of the Optical Society of America A* **5:**1374–1378 (1988).

153. P. Lennie and M. D'Zmura, "Mechanisms of Color Vision," *CRC Critical Reviews in Neurobiology* **3:**333–400 (1988).

154. P. K. Kaiser, B. B. Lee, P. R. Martin, and A. Valberg, "The Physiological Basis of the Minimally Distinct Border Demonstrated in the Ganglion Cells of the Macaque Retina," *Journal of Physiology* **422:**153–183 (1990).

155. P. Gouras and E. Zrenner, "Enhancement of Luminance Flicker by Color-Opponent Mechanisms," *Science* **205:**587–589 (1979).

156. J. L. Brown, L. Phares, and D. E. Fletcher, "Spectral Energy Thresholds for the Resolution of Acuity Targets," *Journal of the Optical Society of America* **50:**950–960 (1960).

157. J. Pokorny, C. H. Graham, and R. N. Lanson, "Effect of Wavelength on Foveal Grating Acuity," *Journal of the Optical Society of America* **58:**1410–1414 (1968).

158. C. R. Ingling, S. S. Grigsby, and R. C. Long, "Comparison of Spectral Sensitivity Using Heterochromatic Flicker Photometry and an Acuity Criterion," *Color Research & Application* **17:**187–196 (1992).

159. M. Ikeda, "Study of Interrelations between Mechanisms at Threshold," *Journal of the Optical Society of America A* **53:**1305–1313 (1963).

160. S. L. Guth, "Luminance Addition: General Considerations and Some Results at Foveal Threshold," *Journal of the Optical Society of America* **55:**718–722 (1965).

161. S. L. Guth, "Nonadditivity and Inhibition Among Chromatic Luminances at Threshold," *Vision Research* **7:**319–328 (1967).

162. S. L. Guth, J. V. Alexander, J. I. Chumbly, C. B. Gillman, and M. M. Patterson, "Factors Affecting Luminance Additivity at Threshold Among Normal and Color-Blind Subjects and Elaborations of a Trichromatic-Opponent Color Theory," *Vision Research* **8:**913–928 (1968).

163. M. Ikeda, T. Uetsuki, and W. S. Stiles, "Interrelations among Stiles $\pi$ Mechanisms," *Journal of the Optical Society of America* **60:**406–415 (1970).

164. J. E. Thornton and E. N. Pugh, Jr., "Relationship of Opponent-Colors Cancellation Measures to Cone Antagonistic Signals Deduced from Increment Threshold Data," in *Colour Vision: Physiology and Psychophysics,* J. D. Mollon and L. T. Sharpe, eds., Academic Press, London, 1983, pp. 361–373.

165. A. B. Poirson and B. A. Wandell, "The Ellipsoidal Representation of Spectral Sensitivity," *Vision Research* **30:**647–652 (1990).

166. K. Knoblauch and L. T. Maloney, "Testing the Indeterminacy of Linear Color Mechanisms from Color Discrimination Data," *Vision Research* **36:**295–306 (1996).

167. A. B. Poirson and B. A. Wandell, "Pattern-Color Separable Pathways Predict Sensitivity to Simple Colored Patterns" *Vision Research* **36:**515–526 (1996).

168. A. B. Poirson B. A. Wandell, D. C. Varner, and D. H. Brainard, "Surface Characterizations of Color Thresholds," *Journal of the Optical Society of America A* **7:**783–789 (1990).

169. G. R. Cole, C. F. Stromeyer, III, and R. E. Kronauer, "Visual Interactions with Luminance and Chromatic Stimuli," *Journal of the Optical Society of America A* **7:**128–140 (1990).

170. A. Chaparro, C. F. Stromeyer, III, E. P. Huang, R. E. Kronauer, and R. T. Eskew, Jr, "Colour is What the Eye Sees Best," *Nature* **361:**348–350 (1993).

171. R. T. Eskew, Jr., C. F. Stromeyer, III, and R. E. Kronauer, "Temporal Properties of the Red-Green Chromatic Mechanism," *Vision Research* **34:**3127–3137 (1994).

172. M. J. Sankeralli and K. T. Mullen, "Estimation of the L-, M-, and S-cone Weights of the Postreceptoral Detection Mechanisms," *Journal of the Optical Society of America A* **13:**906–915 (1996).

173. A. Chaparro, C. F. Stromeyer, III, R. E. Kronauer, and R. T. Eskew, Jr., "Separable Red-Green and Luminance Detectors for Small Flashes," *Vision Research* **34:**751–762 (1994).

174. G. R. Cole, T. Hine, and W. McIlhagga, "Detection Mechanisms in L-, M-, and S-cone Contrast Space," *Journal of the Optical Society of America A* **10:**38–51 (1993).

175. F. Giulianini and R. T. Eskew, Jr., "Chromatic Masking in the ($\Delta$L/L, $\Delta$M/M) Plane of Cone-Contrast Space Reveals only Two Detection Mechanisms," *Vision Research* **38:**3913–3926(1998).

176. J. R. Newton and R. T. Eskew, Jr., "Chromatic Detection and Discrimination in the Periphery: A Postreceptoral Loss of Color Sensitivity," *Visual Neuroscience* **20:**511–521 (2003).

177. R. T. Eskew, Jr., C. F. Stromeyer, III, C. J. Picotte, and R. E. Kronauer, "Detection Uncertainty and the Facilitation of Chromatic Detection by Luminance Contours," *Journal of the Optical Society of America A* **8:** 394–403 (1991).

178. C. F. Stromeyer, III, J. Lee, and R. T. Eskew, Jr., "Peripheral Chromatic Sensitivity for Flashes: a Post-Receptoral Red-Green Asymmetry," *Vision Research* **32:**1865–1873 (1992).

179. R. T. Eskew, Jr., J. R. Newton, and F. Giulianini, "Chromatic Detection and Discrimination Analyzed by a Bayesian Classifier," *Vision Research* **41:**893–909 (2001).

180. R. M. Boynton, A. L. Nagy, and C. X. Olson, "A Flaw in Equations for Predicting Chromatic Differences," *Color Research and Application* **8:**69–74 (1983).

181. C. F. Stromeyer, III, A. Chaparro, C. Rodriguez, D. Chen, E. Hu, and R. E. Kronauer, "Short-Wave Cone Signal in the Red-Green Detection Mechanism," *Vision Research* **38:**813–826 (1998).

182. C. F. Stromeyer, III and J. Lee, "Adaptational Effects of Short Wave Cone Signals on Red-Green Chromatic Detection," *Vision Research* **28:**931–940 (1988).

183. J. D. Mollon and C. R. Cavonius, "The Chromatic Antagonisms of Opponent-Process Theory are not the Same as Those Revealed in Studies of Detection and Discrimination," in *Colour Deficiencies VIII, Documenta Ophthalmologica Proceedings Series, 46*, G. Verriest, ed., Nijhoff-Junk, Dordrecht, 1987, pp. 473–483.

184. H. De Lange, "Research into the Dynamic Nature of the Human Fovea-Cortex Systems with Intermittent and Modulated Light. II. Phase Shift in Brightness and Delay in Color Perception.," *Journal of the Optical Society of America* **48:**784–789 (1958).

185. D. Regan and C. W. Tyler, "Some Dynamic Features of Colour Vision," *Vision Research* **11:**1307–1324 (1971).

186. D. H. Kelly and D. van Norren, "Two-Band Model of Heterochromatic Flicker," *Journal of the Optical Society of America* **67:**1081–1091 (1977).

187. D. J. Tolhurst, "Colour-Coding Properties of Sustained and Transient Channels in Human Vision," *Nature* **266:**266–268 (1977).

188. C. E. Sternheim, C. F. Stromeyer, III, and M. C. K. Khoo, "Visibility of Chromatic Flicker upon Spectrally Mixed Adapting Fields," *Vision Research* **19:**175–183 (1979).

189. V. C. Smith, R. W. Bowen, and J. Pokorny, "Threshold Temporal Integration of Chromatic Stimuli," *Vision Research* **24:**653–660 (1984).

190. A. B. Metha and K. T. Mullen, "Temporal Mechanisms Underlying Flicker Detection and Identification for Red-Green and Achromatic Stimuli," *Journal of the Optical Society of America A* **13:**1969–1980 (1996).

191. A. Stockman, M. R. Williams, and H. E. Smithson, "Flicker-Clicker: Cross Modality Matching Experiments," *Journal of Vision* **4:**86a (2004).

192. G. J. C. van der Horst, C. M. M. de Weert, and M. A. Bouman, "Transfer of Spatial Chromaticity-Contrast at Threshold in the Human Eye," *Journal of the Optical Society of America* **57:**1260–1266 (1967).

193. G. J. C. van der Horst and M. A. Bouman, "Spatio-Temporal Chromaticity Discrimination," *Journal of the Optical Society of America* **59:**1482–1488 (1969).

194. R. Hilz and C. R. Cavonius, "Wavelength Discrimination Measured with Square-Wave Gratings," *Journal of the Optical Society of America* **60:**273–277 (1970).

195. E. M. Granger and J. C. Heurtley, "Visual Chromaticity-Modulation Transfer Function," *Journal of the Optical Society of America* **63:**1173–1174 (1973).

196. C. F. Stromeyer, III and C. E. Sternheim, "Visibility of Red and Green Spatial Patterns upon Spectrally Mixed Adapting Fields," *Vision Research* **21:**397–407 (1981).

197. K. T. Mullen and J. J. Kulikowski, "Wavelength Discrimination at Detection Threshold," *Journal of the Optical Society of America A* **7:**733–742 (1990).

198. N. Sekiguchi, D. R. Williams, and D. H. Brainard, "Efficiency in Detection of Isoluminant and Isochromatic Interference Fringes," *Journal of the Optical Society of America A* **10:**2118–2133 (1993).

199. N. Sekiguchi, D. R. Williams, and D. H. Brainard, "Aberration-Free Measurements of the Visibility of Isoluminant Gratings," *Journal of the Optical Society of America A* **10:**2105–2117(1993).

200. D. R. Williams, N. Sekiguchi, and D. H. Brainard, "Color, Contrast Sensitivity, and the Cone Mosaic," *Proceedings of the National Academy of Science of the United States of America* **90:**9770–9777 (1993).

201. E. N. Pugh, Jr. and C. Sigel, "Evaluation of the Candidacy of the $\pi$-Mechanisms of Stiles for Color-Matching Fundamentals," *Vision Research* **18:**317–330 (1978).

202. O. Estévez, "On the Fundamental Database of Normal and Dichromatic Color Vision," PhD thesis, Amsterdam University, Amsterdam 1979.

203. H. J. A. Dartnall, J. K. Bowmaker, and J. D. Mollon, "Human Visual Pigments: Microspectrophotometric Results from the Eyes of Seven Persons," *Proceedings of the Royal Society of London. Series B: Biological Sciences* **B 220:**115–130 (1983).

204. H. De Vries, "The Luminosity Curve of the Eye as Determined by Measurements with the Flicker Photometer," *Physica* **14:**319–348 (1948).

205. M. Ikeda and M. Urakubo, "Flicker HRTF as Test of Color Vision," *Journal of the Optical Society of America* **58:**27–31 (1968).

206. L. E. Marks and M. H. Bornstein, "Spectral Sensitivity by Constant CFF: Effect of Chromatic Adaptation," *Journal of the Optical Society of America* **63:**220–226 (1973).

207. P. E. King-Smith and J. R. Webb, "The Use of Photopic Saturation in Determining the Fundamental Spectral Sensitivity Curves," *Vision Research* **14:**421–429 (1974).

208. A. Eisner, "Comparison of Flicker-Photometric and Flicker-Threshold Spectral Sensitivities While the Eye is Adapted to Colored Backgrounds," *Journal of the Optical Society of America* **72:**517–518 (1982).

209. W. H. Swanson, "Chromatic Adaptation Alters Spectral Sensitivity at High Temporal Frequencies," *Journal of the Optical Society of America A* **10:**1294–1303 (1993).

210. C. F. Stromeyer, III, A. Chaparro, A. S. Tolias, and R. E. Kronauer, "Colour Adaptation Modifies the Long-Wave Versus Middle-Wave Cone Weights and Temporal Phases in Human Luminance (but not red-green) Mechanism," *Journal of Physiology* **499:**227–254 (1997).

211. W. B. Cushman and J. Z. Levinson, "Phase Shift in Red and Green Counter-Phase Flicker at High Frequencies," *Journal of the Optical Society of America* **73:**1557–1561 (1983).

212. P. L. Walraven and H. J. Leebeek, "Phase Shift of Sinusoidally Alternating Colored Stimuli," *Journal of the Optical Society of America* **54:**78–82 (1964).

213. D. T. Lindsey, J. Pokorny, and V. C. Smith, "Phase-Dependent Sensitivity to Heterochromatic Flicker," *Journal of the Optical Society of America A* **3:**921–927 (1986).

214. W. H. Swanson, J. Pokorny, and V. C. Smith, "Effects of Temporal Frequency on Phase-Dependent Sensitivity to Heterochromatic Flicker," *Journal of the Optical Society of America A* **4:**2266–2273 (1987).

215. V. C. Smith, B. B. Lee, J. Pokorny, P. R. Martin, and A. Valberg, "Responses of Macaque Ganglion Cells to the Relative Phase of Heterochromatically Modulated Lights," *Journal of Physiology* **458:**191–221 (1992).

216. A. Stockman, D. J. Plummer, and E. D. Montag, "Spectrally-Opponent Inputs to the Human Luminance Pathway: Slow +M and –L Cone Inputs Revealed by Intense Long-Wavelength Adaptation," *Journal of Physiology* **566:**61–76 (2005).

217. A. Stockman and D. J. Plummer, "Spectrally-Opponent Inputs to the Human Luminance Pathway: Slow +L and –M Cone Inputs Revealed by Low to Moderate Long-Wavelength Adaptation," *Journal of Physiology* **566:**77–91 (2005).

218. A. Stockman, E. D. Montag, and D. J. Plummer, "Paradoxical Shifts in Human Colour Sensitivity Caused by Constructive and Destructive Interference between Signals from the Same Cone Class," *Visual Neuroscience* **23:**471–478 (2006).

219. A. Stockman, E. D. Montag, and D. I. A. MacLeod, "Large Changes in Phase Delay on Intense Bleaching Backgrounds," *Investigative Ophthalmology and Visual Science (supplement)* **32:**841 (1991).

220. A. Stockman and D. J. Plummer, "The Luminance Channel Can be Opponent??," *Investigative Ophthalmology and Visual Science (supplement)* **35:**1572 (1994).

221. C. F. Stromeyer, III, P. D. Gowdy, A. Chaparro, S. Kladakis, J. D. Willen, and R. E. Kronauer, "Colour Adaptation Modifies the Temporal Properties of the Long- and Middle-Wave Cone Signals in the Human Luminance Mechanism," *Journal of Physiology* **526:**177–194 (2000).

222. A. Stockman, "Multiple Cone Inputs to Luminance," *Investigative Ophthalmology and Visual Science (supplement)* **42:**S320 (2001).

223. A. Stockman and D. J. Plummer, "Long-Wavelength Adaptation Reveals Slow, Spectrally Opponent Inputs to the Human Luminance Pathway," *Journal of Vision* **5:**702–716 (2005).

224. J. D. Mollon and P. G. Polden, "Saturation of a Retinal Cone Mechanism," *Nature* **259:**243–246 (1977).

225. C. F. Stromeyer, III, R. E. Kronauer, and J. C. Madsen, "Response Saturation of Short-Wavelength Cone Pathways Controlled by Color-Opponent Mechanisms," *Vision Research* **19:**1025–1040 (1979).

226. E. N. Pugh, Jr., "The Nature of the $\pi_1$ Mechanism of W. S. Stiles," *Journal of Physiology* **257:**713–747 (1976).

227. P. G. Polden and J. D. Mollon, "Reversed Effect of Adapting Stimuli on Visual Sensitivity," *Proceedings of the Royal Society of London. Series B: Biological Sciences* **B 210:**235–272 (1980).

228. E. N. Pugh, Jr. and J. Larimer, "Test of the Identity of the Site of Blue/Yellow Hue Cancellation and the Site of Chromatic Antagonism in the $\pi_1$ Pathway," *Vision Research* **19:**779–788 (1980).

229. D. B. Kirk, "The Putative $\pi_4$ Mechanism: Failure of Shape Invariance and Field Additivity," *Investigative Ophthalmology and Visual Science* (*supplement*) **26:**184 (1985).

230. A. Reeves, "Field Additivity of Stiles's Pi-4 Color Mechanism," *Journal of the Optical Society of America A* **4:**525–529 (1987).

231. E. N. Pugh, Jr. and J. D. Mollon, "A Theory of the $\pi_1$ and $\pi_3$ Color Mechanisms of Stiles," *Vision Research* **20:**293–312 (1979).

232. J. L. Schnapf, B. J. Nunn, M. Meister, and D. A. Baylor, "Visual Transduction in Cones of the Monkey Macaca Fascicularis," *Journal of Physiology* **427:**681–713 (1990).

233. D. C. Hood and D. G. Birch, "Human Cone Receptor Activity: The Leading Edge of the A-Wave and Models of Receptor Activity," *Visual Neuroscience* **10:**857–871 (1993).

234. B. B. Lee, D. M. Dacey, V. C. Smith, and J. Pokorny, "Horizontal Cells Reveal Cone Type-Specific Adaptation in Primate Retina," *Proceedings of the National Academy of Sciences of the United States of America* **96:**14611–14616 (1999).

235. B. B. Lee, D. M. Dacey, V. C. Smith, and J. Pokorny, "Dynamics of Sensitivity Regulation in Primate Outer Retina: The Horizontal Cell Network," *Journal of Vision* **3:**513–526 (2003).

236. G. J. Burton, "Evidence for Nonlinear Response Processes in the Human Visual System from Measurements on the Thresholds of Spatial Beat Frequencies," *Vision Research* **13:**1211–1225(1973).

237. D. I. A. MacLeod, and S. He "Visible Flicker from Invisible Patterns," *Nature* **361:**256–258 (1993).

238. D. I. A. MacLeod D. R. Williams, and W. Makous, "A Visual Nonlinearity Fed by Single Cones," *Vision Research* **32:**347–363 (1992).

239. O. Estévez and H. Spekreijse, "The 'Silent Substitution' Method in Visual Research," *Vision Research* **22:**681–691 (1982).

240. T. Benzschawel and S. L. Guth, "Post-Receptor Chromatic Mechanisms Revealed by Flickering vs Fused Adaptation," *Vision Research* **22:**69–75 (1982).

241. J. Krauskopf, D. R. Williams, M. B. Mandler, and A. M. Brown, "Higher Order Color Mechanisms," *Vision Research* **26:**23–32 (1986).

242. H. B. Barlow and P. Foldiak, "Adaptation and Decorrelation in the Cortex," in *The Computing Neuron*, R. Durbin, C. Miall, and G. J. Mitchison, eds., Addison-Wesley, Wokingham, 1989, pp. 54–72.

243. Q. Zaidi and A. G. Shapiro, "Adaptive Orthogonalization of Opponent-Color Signals," *Biological Cybernetics* **69:**415–428 (1993).

244. J. J. Atick, Z. Li, and A. N. Redlich, "What Does Post-Adaptation Color Appearance Reveal about Cortical Color Representation?," *Vision Research* **33:**123–129 (1993).

245. K. Gegenfurtner and D. C. Kiper, "Contrast Detection in Luminance and Chromatic Noise," *Journal of the Optical Society of America A* **9:**1880–1888 (1992).

246. M. J. Sankeralli and K. T. Mullen, "Postreceptoral Chromatic Detection Mechanisms Revealed by Noise Masking in Three-Dimensional Cone Contrast Space," *Journal of the Optical Society of America A* **14:**2633–2646 (1997).

247. T. Hansen and K. Gegenfurtner, "Higher Level Chromatic Mechanisms for Image Segmentation," *Journal of Vision* **6:**239–259 (2006).

248. M. D'Zmura and K. Knoblauch, "Spectral Bandwidths for the Detection of Colour," *Vision Research* **38:**3117–3128 (1998).

249. G. Monaci, G. Menegaz, S. Süsstrunk, and K. Knoblauch, "Chromatic Contrast Detection in Spatial Chromatic Noise," *Visual Neuroscience* **21:**291–294 (2005).

250. F. Giulianini and R. T. Eskew, Jr., "Theory of Chromatic Noise Masking Applied to Testing Linearity of S-cone Detection Mechanisms," *Journal of the Optical Society of America A* **24:**2604–2021 (2007).

251. D. L. MacAdam, "Visual Sensitivities to Color Differences in Daylight," *Journal of the Optical Society of America* **32:**247–274 (1942).

252. Y. Le Grand, "Les Seuils Différentiels de Couleurs dans la Théorie de Young," *Revue d'Optique* **28:**261–278 (1949).

253. R. M. Boynton and N. Kambe, "Chromatic Difference Steps of Moderate Size Measured Along Theoretically Critical Axes," *Color Research and Application* **5:**13–23 (1980).

254. A. L. Nagy, R. T. Eskew, Jr., and R. M. Boynton, "Analysis of Color-Matching Ellipses in a Cone-Excitation Space," *Journal of the Optical Society of America A* **4:**756–768 (1987).

255. J. Krauskopf and K. Gegenfurtner, "Color Discrimination and Adaptation," *Vision Research* **11:**2165–2175 (1992).

256. J. Romero, J. A. Garcia, L. Jiménez del Barco, and E. Hita, "Evaluation of Color-Discrimination Ellipsoids in Two-color Spaces," *Journal of the Optical Society of America A* **10:**827–837 (1993).

257. R. W. Rodieck, *The Vertebrate Retina,* Freeman, San Francisco, 1973.

258. R. M. Boynton, R. T. Eskew, Jr., and A. L. Nagy, "Similarity of Normalized Discrimination Ellipses in the Constant-Luminance Chromaticity Plane," *Perception* **15:**755–763 (1986).

259. R. T. Eskew, Jr., Q. Wang, and D. P. Richters, "A Five-Mechanism Model of Hue Sensations," *Journal of Vision* **4:**315 (2004).

260. T. N. Cornsweet, and H. M. Pinsker, "Luminance Discrimination of Brief Flashes Under Various Conditions of Adaptation," *Journal of Physiology* **176:**294–310 (1965.)

261. F. W. Campbell and J. J. Kulikowski, "Orientation Selectivity of the Human Visual System," *Journal of Physiology* **187:**437–445 (1966).

262. J. Nachmias and E. C. Kocher, "Discrimination of Luminance Increments," *Journal of the Optical Society of America* **60:**382–389 (1970).

263. J. Nachmias and R. V. Sansbury, "Grating Contrast: Discrimination May Be Better Than Detection," *Vision Research* **14:**1039–1042 (1974).

264. J. M. Foley and G. Legge, "Contrast Detection and Near-Threshold Discrimination in Human Vision," *Vision Research* **21:**1041–1053 (1981).

265. K. K. De Valois and E. Switkes, "Simultaneous Masking Interactions between Chromatic and Luminance Gratings," *Journal of the Optical Society of America* **73:**11–18(1983).

266. C. F. Stromeyer, III and S. Klein, "Spatial Frequency Channels in Human Vision as Asymmetric (edge) Mechanisms," *Vision Research* **14:**1409–1420 (1974).

267. D. G. Pelli, "Uncertainty Explains Many Aspects of Visual Contrast Detection and Discrimination," *Journal of the Optical Society of America A* **2:**1508–1532 (1985).

268. E. Switkes, A. Bradley, and K. K. De Valois, "Contrast Dependence and Mechanisms of Masking Interactions among Chromatic and Luminance Gratings," *Journal of the Optical Society of America A* **5:**1149–1162 (1988).

269. K. T. Mullen and M. A. Losada, "Evidence for Separate Pathways for Color and Luminance Detection Mechanisms," *Journal of the Optical Society of America A* **11:**3136–3151 (1994).

270. R. W. Bowen and J. K. Cotten, "The Dipper and Bumper: Pattern Polarity Effects in Contrast Discrimination," *Investigative Ophthalmology and Visual Science (supplement)* **34:**708 (1993).

271. R. Hilz, G. Huppmann, and C. R. Cavonius, "Influence of Luminance Contrast on Hue Discrimination," *Journal of the Optical Society of America* **64:**763–766 (1974).

272. C.-C. Chen, J. M. Foley, and D. H. Brainard, "Detection of Chromoluminance Patterns on Chromoluminance Pedestals I: Threshold Measurements," *Vision Research* **40:**773–788 (2000).

273. C.-C. Chen, J. M. Foley, and D. H. Brainard, "Detection of Chromoluminance Patterns on Chromoluminance Pedestals II: Model," *Vision Research* **40:**789–803 (2000).

274. B. A. Wandell, "Measurement of Small Color Differences," *Psychological Review* **89:**281–302(1982).

275. B. A. Wandell, "Color Measurement and Discrimination," *Journal of the Optical Society of America A* **2:**62–71 (1985).

276. A. C. Beare, "Color-Name as a Function of Wavelength," *The American Journal of Psychology* **76:**248–256 (1963).

277. G. S. Brindley, *Physiology of the Retina and the Visual Pathway*, Williams and Wilkins, Baltimore, 1970.

278. E. Schrödinger, "Über das Verhältnis der Vierfarben zur Dreifarbentheorie," *Sitzungberichte. Abt. 2a, Mathematik, Astronomie, Physik, Meteorologie und Mechanik. Akademie der Wissenschaften in Wien, Mathematisch-Naturwissenschaftliche Klasse* **134:**471 (1925).

279. D. Jameson and L. M. Hurvich, "Some Quantitative Aspects of an Opponent-Colors Theory. I. Chromatic Responses and Spectral Saturation," *Journal of the Optical Society of America* **45:**546–552 (1955).

280. L. M. Hurvich and D. Jameson, "Some Quantitative Aspects of an Opponent-Colors Theory. II. Brightness, Saturation, and Hue in Normal and Dichromatic Vision," *Journal of the Optical Society of America* **45:**602–616 (1955).

281. D. Jameson and L. M. Hurvich, "Some Quantitative Aspects of an Opponent-Colors Theory. III. Changes in Brightness, Saturation, and Hue with Chromatic Adaptation," *Journal of the Optical Society of America* **46:**405–415 (1956).

282. L. M. Hurvich and D. Jameson, "Some Quantitative Aspects of an Opponent-Colors Theory. IV. A Psychological Color Specification System," *Journal of the Optical Society of America* **46:**1075–1089 (1956).

283. L. H. Hurvich, *Color Vision*, Sinauer, Sunderland, Massachussets, 1981.

284. R. M. Boynton and J. Gordon, "Bezold-Brücke Hue Shift Measured by a Color-Naming Technique," *Journal of the Optical Society of America* **55:**78–86 (1965).

285. J. Gordon and I. Abramov, "Color Vision in the Peripheral Retina. II. Hue and Saturation," *Journal of the Optical Society of America* **67:**202–207 (1977).

286. J. S. Werner and B. R. Wooten, "Opponent Chromatic Mechanisms: Relation to Photopigments and Hue Naming," *Journal of the Optical Society of America* **69:**422–434 (1979).

287. C. R. Ingling, Jr., J. P. Barley, and N. Ghani, "Chromatic Content of Spectral Lights," *Vision Research* **36:**2537–2551 (1996).

288. A. Brückner, "Zur Frage der Eichung von Farbensystemen," *Zeitschrift für Sinnesphysiologie* **58:**322–362 (1927).

289. E. J. Chichilnisky and B. A. Wandell, "Trichromatic Opponent Color Classification," *Vision Research* **39:**3444–3458 (1999).

290. F. L. Dimmick and M. R. Hubbard, "The Spectral Location of Psychologically Unique Yellow, Green, and Blue," *American Journal of Psychology* **52:**242–254 (1939).

291. M. Ayama, T. Nakatsue, and P. E. Kaiser, "Constant Hue Loci of Unique and Binary Balanced Hues at 10, 100, and 1000 Td," *Journal of the Optical Society of America A* **4:**1136–1144(1987).

292. B. E. Shefrin and J. S. Werner, "Loci of Spectral Unique Hues Throughout the Life-Span," *Journal of the Optical Society of America A* **7:**305–311 (1990).

293. G. Jordan and J. D. Mollon, "Rayleigh Matches and Unique Green," *Vision Research* **35:**613–620 (1995).

294. J. L. Nerger, V. J. Volbrecht, and C. J. Ayde, "Unique Hue Judgments as a Function of Test Size in the Fovea and at 20-deg Temporal Eccentricity," *Journal of the Optical Society of America A* **12:**1225–1232 (1995).

295. V. J. Volbrecht, J. L. Nerger, and C. E. Harlow, "The Bimodality of Unique Green Revisited," *Vision Research* **37:**404–416 (1997).

296. R. W. Pridmore, "Unique and Binary Hues as Functions of Luminance and Illuminant Color Temperature, and Relations with Invariant Hues," *Vision Research* **39:**3892–3908 (1999).

297. R. G. Kuehni, "Variability in Unique Hue Selection: A Surprising Phenomenon," *Color Research and Application* **29:**158–162 (2004).

298. M. A. Webster, E. Miyahara, G. Malkoc, and V. E. Raker, "Variations in Normal Color Vision. II. Unique Hues," *Journal of the Optical Society of America A* **17:**1545–1555 (2000).

299. R. G. Kuehni, "Determination of Unique Hues Using Munsell Color Chips," *Color Research and Application* **26:**61–66 (2001).

300. M. A. Webster, S. M. Webster, S. Bharadwaj, R. Verma, J. Jaikumar, G. Madan, and E. Vaithilingham, "Variations in Normal Color Vision. III. Unique Hues in Indian and United States Observers," *Journal of the Optical Society of America A* **19:**1951–1962 (2002).

301. W. d. W. Abney, "On the Change of Hue of Spectrum Colors by Dilution with White Light," *Proceedings of the Royal Society of London* **A83:**120–127 (1910).

302. K. Richter, "Antagonistische Signale beim Farbensehen und ihr Zusammenhang mit der empfindungsgemässen Farbordnung," PhD thesis, University of Basel, 1969.

303. J. D. Mollon and G. Jordan, "On the Nature of Unique Hues," in *John Dalton's Colour Vision Legacy,* I. M. D. C. C. Dickinson, ed., Taylor and Francis, London, 1997, pp. 381–392.

304. J. H. Parsons, *An Introduction to Colour Vision*, 2nd ed., Cambridge University Press, Cambridge, 1924.

305. A. Valberg, "A Method for the Precise Determination of Achromatic Colours Including White," *Vision Research* **11:**157–160 (1971).

306. D. Jameson and L. M. Hurvich, "Opponent-Response Functions Related to Measured Cone Photopigments," *Vision Research* **58:**429–430 (1968).

307. J. Larimer, D. H. Krantz, and C. M. Cicerone, "Opponent-Process Additivity—I: Red/Green Equilibria," *Vision Research* **14:**1127–1140 (1974).

308. C. R. Ingling, Jr., "The Spectral Sensitivity of the Opponent-Color Channels," *Vision Research* **17:**1083–1089 (1977).

309. J. Larimer, D. H. Krantz, and C. M. Cicerone, "Opponent-Process Additivity—II: Yellow/Blue Equilibria and Nonlinear Models," *Vision Research* **15:**723–731 (1975).

310. J. G. W. Raaijmakers and C. M. M. de Weert, "Linear and Nonlinear Opponent Color Coding," *Perception and Psychophysics* **18:**474–480 (1975).

311. Y. Ejima and Y. Takahashi, "Bezold-Brücke Hue Shift and Nonlinearity in Opponent-Color Process" *Vision Research* **24:**1897–1904 (1984).

312. S. Takahashi and Y. Ejima, "Spatial Properties of Red-Green and Yellow-Blue Perceptual Opponent-Color Response," *Vision Research* **24:**987–994 (1984).

313. M. Ayama, P. K. Kaiser, and T. Nakatsue, "Additivity of Red Chromatic Valence," *Vision Research* **25:**1885–1891 (1985).

314. C. R. Ingling, Jr., P. W. Russel, M. S. Rea, and B. H.-P. Tsou, "Red-Green Opponent Spectral Sensitivity: Disparity between Cancellation and Direct Matching Methods," *Science* **201:**1221–1223 (1978).

315. C. H. Elzinga and C. M. M. de Weert, "Nonlinear Codes for the Yellow/Blue Mechanism," *Vision Research* **24:**911–922 (1984).

316. M. Ayama and M. Ikeda, "Additivity of Yellow Chromatic Valence," *Vision Research* **26:**763–769 (1985).

317. K. Knoblauch and S. K. Shevell, "Relating Cone Signals to Color Appearance: Failure of Monotonicity in Yellow/Blue," *Visual Neuroscience* **18:**901–906 (2001).

318. M. Ikeda and M. Ayama, "Non-linear Nature of the Yellow Chromatic Valence," in *Colour Vision: Physiology and Psychophysics,* J. D. Mollon and L. T. Sharpe, eds., Academic Press, London, 1983, pp. 345–352.

319. K. Knoblauch, L. Sirovich, and B. R. Wooten, "Linearity of Hue Cancellation in Sex-Linked Dichromacy," *Journal of the Optical Society America A* **2:**136–146 (1985).

320. W. von Bezold, "Über das Gesetz der Farbenmischung und die physiologischen Grundfarben," *Annalen der Physiologie und Chemie* **150:**221–247 (1873).

321. E. W. Brücke, "Über einige Empfindungen im Gebiete der Sehnerven," *Sitzungsberichte der Akademie der Wissenschaften in Wien, Mathematisch-Naturwissenschaftliche Klasse, Abteilung 3* **77:**39–71 (1878).

322. D. M. Purdy, "Spectral Hue as a Function of Intensity," *American Journal of Psychology* **63:**541–559 (1931).

323. J. J. Vos, "Are Unique and Invariant Hues Coupled?," *Vision Research* **26:**337–342 (1986).

324. P. L. Walraven, "On the Bezold-Brücke Phenomenon," *Journal of the Optical Society of America* **51:**1113–1116 (1961).

325. J. Walraven, "Discounting the Background—The Missing Link in the Explanation of Chromatic Induction," *Vision Research* **16:**289–295 (1976).

326. S. K. Shevell, "The Dual Role of Chromatic Backgrounds in Color Perception," *Vision Research* **18:**1649–1661 (1978).

327. S. K. Shevell, "Color Perception under Chromatic Adaptation: Equilibrium Yellow and Long-Wavelength Adaptation," *Vision Research* **22:**279–292 (1982).

328. P. Whittle, "The Brightness of Coloured Flashes on Backgrounds of Various Colours and Luminances," *Vision Research* **13:**621–638 (1973).

329. C. M. Cicerone, D. H. Krantz, and J. Larimer, "Opponent-Process Additivity—III: Effect of Moderate Chromatic Adaptation," *Vision Research* **15:**1125–1135 (1975).

330. J. von Kries, "Influence of Adaptation on the Effects Produced by Luminous Stimuli," in *Sources of Color Science (1970),* D. L. MacAdam, ed., MIT Press, Cambridge, MA, 1905, pp. 120–1126.

331. R. W. Burnham, R. W. Evans, and S. M. Newhall, "Influence on Color Perception of Adaptation to Illumination," *Journal of the Optical Society of America* **42:**597–605 (1952).

332. H. V. Walters, "Some Experiments on the Trichromatic Theory of Vision," *Proceedings of the Royal Society of London* **131:**27–50 (1942).

333. D. L. MacAdam, "Influence of Chromatic Adaptation on Color Discrimination and Color Perception," *Die Farbe* **4:**133–143 (1955).

334. E. J. Chichilnisky and B. A. Wandell, "Photoreceptor Sensitivity Changes Explain Color Appearance Shifts Induced by Large Uniform Backgrounds in Dichoptic Matching," *Vision Research* **35:**239–254 (1995).

335. L. H. Hurvich and D. Jameson, "Further Developments of a Quantified Opponent Colors Theory," in *Visual Problems of Colour,* Volume 2, Her Majesty's Stationery Office, London, 1958, pp. 691–723.

336. D. Jameson and L. M. Hurvich, "Sensitivity, Contrast, and Afterimages," in *Visual Psychophysics,* Vol. VII/4, *Handbook of Sensory Physiology,* D. Jameson and L. H. Hurvich, eds., Springer-Verlag, Berlin, 1972, pp. 568–581.

337. S. K. Shevell, "Color Appearance," in *The Science of Color*, (2nd ed.), S. K. Shevell, ed., Elsevier, Oxford, 2003, pp. 149–190.

338. J. Walraven, "No Additive Effect of Backgrounds in Chromatic Induction," *Vision Research* **19:**1061–1063 (1979).

339. S. K. Shevell, "Unambiguous Evidence for the Additive Effect in Chromatic Adaptation," *Vision Research* **20:**637–639 (1980).

340. B. Drum, "Additive Effect of Backgrounds in Chromatic Induction," *Vision Research* **21:**959–961 (1981).

341. E. H. Adelson, "Looking at the World through a Rose-Colored Ganzfeld," *Vision Research* **21:**749–750 (1981).

342. J. Larimer, "Red/Green Opponent Colors Equilibria Measured on Chromatic Adapting Fields: Evidence for Gain Changes and Restoring Forces," *Vision Research* **21:**501–512 (1981).

343. J. Wei and S. K. Shevell, "Color Appearance under Chromatic Adaptation Varied Along Theoretically Significant Axes in Color Space," *Journal of the Optical Society of America A* **12:**36–46 (1995).

344. O. Rinner and K. Gegenfurtner, "Time Course of Chromatic Adaptation for Color Appearance and Discrimination," *Vision Research* **40:**1813–1826 (2000).

345. J. M. Hillis and D. H. Brainard, "Distinct Mechanisms Mediate Visual Detection and Identification," *Current Biology* **17:**1714–1719 (2007).

346. P. K. Kaiser, "Minimally Distinct Border as a Preferred Psychophysical Criterion in Heterochromatic Photometry," *Journal of the Optical Society of America* **61:**966–971 (1971).

347. A. Kohlrausch, "Theoretisches und Praktisches zur heterochromen Photometrie," *Pflügers Archiv für die gesamte Physiologie des Menschen und der Tiere* **200:**216–220 (1923).

348. H. Helson and V. B. Jeffers, "Fundamental Problems in Color Vision. II. Hue, Lightness, and Saturation of Selective Samples in Chromatic Illumination," *Journal of Experimental Psychology* **26:**1–27 (1940).

349. R. W. Burnham, R. M. Evans, and S. M. Newhall, "Prediction of Color Appearance with Different Adaptation Illuminations," *Journal of the Optical Society of America* **47:**35–42 (1957).

350. J. J. McCann, S. P. McKee, and T. H. Taylor, "Quantitative Studies in Retinex Theory: A Comparison between Theoretical Predictions and Observer Responses to the 'Color Mondrian' Experiments," *Vision Research* **16:**445–458 (1976).

351. L. E. Arend and A. Reeves, "Simultaneous Color Constancy," *Journal of the Optical Society of America A* **3:**1743–1751 (1986).

352. D. H. Brainard, W. A. Brunt, and J. M. Speigle, "Color Constancy in the Nearly Natural Image. 1. Asymmetric Matches," *Journal of the Optical Society of America A* **14:**2091–2110.(1997).

353. D. H. Brainard, "Color Constancy in the Nearly Natural Image. 2. Achromatic Loci," *Journal of the Optical Society of America A* **15:**307–325 (1998).

354. J. M. Kraft and D. H. Brainard, "Mechanisms of Color Constancy under Nearly Natural Viewing," *Proceedings of the National Academy of Sciences of the United States of America,* **96:**307–312 (1999).

355. D. H. Brainard, "Color Constancy," in *The Visual Neurosciences,* L. Chalupa and J. Werner, eds., MIT Press, Cambridge, MA, 2004, pp. 948–961.

356. H. E. Smithson, "Sensory, Computational, and Cognitive Components of Human Color Constancy," *Philosophical Transactions of the Royal Society of London B* **360:**1329–1346 (2005).

357. S. K. Shevell and F. A. A. Kingdom, "Color in Complex Scenes," *Annual Review of Psychology* **59:**143–166 (2008).

358. G. Buchsbaum, "A Spatial Processor Model for Object Colour Perception," *Journal of the Franklin Institute* **310:**1–26 (1980).

359. L. T. Maloney and B. A. Wandell, "Color Constancy: A Method for Recovering Surface Spectral Reflectances," *Journal of the Optical Society of America A* **3:**29–33 (1986).

360. D. H. Brainard and W. T. Freeman, "Bayesian Color Constancy," *Journal of the Optical Society of America A* **14:**1393–1411 (1997).

361. B. V. Funt, M. S. Drew, and J. Ho, "Color Constancy from Mutual Reflection," *International Journal of Computer Vision* **6:**5–24 (1991).

362. M. D'Zmura and G. Iverson, "Color Constancy. III. General Linear Recovery of Spectral Descriptions for Lights and Surfaces," *Journal of the Optical Society of America A* **11:**2389–2400 (1994).

363. G. D. Finlayson, P. H. Hubel, and S. Hordley, "Color by Correlation," in *Proceedings of the IS&T/SID Fifth Color Imaging Conference,* Scottsdale, AZ, 1997, pp. 6–11.

364. A. C. Hurlbert, "Computational Models of Color Constancy," in *Perceptual Constancy: Why Things Look As They Do*, V. Walsh and J. Kulikowski, eds., Cambridge University Press, Cambridge, 1998, pp. 283–322.

365. L. T. Maloney and J. N. Yang, "The Illuminant Estimation Hypothesis and Surface Color Perception," in *Colour Perception: From Light to Object,* R. Mausfeld and D. Heyer, eds., Oxford University Press, Oxford, 2001, pp. 335–358.

366. D. H. Brainard, J. M. Kraft, and P. Longère, "Color Constancy: Developing Empirical Tests of Computational Models," in *Colour Perception: Mind and the Physical World,* R. Mausfeld and D. Heyer, eds., Oxford University Press, Oxford, 2003, pp. 307–334.

367. D. H. Brainard, P. Longere, P. B. Delahunt, W. T. Freeman, J. M. Kraft, and B. Xiao, "Bayesian Model of Human Color Constancy," *Journal of Vision* **6:**1267–1281 (2006).

368. H. Boyaci, L. T. Maloney, and S. Hersh, "The Effect of Perceived Surface Orientationon Perceived Surface Albedo in Binocularly Viewed Scenes," *Journal of Vision* **3:**541–553 (2003).

369. H. Boyaci, K. Doerschner, and L. T. Maloney, "Perceived Surface Color in Binocularly Viewed Scenes with Two Light Sources Differing in Chromaticity," *Journal of Vision* **4:**664–679 (2004).

370. M. Bloj, C. Ripamonti, K. Mitha, S. Greenwald, R. Hauck, and D. H. Brainard, "An Equivalent Illuminant Model for the Effect of Surface Slant on Perceived Lightness," *Journal of Vision* **4:**735–746 (2004).

371. E. H. Land and J. J. McCann, "Lightness and Retinex Theory," *Journal of the Optical Society of America* **61:**1–11 (1971).

372. E. H. Land, "The Retinex Theory of Color Vision," *Scientific American* **237:**108–128 (1977).

373. E. H. Land, "Recent Advances in Retinex Theory," *Vision Research* **26:**7–21 (1986).

374. A. Hurlbert, "Formal Connections between Lightness Algorithms," *Journal of the Optical Society of America A* **3:**1684–1694 (1986).

375. G. West and M. H. Brill, "Necessary and Sufficient Conditions for von Kries Chromatic Adaptation to Give Color Constancy," *Journal of Mathematical Biology* **15:**249–250 (1982).

376. J. A. Worthey and M. H. Brill, "Heuristic Analysis of von Kries Color Constancy," *Journal of the Optical Society of America A* **3:**1708–1712 (1986).

377. D. H. Brainard and B. A. Wandell, "Analysis of the Retinex Theory of Color Vision," *Journal of the Optical Society of America A* **3:**1651–1661 (1986).

378. D. H. Foster and S. M. C. Nascimento, "Relational Colour Constancy from Invariant Cone-Excitation Ratios," *Proceedings of the Royal Society of London. Series B: Biological Sciences* **257:**115–121 (1994).

379. M. A. Webster and J. D. Mollon, "Colour Constancy Influenced by Contrast Adaptation," *Nature* **373:**694–698 (1995).

380. Q. Zaidi, B. Spehar, and J. DeBonet, "Color Constancy in Variegated Scenes: Role of Low-level Mechanisms in Discounting Illumination Changes," *Journal of the Optical Society America A* **14:**2608–2621 (1997).

381. M. D'Zmura and B. Singer, "Contast Gain Control," in *Color Vision: From Molecular Genetics to Perception,* K. Gegenfurtner and L. T. Sharpe, eds., Cambridge University Press, Cambridge, 1999, pp. 369–385.

382. W. S. Stiles, "Mechanism Concepts in Colour Theory," *Journal of the Colour Group* **11:**106–123 (1967).

383. D. Krantz, "A Theory of Context Effects Based on Cross-Context Matching," *Journal of Mathematical Psychology* **5:**1–48 (1968).

384. D. H. Brainard and B. A. Wandell, "Asymmetric Color-matching: How Color Appearance Depends on the Illuminant," *Journal of the Optical Society of America A* **9:**1433–1448(1992).

385. Q. Zaidi, "Identification of Illuminant and Object Colors: Heuristic-Based Algorithms," *Journal of the Optical Society America A* **15:**1767–1776 (1998).

386. J. Golz and D. I. A. MacLeod, "Influence of Scene Statistics on Colour Constancy," *Nature* **415:**637–640 (2002).

387. R. M. Boynton, M. M. Hayhoe, and D. I. A. MacLeod, "The Gap Effect: Chromatic and Achromatic Visual Discrimination as Affected by Field Separation," *Optica Acta* **24:**159–177(1977).

388. R. T. Eskew, Jr. and R. M. Boynton, "Effects of Field Area and Configuration on Chromatic and Border Discriminations," *Vision Research* **27:**1835–1844 (1987).

389. B. W. Tansley and R. M. Boynton, "A Line, Not a Space, Represents Visual Distinctness of Borders Formed by Different Colors" *Science* **191:**954–957 (1976).

390. B. Pinna, "Un Effetto di Colorazione," in *Il laboratorio e la città. XXI Congresso degli Psicologi Italiani,* V. Majer, M. Maeran, and M. Santinello, eds., Società Italiana di Psicologia, Milano, 1987, p. 158.

391. B. Pinna, G. Brelstaff, and L. Spillmann, "Surface Color from Boundaries: A New 'Watercolor' Illusion," *Vision Research* **41:**2669–2676 (2001).

392. B. Pinna, J. S. Werner, and L. Spillmann, "The Watercolor Effect: A New Principle of Grouping and Figure-ground Organization," *Vision Research* **43:**43–52 (2003).

393. F. Devinck, P. B. Delahunt, J. L. Hardy, L. Spillmann, and J. S. Werner, "The Watercolor Effect: Quantitative Evidence for Luminance-Dependent Mechanisms of Long-Range Color Assimilation," *Vision Research* **45:**1413–1424 (2005).

394. E. D. Montag, "Influence of Boundary Information on the Perception of Color," *Journal of the Optical Society of America A* **14:**997–1006 (1997).

395. R. T. Eskew, Jr. "The Gap Effect Revisited: Slow Changes in Chromatic Sensitivity as Affected by Luminance and Chromatic Borders," *Vision Research* **29:**717–729 (1989).

396. P. D. Gowdy, C. F. Stromeyer, III, and R. E. Kronauer, "Facilitation between the Luminance and Red-Green Detection Mechanisms: Enhancing Contrast Differences Across Edges," *Vision Research* **39:**4098–4112 (1999).

397. L. A. Riggs, F. Ratliff, J. C. Cornsweet, and T. C. Cornsweet, "The Disappearance of Steadily Fixated Visual Test Objects," *Journal of the Optical Society of America* **43:**495–501 (1953).

398. J. Krauskopf, "Effect of Retinal Image Stabilization on the Appearance of Heterochromatic Targets," *Journal of the Optical Society of America* **53:**741–744 (1963).

399. A. L. Yarbus, *Eye Movements and Vision,* Plenum Press, New York, 1967.

400. T. P. Piantanida and J. Larimer, "The Impact of Boundaries on Color: Stabilized Image Studies," *Journal of Imaging Technology* **15:**58–63 (1989).

401. H. D. Crane and T. Piantanida, "On Seeing Reddish Green and Yellowish Blue," *Science* **221:**1078–1080 (1983).

402. V. A. Billock, G. A. Gleason, and B. H. Tsou, "Perception of Forbidden Colors in Retinally Stabilized Equiluminance Images: An Indication of Softwired Cortical Color Opponency," *Journal of the Optical Society of America A* **10:**2398–2403 (2001).

403. J. L. Nerger, T. P. Piantanida, and J. Larimer, "Color Appearance of Filled-in Backgrounds Affects Hue Cancellation, but not Detection Thresholds," *Vision Research* **33:**165–172(1993).

404. J. J. Wisowaty and R. M. Boynton, "Temporal Modulation Sensitivity of the Blue Mechanism: Measurements Made Without Chromatic Adaptation," *Vision Research* **20:**895–909 (1980).

405. T. P. Piantanida, "Temporal Modulation Sensitivity of the Blue Mechanism: Measurements Made with Extraretinal Chromatic Adaptation," *Vision Research* **25:**1439–1444(1985).

406. N. W. Daw, "Why After-Images are Not Seen in Normal Circumstances," *Nature* **196:**1143–1145(1962).

407. R. van Lier and M. Vergeer, "Filling in the Afterimage after the Image," *Perception (ECVP Abstract Supplement)* **36:**200–201 (2007).

408. R. van Lier, M. Vergeer, and S. Anstis, "'Mixing-In' Afterimage Colors," *Perception (ECVP Abstract Supplement)* **37:**84 (2008).

409. C. McCollough, "Color Adaptation of Edge Detectors in the Human Visual System," *Science* **149:**1115–1116 (1965).

410. P. D. Jones and D. H. Holding, "Extremely Long-Term Persistence of the McCollough Effect," *Journal of Experimental Psychology: Human Perception & Performance* **1:**323–327 (1975).

411. E. Vul, E. Krizay, and D. I. A. MacLeod, "The McCollough Effect Reflects Permanent and Transient Adaptation in Early Visual Cortex," *Journal of Vision* **8:**4, 1–12 (2008).

412. G. M. Murch, "Binocular Relationships in a Size and Color Orientation Specific Aftereffect," *Journal of Experimental Psychology* **93:**30–34 (1972).

413. R. L. Savoy, " 'Extinction' of the McCollough Effect does not Transfer Interocularly," *Perception & Psychophysics* **36:**571–576 (1984).

414. E. Vul and D. I. A. MacLeod, "Contingent Aftereffects Distinguish Conscious and Preconscious Color Processing," *Nature Neuroscience* **9:**873–874 (2006).

415. P. Thompson and G. Latchford, "Colour-Contingent After-Effects Are Really Wavelength-Contingent," *Nature* **320:**525–526 (1986).

416. D. H. Hubel and T. N. Wiesel, "Receptive Fields, Binocular Interaction and Functional Architecture in the Cat's Visual Cortex," *Journal of Physiology* **160:**106–154 (1962).

417. D. H. Hubel and T. N. Wiesel, "Receptive Fields and Functional Architecture of Monkey Striate Cortex," *Journal of Physiology* **195:**215–243 (1968).

418. C. F. Stromeyer, III, "Form-Color Aftereffects in Human Vision," in *Perception, Handbook of Sensory Physiology,* Vol. VIII, R. Held, H. W. Leibowitz, and H. L. Teuber, eds., Springer-Verlag, Berlin, 1978, pp. 97–142.

419. D. Skowbo, B. N. Timney, T. A. Gentry, and R. B. Morant, "McCollough Effects: Experimental Findings and Theoretical Accounts," *Psychological Bulletin* **82:**497–510 (1975).

420. H. B. Barlow, "A Theory about the Functional Role and Synaptic Mechanism of Visual After-effects," in *Visual Coding and Efficiency,* C. B. Blakemore, ed., Cambridge University Press, Cambridge, 1990, pp. 363–375.

421. P. Dodwell and G. K. Humphrey, "A Functional Theory of the McCollough Effect," *Psychological Review* **97:**78–89 (1990).

422. G. K. Humphrey and M. A. Goodale, "Probing Unconscious Visual Processing with the McCollough Effect," *Consciousness and Coginition* **7:**494–519 (1998).

423. C. McCollough, "Do McCollough Effects Provide Evidence for Global Pattern Processing?," *Perception & Psychophysics* **62:**350–362 (2000).

424. V. H. Perry, R. Oehler, and A. Cowey, "Retinal Ganglion Cells that Project to the Dorsal Lateral Geniculate Nucleus in the Macaque Monkey," *Neuroscience* **12:**1101–1123 (1984).

425. T. N. Wiesel and D. Hubel, "Spatial and Chromatic Interactions in the Lateral Geniculate Body of the Rhesus Monkey," *Journal of Neurophysiology* **29:**1115–1156 (1966).

426. R. L. De Valois and P. L. Pease, "Contours and Contrast: Responses of Monkey Lateral Geniculate Nucleus Cells to Luminance and Color Figures," *Science* **171:**694–696 (1971).

427. H. Kolb and L. Dekorver, "Midget Ganglion Cells of the Parafovea of the Human Retina: A Study by Electron Microscopy and Serial Reconstructions," *Journal of Comparative Neurology* **303:**617–636 (1991).

428. D. J. Calkins, S. J. Schein, Y. Tsukamoto, and P. Sterling, "M and L Cones in Macaque Fovea Connect to Midget Ganglion Cells by Different Numbers of Excitatory Synapses," *Nature* **371:**70–72 (1994).

429. B. B. Boycott, J. M. Hopkins, and H. G. Sperling, "Cone Connections of the Horizontal Cells of the Rhesus Monkey's retina," *Proceedings of the Royal Society of London. Series B: Biological Sciences* **B229:**345–379 (1987).

430. W. Paulus and A. Kröger-Paulus, "A New Concept of Retinal Colour Coding," *Vision Research* **23:**529–540 (1983).

431. P. Lennie, P. W. Haake, and D. R. Williams, "The Design of Chromatically Opponent Receptive Fields," in *Computational Models of Visual Processing,* M. S. Landy and J. A. Movshon, eds., MIT Press, Cambridge, MA, 1991, pp. 71–82.

432. R. C. Reid and R. M. Shapley, "Spatial Structure of Cone Inputs to the Receptive Fields in Primate Lateral Geniculate Nucleus," *Nature* **356:**716–718 (1992).

433. B. B. Lee, J. Kremers and T. Yeh, "Receptive Fields of Primate Retinal Ganglion Cells Studied with a Novel Technique," *Visual Neuroscience* **15:**161–175 (1998).

434. D. M. Dacey, "Parallel Pathways for Spectral Coding in Primate Retina," *Annual Review of Neuroscience* **23:**743–775 (2000).

435. K. T. Mullen and F. A. A. Kingdom, "Differential Distributions of Red-Green and Blue-Yellow Cone Opponency across the Visual Field," *Visual Neuroscience* **19:**109–118 (2002).

436. L. Diller, O. S. Packer, J. Verweij, M. J. McMahon, D. R. Williams, and D. M. Dacey, "L and M Cone Contributions to the Midget and Parasol Ganglion Cell Receptive Fields of Macaque Monkey Retina," *Journal of Neuroscience* **24:**1079–1088 (2004).

437. S. G. Solomon, B. B. Lee, A. J. White, L. Rüttiger, and P. R. Martin, "Chromatic Organization of Ganglion Cell Receptive Fields in the Peripheral Retina," *Journal of Neuroscience* **25:**4527–4539 (2005).

438. C. Vakrou, D. Whitaker, P. V. McGraw, and D. McKeefry, "Functional Evidence for Cone-Specific Connectivity in the Human Retina," *Journal of Physiology* **566:**93–102 (2005).

439. P. Buzas, E. M. Blessing, B. A. Szmajda, and P. R. Martin, "Specificity of M and L Cone Inputs to Receptive Fields in the Parvocellular Pathway: Random Wiring with Functional Bias," *Journal of Neuroscience* **26:**11148–11161 (2006).

440. P. R. Jusuf, P. R. Martin, and U. Grünert, "Random Wiring in the Midget Pathway of Primate Retina," *Journal of Neuroscience* **26:**3908–3917 (2006).

441. R. W. Rodieck, "What Cells Code for Color?," in *From Pigments to Perception. Advances in Understanding Visual Processes,* A. Valberg, and B. B. Lee, eds., Plenum, New York, 1991.

442. T. Cornsweet, *Visual Perception,* Academic Press, New York, 1970.

443. P. Lennie, "Recent Developments in the Physiology of Color Vision," *Trends in Neurosciences* **7:**243–248 (1984).

444. E. Martinez-Uriegas, "A Solution to the Color-Luminance Ambiguity in the Spatiotemporal Signal of Primate X Cells," *Investigative Ophthalmology and Visual Science (supplement)* **26:**183 (1985).

445. V. A. Billock, "The Relationship between Simple and Double Opponent Cells," *Vision Research* **31:**33–42 (1991).

446. F. A. A. Kingdom and K. T. Mullen, "Separating Colour and Luminance Information in the Visual System," *Spatial Vision* **9:**191–219 (1995).

447. J. Nathans, D. Thomas, and S. G. Hogness, "Molecular Genetics of Human Color Vision: The Genes Encoding Blue, Green and Red Pigments," *Science* **232:**193–202 (1986).

448. J. D. Mollon, "'Tho' She Kneel'd in That Place Where They Grew...' The Uses and Origins of Primate Colour Vision," *Journal of Experimental Biology* **146:**21–38 (1989).

449. M. S. Livingstone and D. H. Hubel, "Segregation of Form, Color, Movement, and Depth: Anatomy, Physiology, and Perception," *Science* **240:**740–749 (1988).

450. D. T. Lindsey and A. M. Brown, "Masking of Grating Detection in the Isoluminant Plane of DKL Color Space," *Visual Neuroscience* **21:**269–273 (2004).

451. A. Li and P. Lennie, "Mechanisms Underlying Segmentation of Colored Textures," *Vision Research* **37:**83–97 (1997).

452. T. Hansen and K. Gegenfurtner, "Classification Images for Chromatic Signal Detection," *Journal of the Optical Society of America A* **22:**2081–2089 (2005).

453. H. E. Smithson, S. Khan, L. T. Sharpe, and A. Stockman, "Transitions between Colour Categories Mapped with Reverse Stroop Interference and Facilitation," *Visual Neuroscience* **23:**453–460 (2006).

454. Q. Zaidi and D. Halevy, "Visual Mechanisms That Signal the Direction of Color Changes," *Vision Research* **33:**1037–1051 (1986).

455. M. D'Zmura, "Color in Visual Search," *Vision Research* **31:**951–966 (1991).

456. J. Krauskopf, Q. Zaidi, and M. B. Mandler, "Mechanisms of Simultaneous Color Induction," *Journal of the Optical Society of America A* **3:**1752–1757 (1986).

457. J. Krauskopf, H. J. Wu, and B. Farell, "Coherence, Cardinal Directions and Higher-order Mechanisms," *Vision Research* **36:**1235–1245 (1996).

458. A. Valberg, "Unique Hues: An Old Problem for a New Generation," *Vision Research* **41:**1645–1657 (2001).

459. J. A. Movshon, I. D. Thompson, and D. J. Tolhurst, "Spatial Summation in the Receptive Fields of Simple Cells in the Cat's Striate Cortex," *Journal of Physiology* **283:**53–77 (1978).

460. H. Spitzer and S. Hochstein, "Complex-Cell Receptive Field Models," *Progress in Neurobiology* **31:**285–309 (1988).

461. J. Krauskopf and Q. Zaidi, "Induced Desensitization," *Vision Research* **26:**759–762 (1986).

462. M. J. Sankeralli and K. T. Mullen, "Bipolar or Rectified Chromatic Detection Mechanisms?," *Visual Neuroscience* **18:**127–135 (2001).

463. P. D. Gowdy, C. F. Stromeyer, III, and R. E. Kronauer, "Detection of Flickering Edges: Absence of a Red-Green Edge Detector," *Vision Research* **39:**4186–4191 (1999).

464. M. Sakurai and K. T. Mullen, "Cone Weights for the Two Cone-Opponent Systems in Peripheral Vision and Asymmetries of Cone Contrast Sensitivity," *Vision Research* **46:**4346–4354 (2006).

465. A. Vassilev, M. S. Mihaylovaa, K. Rachevaa, M. Zlatkovab, and R. S. Anderson, "Spatial Summation of S-cone ON and OFF Signals: Effects of Retinal Eccentricity," *Vision Research* **43:**2875–2884 (2003).

466. J. S. McClellan and R. T. Eskew, Jr., "ON and OFF S-cone Pathways Have Different Long-Wave Cone Inputs" *Vision Research* **40:**2449–2465 (2000).

467. A. G. Shapiro and Q. Zaidi, "The Effects of Prolonged Temporal Modulation on the Differential Response of Color Mechanisms," *Vision Research* **32:**2065–2075 (1992).

468. Q. Zaidi, A. G. Shapiro, and D. C. Hood, "The Effect of Adaptation on the Differential Sensitivity of the S-cone Color System," *Vision Research* **32:**1297–1318 (1992).

469. N. V. S. Graham, *Visual Pattern Analyzers*, Oxford University Press, New York, 1989.

470. A. B. Watson and J. G. Robson, "Discrimination at Threshold: Labelled Detectors in Human Vision," *Vision Research* **21:**1115–1122 (1981).

471. S. L. Guth, "Comments on 'A Multi-Stage Color Model' " *Vision Research* **36:**831–833 (1996).

472. R. L. De Valois and K. K. De Valois, "On 'A Three-Stage Color Model'," *Vision Research* **36:**833–836 (1996).

473. M. E. Chevreul, *De la loi du Contraste Simultané des Couleurs,* Pitois-Levreault, Paris, 1839.

474. A. Kitaoka, "Illusion and Color Perception," *Journal of the Color Science Association of Japan* **29:**150–151 (2005).

475. K. Sakai, "Color Representation by Land's Retinex Theory and Belsey's Hypothesis," Graduational thesis, *Department of Psychology*, Ritsumeikan University, Japan, 2003.

476. W. von Bezold, *Die Farbenlehre in Hinblick auf Kunst und Kunstgewerbe*, Westermann, Braunschweig, 1874.

477. L. T. Sharpe, A. Stockman, H. Jägle, and J. Nathans, "Opsin Genes, Cone Photopigments, Color Vision and Colorblindness," in *Color Vision: From Genes to Perception,* K. Gegenfurtner and L. T. Sharpe, eds., Cambridge University Press, Cambridge, 1999, pp. 3–51.

478. P. Lennie, "Parallel Visual Pathways: A Review," *Vision Research* **20:**561–594 (1980).